Universitetet i Stavanger

FACULTY OF SCIENCE AND TECHNOLOGY

MASTER'S THESIS

Study programme/specialisation: Marine and Offshore Technology - Semisubmersible design	Spring semester, 2019 Open
Author: José Antonio Torres	

Programme coordinator: Muk Chen Ong

Supervisor: Sverre Haver

Title of master's thesis:

Assessment of necessary airgap of a semisubmersible using a Peak-Over-Threshold long term analysis

Credits: 30

Keywords: airgap, semisubmersible, relative surface elevation, significant wave height, peak period, peak over threshold, contours, extremes, severity, probability of exceedance, transfer functions, long term, short-term variability, Weibull, Gumbel	Number of pages: 102 Stavanger, June 10, 2019

ABSTRACT

The airgap of a column stabilized floating structure is the distance from a point on the underside of the deck to the water level instantly and directly below it; when the sea is not calm, it varies with time and for different locations of the deck due to the wave motions. The initial airgap, the vertical distance from the underside of the deck to the mean water level, is of critical importance to make sure that wave to deck impacts are avoided; for these can result in unwanted roll or pitch motions or even damage to the topside. Safety standards require that the probability of a wave hitting the deck corresponds to 1 in 100 years for the ultimate limit state design (ULS) and 1 in 10,000 years for an accidental limit state deign (ASL). The complexity of calculating the required airgap goes far beyond estimating extreme values of the wave heights and periods because 1) the structure moves in different ways with different waves and different directions, 2) the wave field changes below the deck due to disturbances created by the structure itself 3) the surface elevation and the responses are stochastic processes. At the same time, there are several reasons to avoid ending up with an airgap that is larger than the minimum required.

The geometry of a semisubmersible that was to be built offshore Norway was given along with the transfer functions that describe its motions and the functions that describe the disturbed wave elevation under the deck. These were previously computed with a finite element analysis for 16 different directions of incidence of the waves. Besides, hindcast data from the northern north-sea over the last 61 years was accessible; this describes the significant wave height (H_s), peak period (T_p) and direction of 3-hour sea states. Wind waves were of interest and the effect of swell was ignored due to its negligible effect. In order to determine the minimum required initial airgap for both limit state designs, statistical analyses of the responses were done for which all of the measured 3-hour sea states were examined. A peak-over-threshold (POT) approach was adopted at first, where responses are modelled for storms with 3-hour significant wave heights above the threshold. The results are compared for many cases (different thresholds and two different POT versions) and an additional analysis was made, the latter required the estimation of extreme sea states from probability contours that were generated on the H_s, T_p scatter plot of the data. The work also presents a measure of the storm severity for different directional sectors and the estimated extreme values of the significant wave height for various analytical setups.

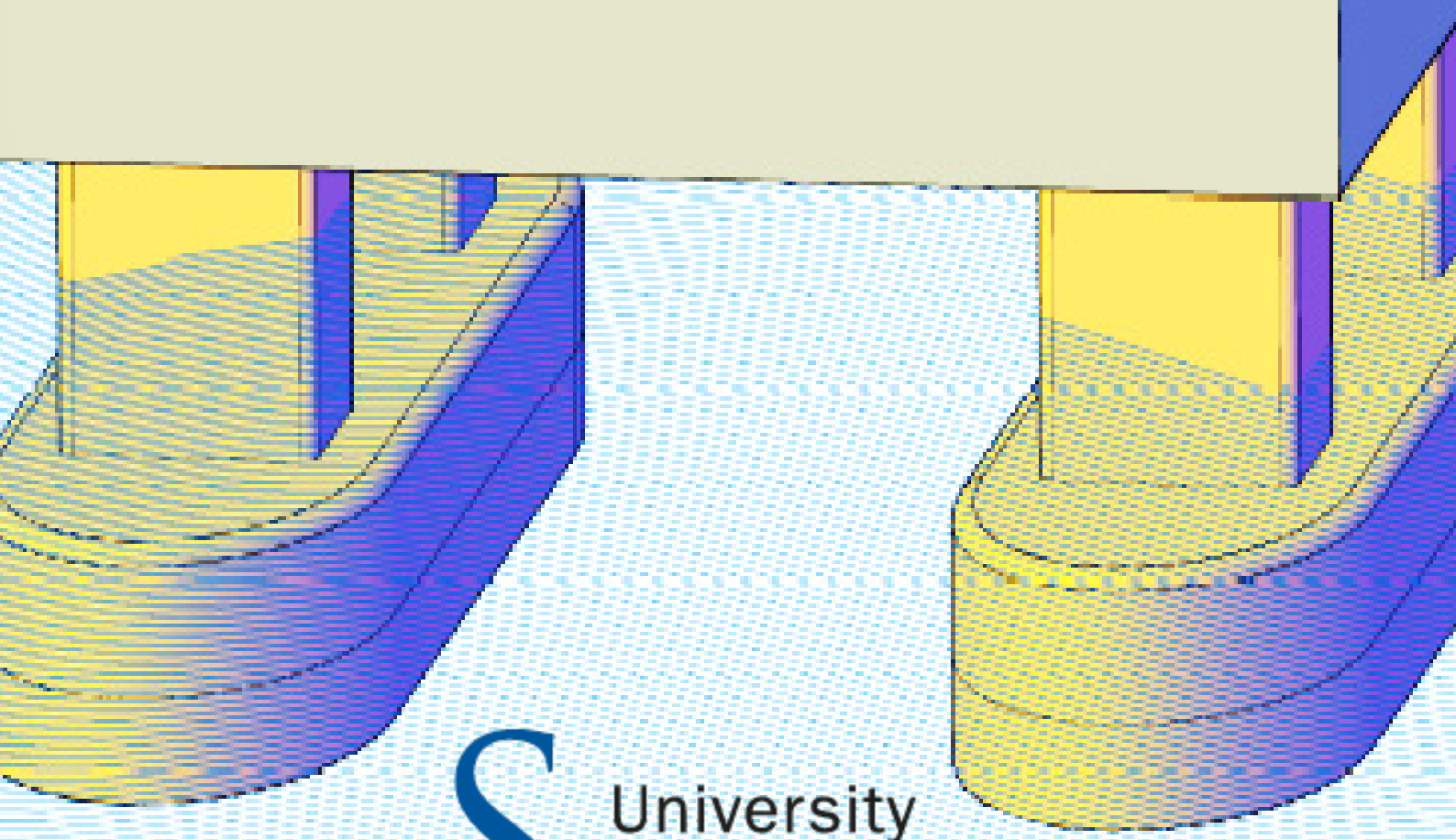

University of Stavanger

José Antonio Torres

Master's thesis in Marine Technology

Assessment of necessary airgap of a semisubmersible using a Peak-Over-Threshold long term analysis

Program coordinator: Muk Chen Ong
Supervisor: Sverre Haver

Spring, 2019

ACKNOWLEDGEMENTS

This master's thesis was done under the supervision and with the help of Sverre Haver. Not only do I thank him for the great support throughout the semester, but I want to emphasize on how remarkable his knowledge on the topic is as well as his ability to notice the smallest details. His dedication and kindness reflected a true passion for this science. I am proud of having worked with someone so achieved in the field who made a big effort to help me learn as much as possible.

During the whole project I had the support of many people who encouraged me to work smarter and to try and achieve more than what was required. I thank my close friends Alla and Charlotte for all those times when they managed to motivate me, Julio Patiño for his proficient previous work which I often read to guide me, and Professor Muk Chen Ong for his keenness on making the most competent students.

TABLE OF CONTENTS

ABBREVIATIONS AND SYMBOLS

ALS	Accidental limit state
CDF	Cumulative distribution function
E	Expectancy
F	Value of a CDF, in the range of [0, 1]
F_{ALS}	Value that a CDF takes for the ALS design
F_R	CDF of the maximum relative surface elevation
$F_{R,i}$	CDF of the maximum relative surface elevation for storm i
$F_{R,j}$	CDF of the maximum relative surface elevation for storm step j
F_R^*	Long-term (cumulative) distribution of the maximum relative surface elevation accounting for the short-term variability
$F(T_p \mid H_s)$	Cumulative distribution of the peak period given a significant wave height
F_{ULS}	Value that a CDF takes for the ULS design
f	Probability density function of a random variable
f_R	Probability density function of the most probable storm maximum relative surface elevation
H_s	Significant wave height
$H_{s,ALS}$	Significant wave height with probability of exceedance of 1 in 10,000 years
$H_{s,ULS}$	Significant wave height with probability of exceedance of 1 in 100 years
$h_{H,p}$	Disturbed surface elevation transfer function under point p under the deck
$h_{R,p}$	Relative surface elevation process
$h_{z,p}$	Heave transfer function accounting for roll and pitch motions under point p under the deck
k	A directional WAMIT sector
$MPSM$	Most probable storm maximum relative surface elevation
MWL	Mean water level
N_{1y}^*	Expected number of annual 3-hour events above a threshold. Or expected number of annual storms when only the storm peaks are analysed
n_{3h}	Expected number of zero up-crossings in three hours
P	Probability
PDF	Probability density function

POT	Peak over threshold
p	A specific point under the deck
RAO	Response amplitude operator
r	Maximum relative surface elevation in a 3-hour event (a random variable)
$\tilde{r}$	Domain of the most probable storm maximum relative surface elevation
$\tilde{r}^*_{100}$	100-years MPSM without accounting for short-term variability
$\tilde{r}^*_{10K}$	10,000-years MPSM without accounting for short-term variability
S_J	JONSWAP wave spectrum
$S_{R,p}$	Spectrum of the relative surface elevation process
S_{Ξ}	Wave spectrum
T	Threshold
T_p	Peak period
T_p^*	Peak period as a fitted function of the significant wave height
T_z	Expected zero up-crossing period
ULS	Ultimate limit state
$\tilde{z}$	Sea-state maximum relative surface elevation (the expected maximum relative surface elevation during a specific sea state)
α	Scale parameter in the Weibull distribution Wave asymmetry factor
β	Shape parameter in the Weibull distribution
β_G	Beta parameter in the Gumbel distribution
γ	Peak shape parameter in the JONSWAP spectrum
γ_1	Skewness of the significant wave height given a threshold
μ	Mean / expected value
λ	Location parameter in the Weibull distribution
σ	Standard deviation
σ^2	Variance
σ_{R_p}	Variance of the spectrum of the relative surface elevation process for point p under the deck
θ	NORA10 direction (direction in the meteorological convention)
ω	Angular frequency in radians per second
ω_p	Peak angular frequency

INTRODUCTION

All floating structures experience motion responses from the natural loads at the sea, particularly wave loads. These motions, when excessive, will force the operations to be temporarily shut down. In the Oil and Gas industry, bearing rough sea conditions and large water depths is key; not only for production and drilling, but for exploration and installations as well. A floating production unit that handles larger and steeper waves while maintaining its operability essentially translates into a better rate of production.

When the first Mobile Offshore Drilling Unit was built in 1954 by Ocean Drilling and Exploration Co. (ODECO) the maximum operational water depth reached only 12 meters. It was a submersible; a barge that would lower itself down until making contact with the seabed. The drawbacks were clear considering that the whole topside had to stand well above the water level, but it was the beginning of offshore oil and gas exploration. The jackups were the next big innovation: carrying several 'legs' on top of them which can be lowered to work as columns when the desired location is reached, jackups are used broadly for installations, but their obvious restraint is the depth of the water at which they can operate. Maersk has reached 150 m with the *Invincible*. Gravity based structures have proven to work well for permanent solutions at even larger depths; the first offshore drilling units were in fact gravity-based structures. Many were built in the Gulf of Mexico in the early 1900s, nowadays, these have reached great depths. The famous *Troll-A,* built in the south west of Norway by Statoil, lays on waters with a depth of almost 370 m and is built with concrete. Whereas for steel gravity-based structures (Jackets) Chevron holds the record with the *Petronius* at a water depth of 530 m. As explorations activities became more ambitious, the need for effective floaters grew and in 1961 Shell Oil converted the submersible *Bluewater I* into a semisubmersible by implementing a mooring system in it. Then in 1963 ODECO (now Diamond Offshore) build the first purpose-built semisubmersible - or "column stabilized vessel"-. It was designed for water depths of up to 90 m. As station keeping systems underwent innovations such as the development of Dynamic Positioning systems, it is now not uncommon that production floaters operate at water depths exceeding 2,000 m. These also include drillships and spars. Some examples of the greatest achievements are the *CNOOC981* by China's National Offshore Oil Corporation, a semisubmersible designed to operate at depths of 3,000

meters. Shell's *Perdido* spar, east of Texas, is designed to operate at depths of up to 2400m, and BP's *Atlantis* semisubmersible, currently located at the south of New Orleans floats over 2,150 m of water.

From an investment perspective, gravity-based structures are more profitable than floaters at large water depths. The question on what the water depth limit for gravity-based structures is remains subjective, but it seems clear that floaters are the only option in ultradeep waters. Semisubmersibles and spars are the state-of-the-art floating production system types. The idea behind a semisubmersible is that the restoring forces in the heave motion are much smaller than those of a ship due to having a small waterplane area -the intersection between the structure and the water surface- while still being heavy. The pontoons that they lie on are in some cases used for transportation, but they are fully submerged for operational conditions and filled with ballast weight. They also make up for most of the buoyancy. The newer alternative to semisubmersibles are the spars, with only one big column, no pontoons and a large ballast mass at the bottom to provide stability. These are not as stable as semisubmersibles but that results in larger natural periods in all degrees of freedom, which is convenient. Spars have an even smaller waterplane area than semisubmersibles and can protect the risers from the wave forces, but their big disadvantage is that they need to be towed in parts for their transportation. Drillships on the other hand are more responsive to wave motions and thus their operability is certainly lower than that of the named column stabilized units. They are very common though, for their versatility and the weight of the drillships used in the Oil and Gas industry is so large that their natural periods are in some cases comparable to those of a semisubmersible. However, they require more complex heave compensation systems.

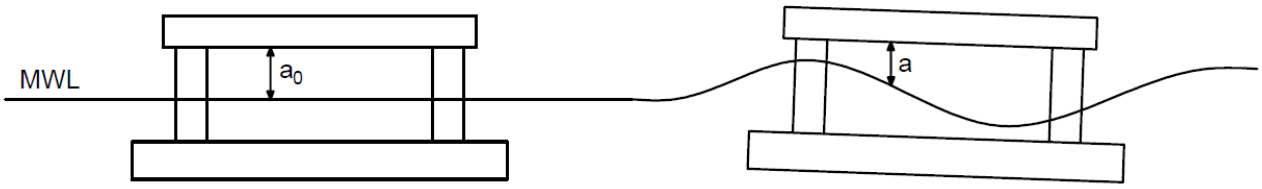

***Figure 1**: Initial airgap vs true airgap*

One of the main issues with column stabilized structures when it comes to design is the airgap, which is the vertical distance between the underside of a point of the deck and the water level directly below it. It is analogous to the freeboard of a ship, but not comparable. With this definition, the difference between airgap and still water airgap -or initial airgap- should be made clear: there is an airgap for

every point under the deck at any given time and they would all be the same for the condition when the sea is totally calm, the still water airgap. In the case of a gravity-based structure -or 'bottom fixed structure'- such as a jacket this distance is only a function of the wave height if the diffraction of the waves is not considered. It basically depends only on the sea state, since the structure is fixed. Semisubmersibles and spars, although moored or dynamically positioned, follow the waves. They are by no means static. This implies that designing for the airgap depends on how the structure reacts to different waves and for every point, the induced motions must be considered. Surge, sway and yaw are not relevant, but pitch and a roll motions decrease the airgap for half of the platform area.

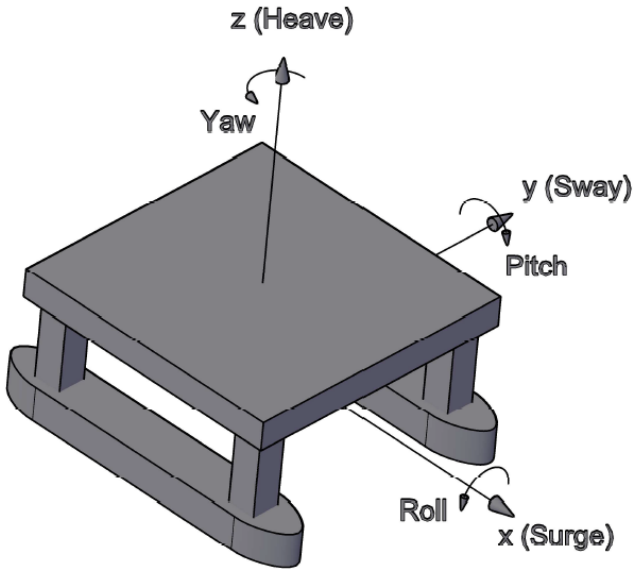

***Figure 2**: All six degrees of freedom of a floating structure*

The aim of the design airgap being equal or larger than the airgap at a specific point and time when the water level is at its highest relative to the structure is to avoid wave to deck impacts. Several accidents have occurred with wave to deck impacts in the history of semisubmersibles, such as that of the COSL Innovator in 2015[1]. In the case of bottom fixed structures there is a substantial increase of the base shear[2] which is equivalent to an increase in loads and motions in surge, sway, roll or pitch for column stabilized vessels thus increasing the loads in mooring lines or contributing to

[1] Veld, K. (2016). From cosl.no
[2] Haver, S. (2019)

inconvenient motions of the risers. It has also been shown that deck structures can suffer significantly greater loads with the impact of waves[3].

For these kind of problems where it is necessary to describe of the sea states, different models of wave spectra exist. They have each been developed for a specific sea and the semisubmersible whose airgap is assessed in this work was a project for an oil field in the Norwegian continental shelf. It was never built, but several simulations with the finite element method were run on the model to compute its response properties. This work considers a site in the northern North Sea where the full JONSWAP spectrum is the most suitable. The location of the semisubmersible is considered to be in the geographical position of 67.05° North and 7° East. The hindcast data that was used in this thesis was obtained from NORA10 for this location.

Estimating the minimum airgap requires an extensive statistical analysis. The relative wave elevation -I.e. above the mean water level relative to the columns of the floater- is to be computed given certain physical models and the hindcast data. It is in the end the extreme values that are of interest, thus one of the main topics treated is extreme value statistics. The data analysed describes three-hour sea states for the last 61 years and the main process for this work follows the Peak-Over-Threshold (POT) method, introduced by Yoshimi Goda in 1988. The POT method consists on taking only the data that corresponds to a significant wave height that exceeds a certain value, hence treating every group of 3-hour events above the threshold as a storm. The responses are analysed for each storm. Besides, the distribution of the significant wave height is very difficult to model precisely considering all the values that it takes, omitting the smaller ones (close to zero) yields more realistic estimations for the extremes[4]. The method can also be referred to as All Storms Approach, in the sense that implementing a threshold divides the valid data into 'storms' every time that the threshold is crossed. A variation of the POT method was also implemented, where only the storm peaks were analysed. Additionally, probability contours were generated to estimate combinations of 'significant wave height' and 'peak period' with a certain probability of exceedance and the response analysis was performed from these combinations to find the critical. Several comparisons amongst the different methods and thresholds are shown.

[3] Skjeggedal, E. (2017)
[4] Ferreira, J.A. & Soares, C. G. (1998)

SOME THEORY ON THE RELATIVE SURFACE ELEVATION

The motions of a floater in a particular degree of freedom due to waves are understood as oscillatory motions that can be well modelled by amplitudes and frequencies, where the amplitude of the responses depend on both the amplitude and the frequency of the exciting motions (the wave particle motions) and the frequency of the response is the same as the frequency of the exiting motions. Besides, a phase shift exists between the exciting motions and the response motions, meaning that there is a 'delay' in the response motions. The existence of such phase shift is inherent due to the mass of the floater: all free bodies with a mass experience an acceleration when a force is applied to them, not an instant velocity.

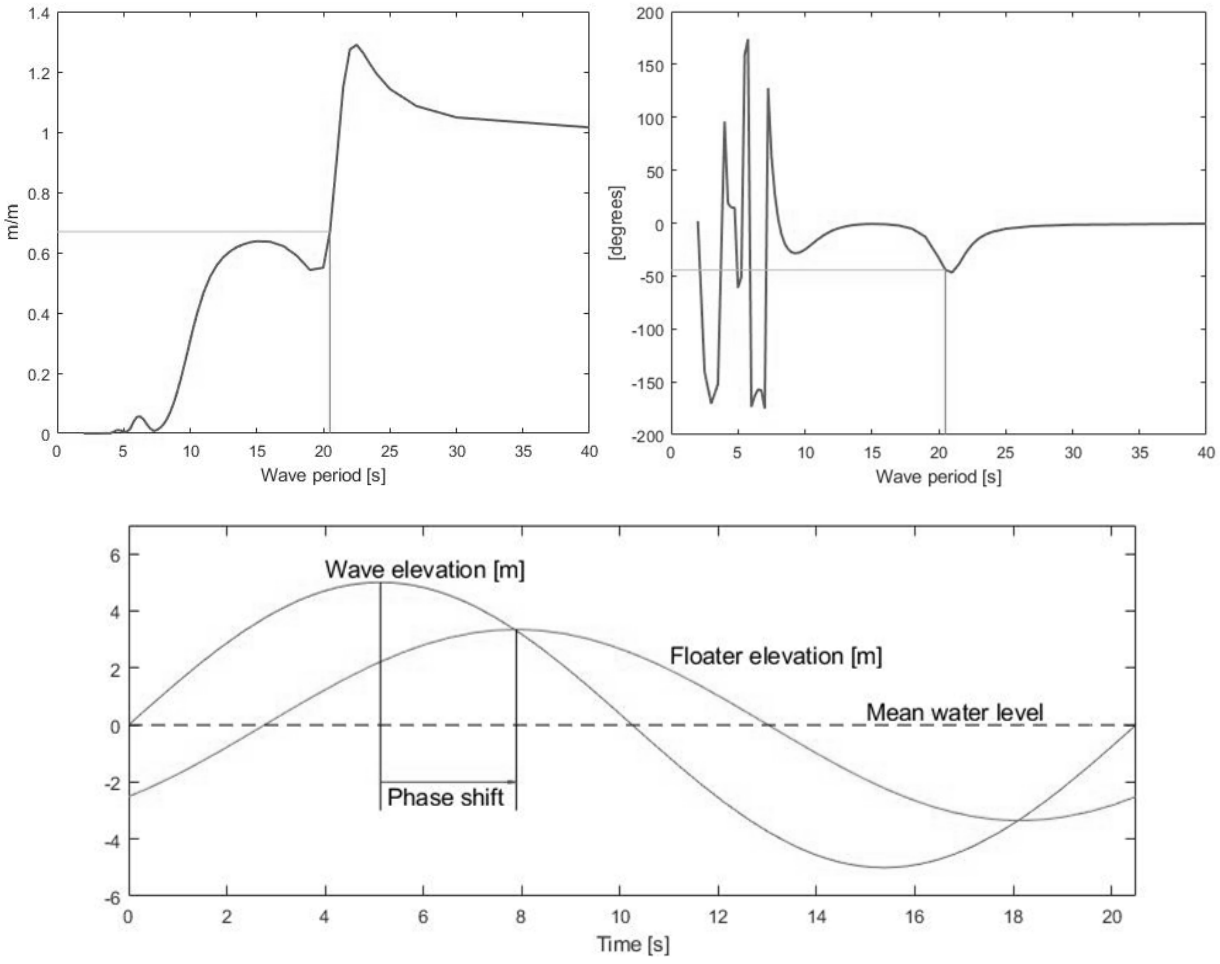

***Figure 3**: Example of heave RAO and phase shift of the centre of the given semisubmersible for an incoming wave at 22.5° from x to y axis (figure 11) with a height of 10 m and period of 20.5 s. The lower subfigure shows that for the given wave the amplitude of the response motion is scaled by 0.67 and the phase shift of 44.2° corresponds to a delay of 2.7 seconds.*

For the centre of flotation of a ship, or the point at the centre of the underside of the deck for a semisubmersible, the resultant motions can be described by the vessel's Response Amplitude Operators (RAOs) along with their phase shifts. Both RAOs and phase shifts are functions of the wave frequencies, in radians per second. A RAO's value tells the ratio between the amplitude of the motion of the floater to the amplitude of the wave particle motions at the surface. By this definition it can be deducted that the RAO's minimum value would tend to zero if the wave frequencies were 'too high to allow the vessel to move' and tends to one when frequencies of the waves are so low that vessel would 'follow the wave'. In the case when the heave, roll and pitch RAOs tend to one, with very low wave frequencies or equivalently, very high wave periods, the vessel would move with the waves and the relative surface elevation (the upwell, or elevation of the sea surface relative to the waterline of the vessel) would remain close to zero. On the other hand, the case of the RAOs taking very low values close to zero would occur when the waves are very, very frequent, with periods of short duration. Here the structure would remain quasi-static and the relative surface elevation would approach the wave height.

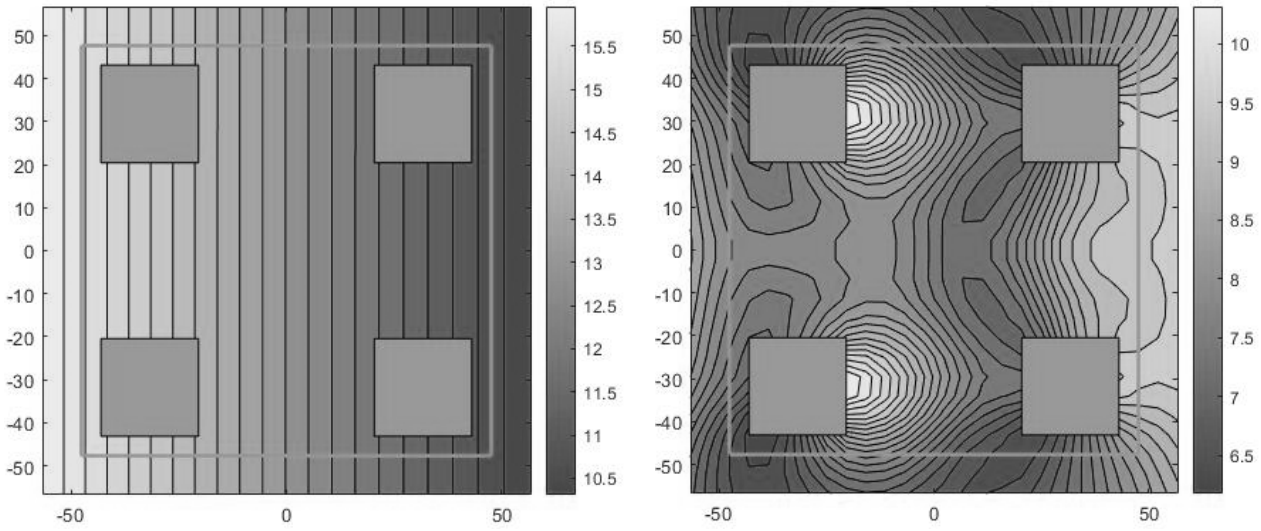

***Figure 4**: Example of the influence of the disturbance of the wave crests by the semisubmersible. Here, the expected maximum values for the relative surface elevation are plotted with vs without the disturbances for a 3-hour sea state that has a significant wave height of 9.6 m and a peak period of 15.3 s, with a direction of 180° WAMIT. For the given sea state, the expected maximum values decreased, but they might increase with different peak periods.*

The RAOs of a vessel are given for a fixed point (and wave direction direction) which is at the centre of the underside of the deck for a semisubmersible. However, a corrected RAO must be used for the location of every single point that is to be worked with. Since the waves move the floater in several degrees of freedom at the same time, it becomes obvious that the pitch or roll motions affect the airgap in a very large extent at all points far from the centre. Moreover, the waves get disturbed by the structure itself, so the height of the wave crests under a particular point of the deck actually differs from the height of the crests if the structure was not there. For every point under the deck then, and for a given direction of the incoming waves, this disturbances are modelled as wave RAOs, which express the ratio of the disturbed crest heights to the undisturbed (figure 4).

It is important to notice at this point that the waves are modelled as linear waves while in reality the most accurate models follow the stokes' 5^{th} profile. For an assessment of an airgap though, a simple correction is made with an asymmetry factor to account for the crests being higher than the troughs.

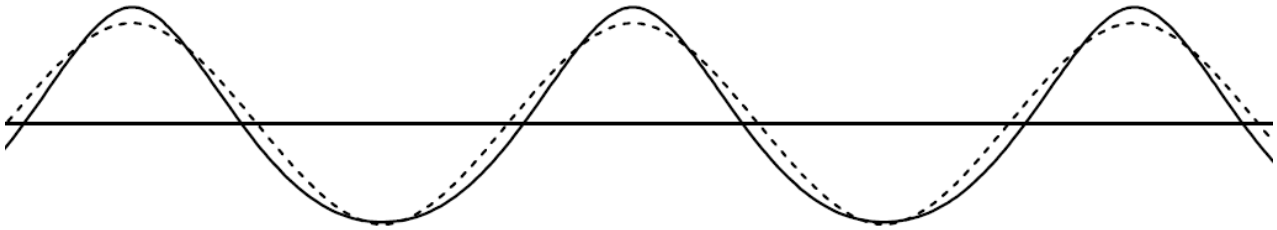

Figure 5: *Sinusoidal profile (dashed line) vs real profile (approximation)*

PROBLEM SETUP

HINDCAST DATA

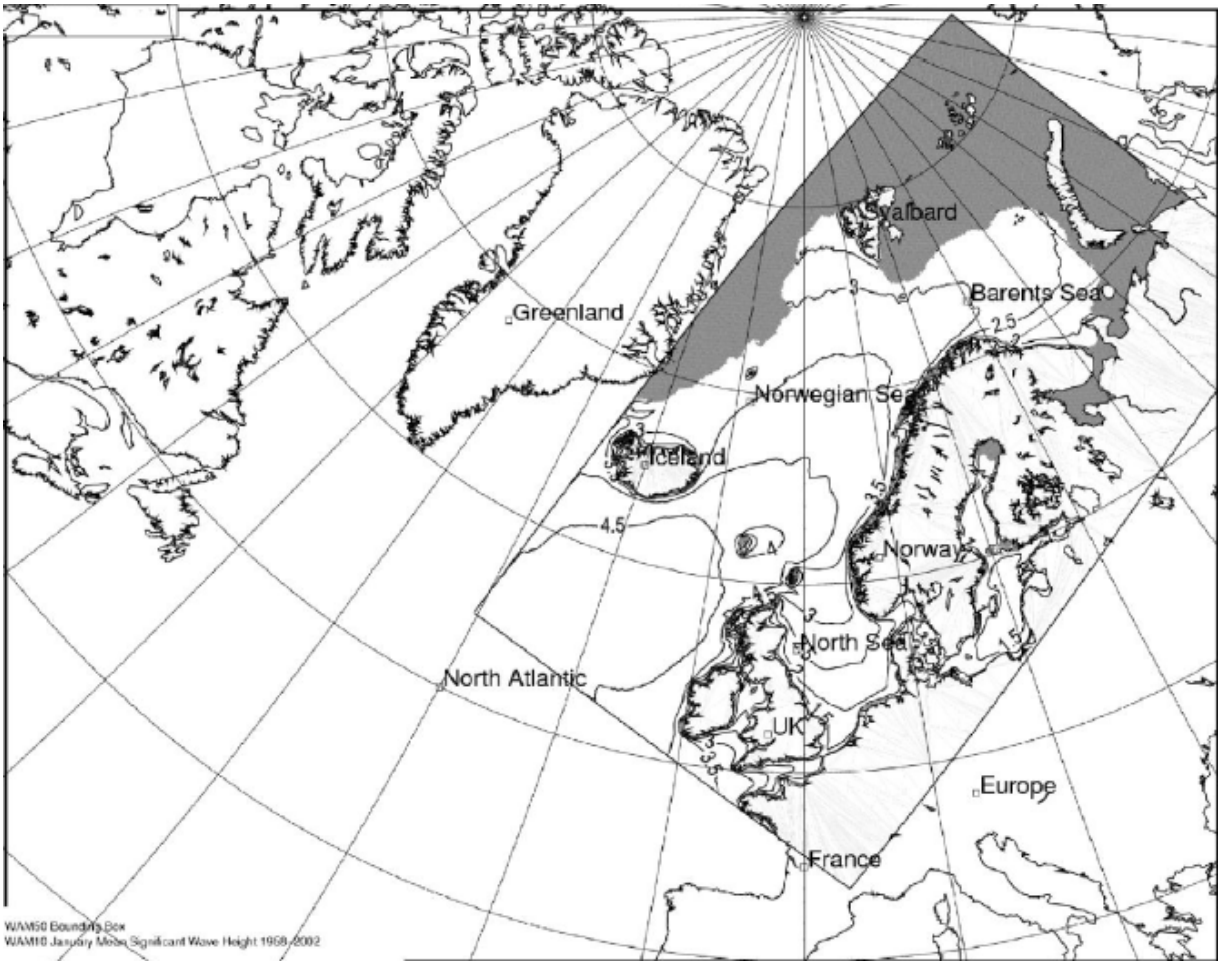

Figure 6: *Area covered by the NORA10 database. The work's location is West of the Lofoten peninsula. (Reistad et al., 2011)*

The NORA10 data used from which the sea states are known corresponds to a geographical position of 67.05° North and 7° East. This is arguably the zone with the rougher seas in the world, influenced by the North Atlantic current, a branch of the Gulf Stream that follows the West coast of Norway and northwards. The data comprises 178,725 three-hour measurements for the sea states from September 1 of 1957 till October 31 of 2018. The data has information on significant wave heights, peak periods, and directions for the waves generated from the wind, swell waves, and the total sea as a superposition of the wind sea and swell sea.

WAM106705N0700E																
YEAR	M	D	H	WSP	DIR	HS	TP	TM	DIRP	DIRM	HS1	TP1	DIRP1	HS2	TP2	DIRP2
Nu...	...	...	...	Number	Nu...	Number	Nu...	Nu...	Nu...	Nu...	Number	Nu...	Nu...	Number	Nu...	Nu...
WAM	WIN	D A	ND	WAVES												
LATI	TUD	E:	67.	05, LON	GITUD	E:	7.	00								
				WI	ND			TOTAL	SEA		WI	ND SE	A	S	WELL	
YEAR	M	D	H	WSP	DIR	HS	TP	TM	DIRP	DIRM	HS	TP	DIRP	HS	TP	DIRP
1957	9	1	6	7.9	42.	1.2	5.2	4.3	36.	37.	1.0	5.2	36.	0.6	6.3	6.
1957	9	1	9	9.5	33.	1.3	5.2	4.3	36.	38.	1.2	5.2	36.	0.4	6.9	81.
1957	9	1	12	10.0	36.	1.5	5.7	4.5	36.	39.	1.5	5.7	36.	0.4	6.9	81.

Figure 7: *Segment of NORA10 database for the selected location*

Since it has been shown that the influence of the swell waves is negligible for airgap assessments[5], the present work only considers the wind sea. Apart from that, all of the 'measurements' that correspond to a significant wave height (H_s) of less than 0.4 m were sorted out of the dataset. By looking at the occurrences of the sorted H_s values for this case, it was concluded that the H_s larger than 0.3 m follow the same distribution, while the H_s smaller than 0.4 don't. For the statistical analyses of H_s extremes, this assumption suggests more precise results. In chapter 3, a comparison shows that sorting out these numbers is indeed better for the probabilistic fits, though the analysis of all sea states is only useful for the contour method anyway.

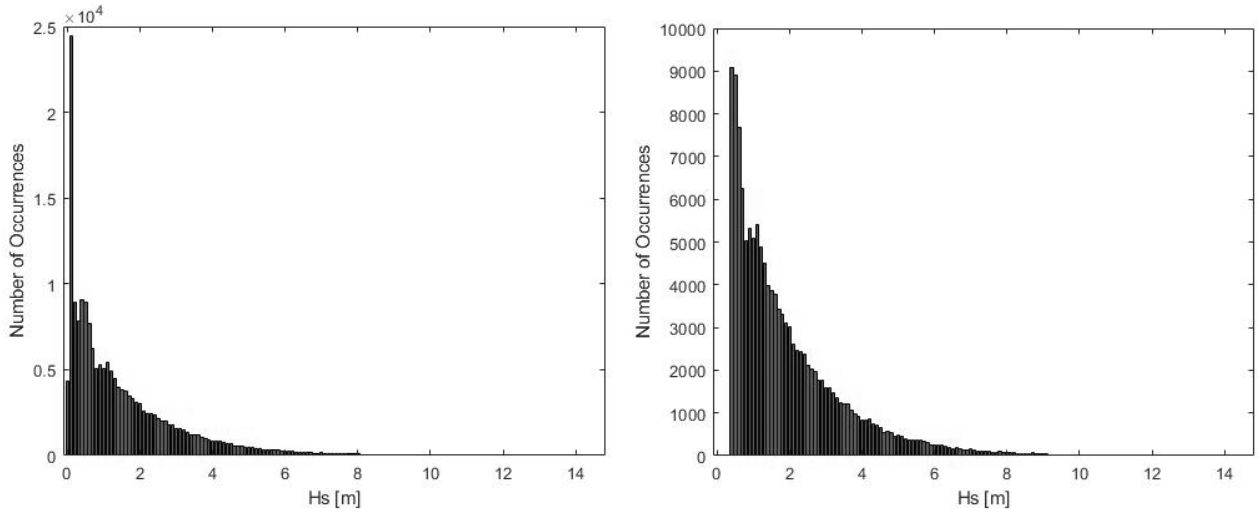

Figure 8: *Modified data set for all sea states. The bars show the occurrences of the sorted H_s values.*

[5] Patiño, J. (2018)

Another alteration that was done on the NORA10 dataset was correcting the spectral peak period (T_p) values: this was done following the procedure proposed by Odd Jan Andersen[6] in which the discrete values in the T_p domain are transformed to random values within specific intervals:

> originally, there are 22 values for the peak period , being the lowest 2.4 seconds, then 2.7… and up until the highest with 18 seconds without a fixed increment, as seen in the first subfigure below. It was found that this numbers are obtained by
>
> $$T_p = 3.244\ exp\{0.09525(i-1)\} \qquad i = 1,2,3,\dots,22$$
>
> the limits of the intervals, then, are
>
> $$3.244\ exp\{0.09525(i-1\pm 0.5)\}$$
>
> so, the correction for each T_p becomes
>
> $$T_p = 3.244\ exp\{0.09525(i-0.5-rnd)\} \tag{1}$$

with '*rnd*' being a uniformly distributed random number from 0 to 1

In order to apply equation (1), the i value for every T_p had to be found:

$$i = Round\left[1+\frac{ln(T_p/3.244)}{0.09525}\right] \tag{2}$$

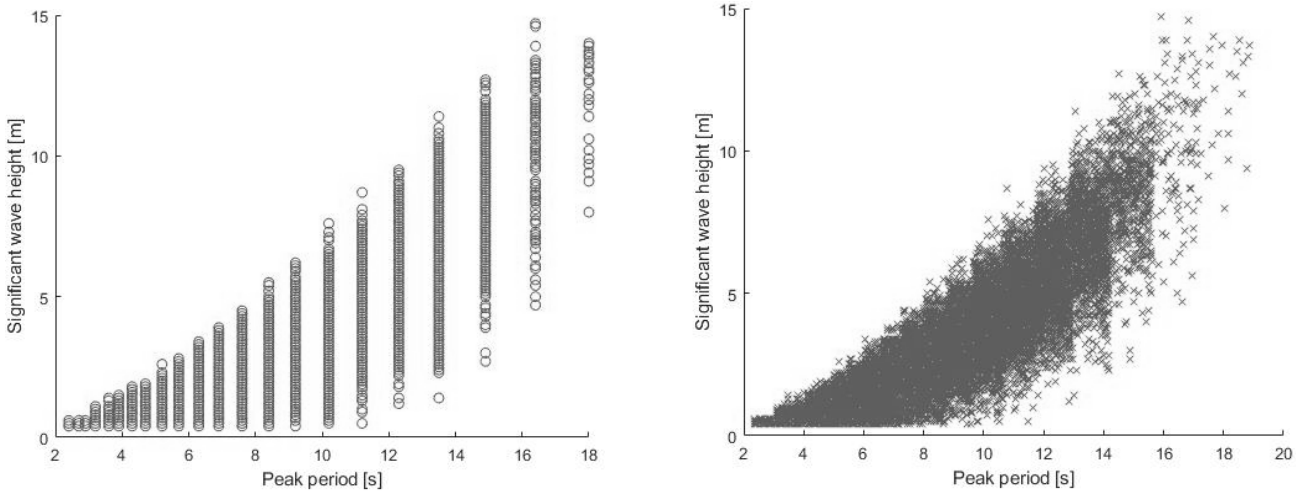

Figure 9: *Scatter plot H_s vs T_p for all of the 3-hour sea states from the wind. The resolution of the peak period was corrected.*

[6] Andersen, O. J. (2009): Appendix D of Haver, S.'s METOCEAN MODELLING AND PREDICTION OF EXTREMES (2018)

SEMISUBMERSIBLE ARRANGEMENT

Analysing the data for the wind sea, a wind rose[7] was plotted to visualize the directions where the 3-hour significant wave heights come from. NORA10 follows a meteorological convention, which means that the directions represent where the waves are coming from, with zero degrees being the North and rotating in a clockwise direction. Traditionally, a semisubmersible will have its x axis (forward) pointing towards the direction where the most severe storm come from. Further in this document, storm severity is referred to as a measure of the relative wave elevation that results from a particular storm on the structure.

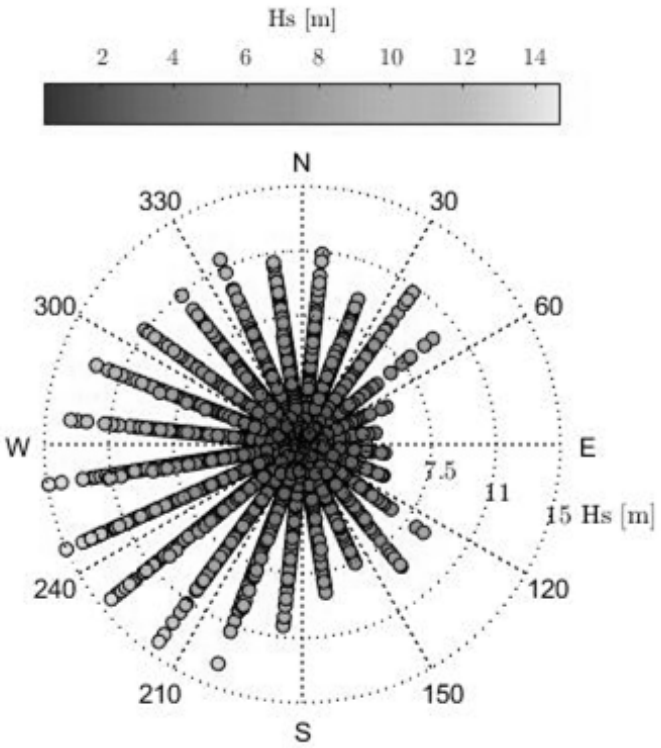

Figure 10: *NORA10 directions for the 3-h wind sea states.*
Highest waves coming from the West, slightly South.

In the way the semisubmersible was designed its response properties for the structure as a whole (rigid body motions) as well as the response properties for every point under the deck and the wave RAOs for every point under the deck are a function of the direction of the incident waves where the incident waves follow the WAMIT convention, starting at zero degrees for the waves following the direction of the x axis (surge) and increasing counter-clockwise with steps of 22.5 degrees. A zero-

[7] Cheynet, E. (2016)

degree wave -or rather for this work, 3-hour sea state- in the WAMIT direction follows the forward surge direction, while a 90-degree wave would move from starboard to port.

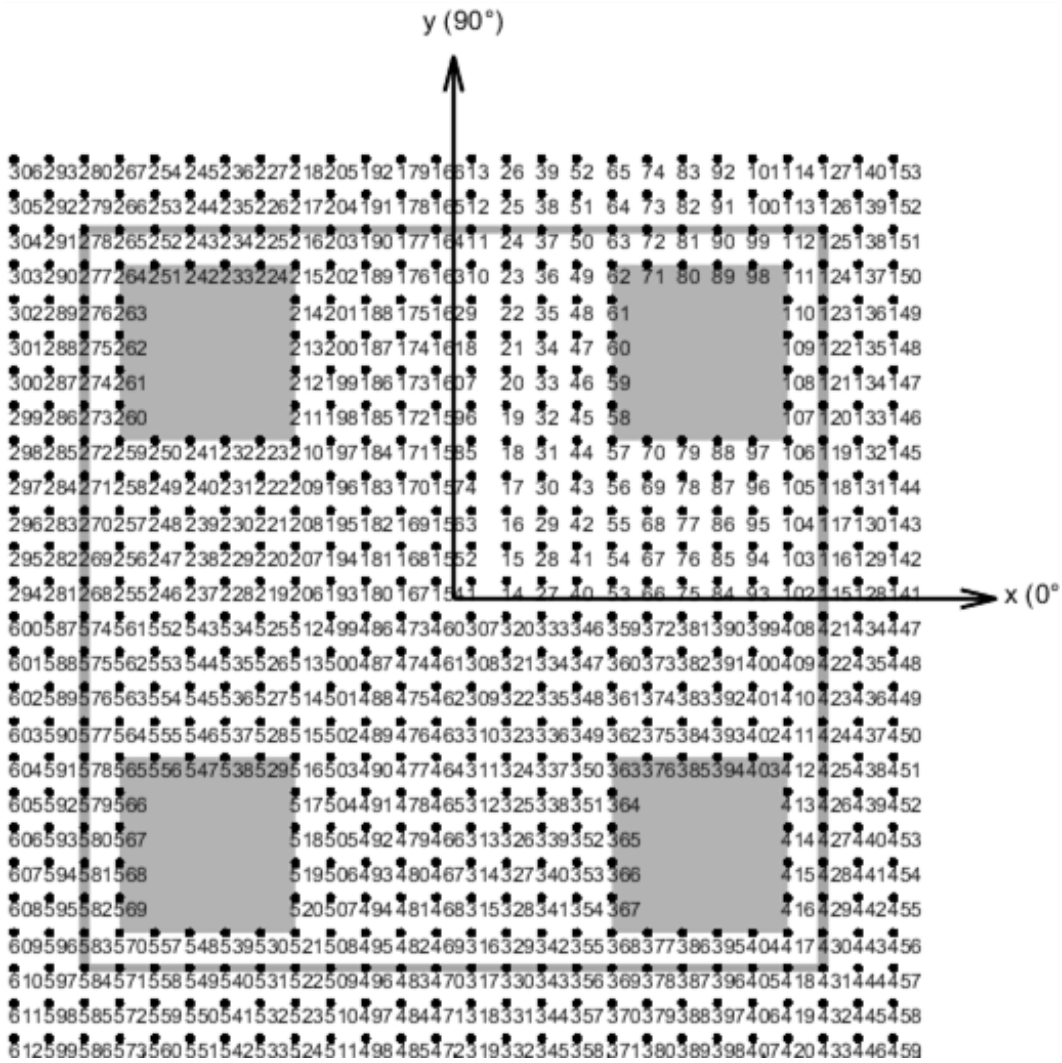

Figure 11: *WAMIT directions with respect to the surge and sway axes and each point number*

Is was therefore necessary to do the two corresponding adjustments for the directions: first, a suitable orientation for the platform was found with the aid of figure 10. Second, once with the deck oriented, the NORA10 directions were converted into WAMIT directions for each of the analyses performed. The wind rose shows that the resolution of the NORA10 directions is also discretized, so although it is difficult to tell exactly where the storm with the highest waves come from, it is clear that they come somewhere from the West and slightly from the South. To stick to the WAMIT convention, the rotation angle was chosen to be a multiple of 22.5; that is, 202.5 degrees.

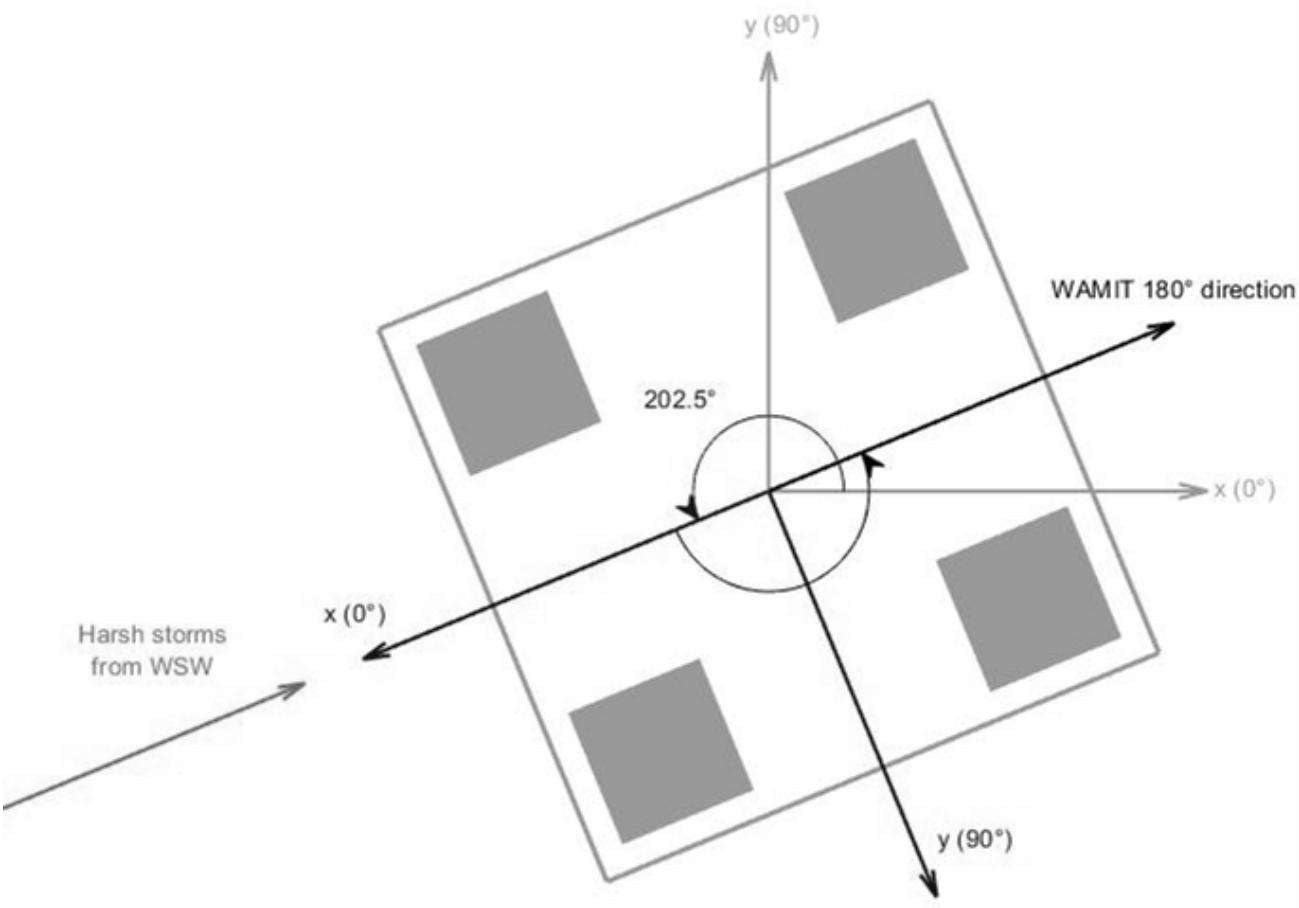

Figure 12: *NORA10 vs WAMIT with the proper orientation of the structure*

Lastly, as figure 11 shows, each modelled point has its exact location and number. Thus the rotation implies that each point is rotated as well. On top of that, It is known that some of the points for which the wave RAOs were modelled lay outside of the deck, meaning that they are not under it and that the critical point for the airgap assessment couldn't be one of these. Below, the deck area is shown with some of its rotated point numbers and with the box that sets the deck edges. It should be noticed that the axes labels express the dimensions of the deck, in meters.

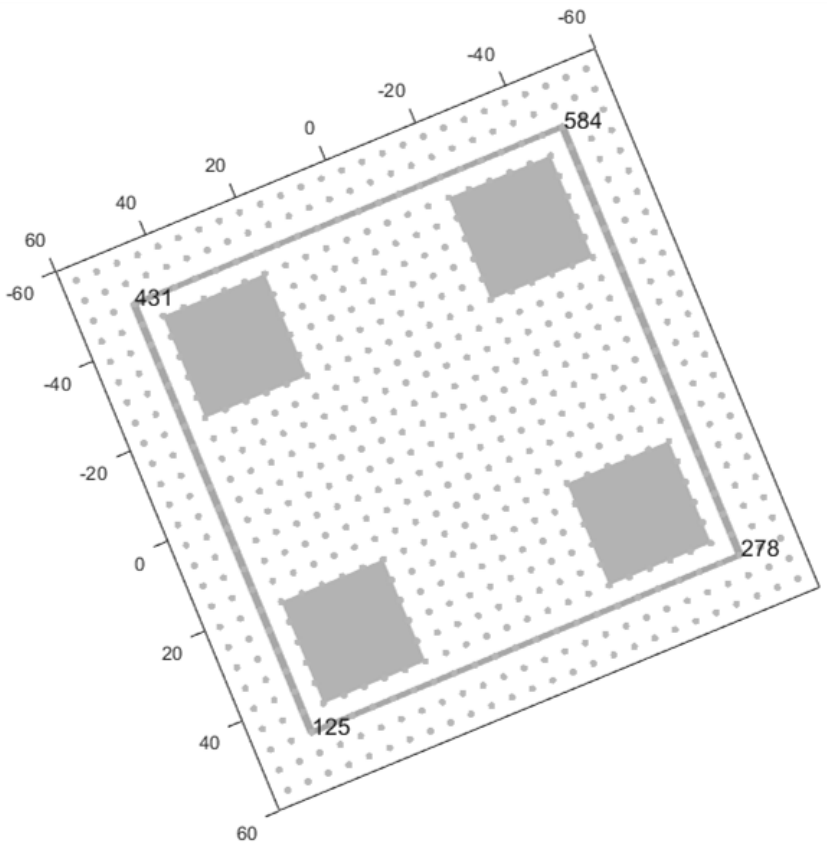

Figure 13: *Oriented deck with some of the critical points shown as well as the deck boundary.*

WAVES AND SEA STATE MODELLING

As mentioned above, only the wind seas are taken into account for this thesis; considering that the swell sea would virtually not contribute to higher relative wave crests. However, the following assumptions are made, which lean slightly to the conservative side

- **Long crested waves** The real waves in the sea are far from long crested, they are chaotic, and their modelling can become extremely complex. Intuitively, a short-crested sea could be worst for floater motions and consequently for relative wave crests, given that a short-crested wave can induce a motion around the axis parallel the wave direction. For example, a wave with a direction from forward to aft (180 degrees WAMIT in the present case) would not induce roll on the floater, but it could in the case of a short-crested sea. Contrary to intuition, Kurian et al.[8] showed that considering infinitely long crests is actually -if any- slightly conservative. long crested waves are considered for this assessment.

[8] Kurian, V.J. Ng, C.Y., & M.S, Liew. (2012)

- **Asymmetry factor** For a given wave, the distance from the mean water level (MWL) to the crest is larger than the distance to its trough, as shown in figure 5. This means that the relative surface elevations are actually higher that what the case would be with, say, sinusoidal waves. The approach to fix this is by multiplying the relative surface elevation by a so-called asymmetry factor, which essentially is the ratio of the MWL to crest for a real wave to the MWL to crest for a linear ('sinusoidal') wave. For the design of a semisubmersible it is accepted to consider an asymmetry factor of 1.2 for all the points under the deck[9].
- **Runup** The vertical forces acting on the underside of the deck from the runup of water along the columns are not significant compared the forces of the true waves (decks are designed to withstand runup forces) and they are vertical, thus it would not contribute to the negative effects of wave to deck impact mentioned in the introduction. The extra relative surface elevation near the columns due to runup is not part of this analysis and is not considered relevant for it.
- **Ergodic , stationary and linear surface process[10]** The models adopted for the sea surface process imply that the wave profiles are linear (Gaussian), with the probability density function of the surface elevation at a point and time being described by the Gaussian distribution

$$f_{\Xi}(\xi) = \frac{1}{\sqrt{2\pi}\sigma_{\Xi}} exp\left\{-0.5\left(\frac{\xi}{\sigma_{\Xi}}\right)^2\right\} \quad (\mathbf{3})$$

  here $\boldsymbol{\sigma_{\Xi}}$ is the standard deviation of the surface process. In other words, the profile of the waves looks like a sine function instead of the stokes 5th profile (reference again to figure 5). Ergodicity means that the mean and standard deviation of the surface elevation process over a time window of a particular duration would tend to be the same for a sea state within a different time window of the same duration. The stationarity of the process is a condition for the ergodicity and is the implication of the characteristics of the sea remaining constant over time: there is not a trend for higher, lower, steeper or flatter seas over the years.

- **Independent events** A response, or a wave elevation is not related to the previous one. This could also, if any, be slightly conservative if the responses were estimated for a design wave elevation process -a series of random waves-.

[9] DNV GL: OTG-13 (2017)
[10] Haver, S. (2018)

- **3-hour sea states** The sea parameters are typically expressed in terms of a significant wave height and peak period for time intervals of 20 min to 3 hours. The sea states for this work represent 3-hour periods where the significant wave height is 4 times the standard deviation of the surface elevation process expressed in equation (2) (previously, the definition of H_s was the average of the highest third of the waves).

POT AND STORM DEFINITIONS

For the Peak-Over-Threshold method storms are defined as adjacent sea states whose significant wave height exceeds the threshold, but an interval where the H_s are lower than the threshold is admitted so that two storms are merged when this interval does not exceed a certain time. 12 hours in between were thought to be a reasonable duration in between for considering only one storm instead of two, this is well illustrated in the figure below.

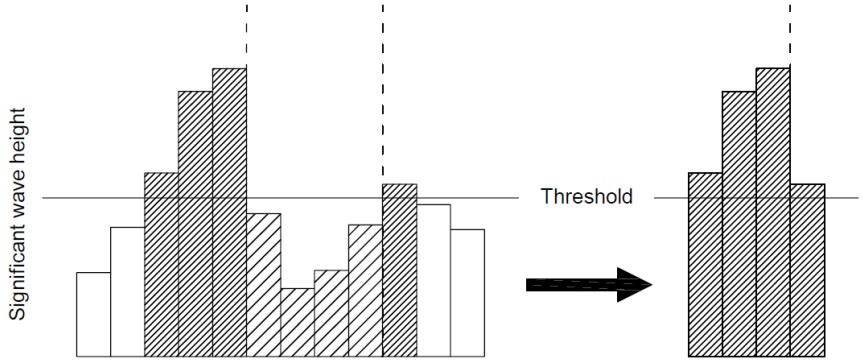

Figure 14: *Example of two 'storms' -with a threshold of 7 m- being merged due to no more than 12 hours in between.*

DESIGN REQUIREMENTS

For the Norwegian continental shelf, two rules regimes exist: the NORSOK standards and the Maritime Regulations by the Norwegian Marine Directorate. For floating installations operating during a limited time (a stage of the project, e.g. a semi that is used only for drilling) the Maritime Regulations require the initial airgap to be large enough so that a wave to deck impact, excluding runup, has a 10^{-2} annual probability of occurrence, which corresponds to the Ultimate Limit State design (ULS). The NORSOK standards also require the initial airgap to be large enough so that such impact has a 10^{-4} annual probability, which corresponds to the Accidental Limit State design (ALS). Both requirements were considered for the present airgap assessment.

MODELLING

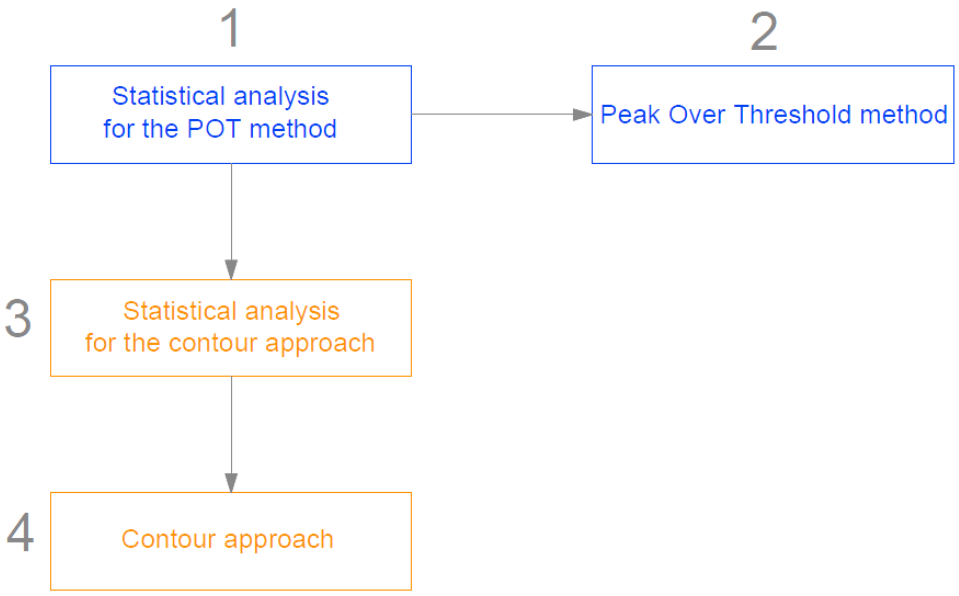
1
Statistical analysis
for the POT method
2
Peak Over Threshold method
3
Statistical analysis
for the contour approach
4
Contour approach

1. Statistical analysis for the POT method

1.1. Definition of case parameters

The Peak-Over-Threshold method for analysing a response process involves the selection of a threshold and the H_s values over the threshold are looked at as storms, as shown in figure 1.1. The responses for the different storms are modelled to estimate extreme values of the response quantities of interest. The sea surface elevation relative to the waterline of the semisubmersible is not a response in itself, but it is analogous when the proper transformations are performed. The responses of the floater are how it moves with respect to a particular wave height, wave period, and direction; they are to be computed for every point under the deck.

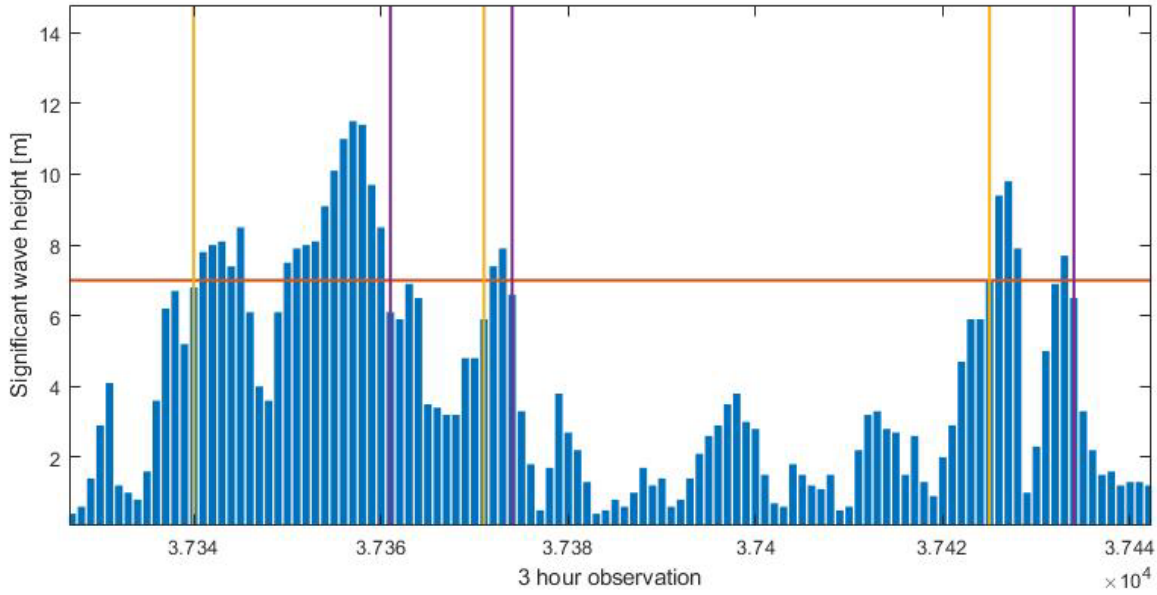

***Figure 1.1**: An example of three storms identified over the period of two weeks when the threshold is 7 m*

Different thresholds are to be compared. Lowering the threshold to around 6 m has previously resulted in the most accurate outcomes, but it is of interest to find the maximum threshold value that yields consistent results. One of the main reasons to use a higher values is that the computations with

lower thresholds, when managing large amounts of data, turn to be very expensive. The computational time required for the POT method is proportional to the number of storms (Table 1.1). and points to be analysed. For the present numerical analyses, the quantity of points remains constant with 612. Commonly, values from 6 to 10 m have been used as threshold values, but there is evidence on 6 to 7 m being the best margin when the data elements represent 3-hour sea states in the northern north sea[11].

***Table 1.1**: Threshold value vs number of storms*

	Threshold		
	6	7	8
Number of storms	797	456	259

As explained in the problem setup, the peak periods were corrected and all data elements corresponding to a significant wave height of less than 0.4 m were sorted out. This required a correction for the original number of 3-hour events in a year $N_{1y,0}$, which is a critical value for estimating annual probabilities of exceedance.

$$N_{1y,0} = (number\ of\ 3\ hour\ events\ in\ a\ day)\ \times 365 = 2{,}920$$

With the small values of H_s sorted out, the size of the data set (3-hour evens) reduces from 178,725 to 133,176. But the length of the 'measurement' period remains the same (22,341.125 days from September 1 of 1957 till October 31 of 2018). So $N_{1y,0}$ was scaled to

$$N_{1y} = N_{1y,0}\left(\frac{133{,}176}{178{,}725}\right) = 2{,}175.8 \tag{1.1}$$

Later, setting a threshold would rescale N_{1y} due to only the values larger than the threshold being taken:

$$N_{1y}^{*} = N_{1y}\left(\frac{N^{*}}{N}\right) \tag{1.2}$$

where (N^{*}/N) is the ratio of the number of 3-hour events over the threshold to the total number of 3-hour events. For the analysis of the storm peaks only, N^{*} is the total number of storm peaks over during the 61 years (N_{1y}^{*} becomes the number of storms per year).

[11] Patiño, J. (2018)

For the wind sea states, two versions of the POT method were used:

1. For each point, the responses were analysed for each storm considering each of its 3-hour steps and the corresponding direction of the step.
2. For each point, the responses were analysed only for the step with the highest significant wave height of each storm and its corresponding peak period. In the case of the highest H_s value being repeated multiple times within a particular storm, The T_p value and direction taken were the ones corresponding to the step with the lowest T_p, fairly assuming that the steepest sea states produce more higher relative elevations.

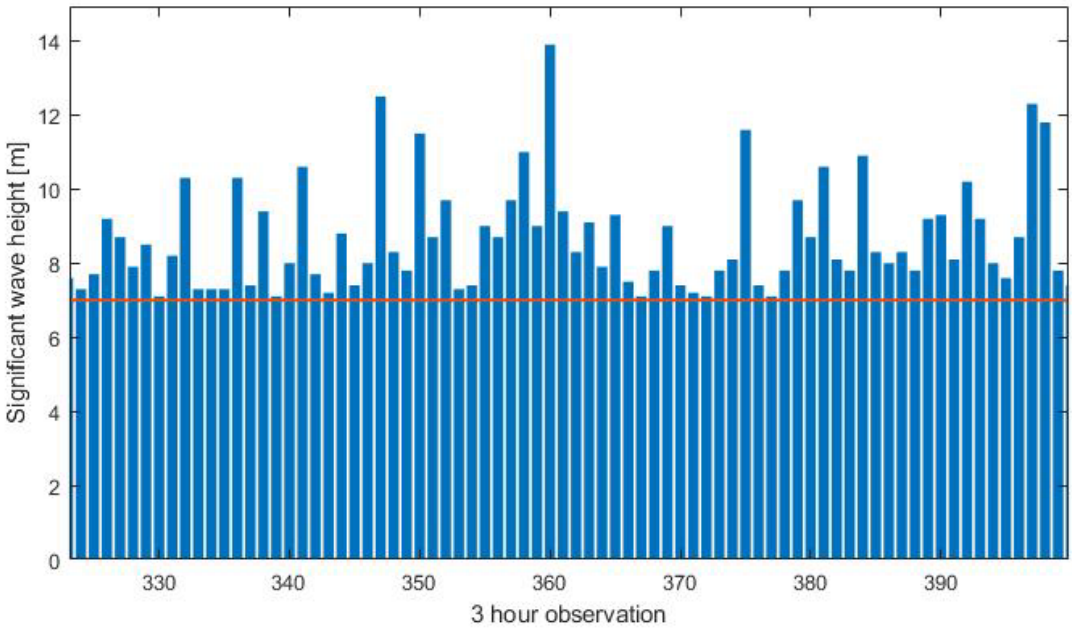

***Figure 1.2**: For the second version of the POT method, only the storm maxima were analysed.*

DIFFERENT FORMS OF THE WEIBULL DISTRIBUTION

In chapters 2 and 3 respectively, the 3-parameter Weibull distribution is implemented for modelling the computed relative surface elevations for every storm and for modelling the distribution of H_s

$$F(H_s) = 1 - exp\left\{-\left(\frac{H_s - \lambda}{\alpha}\right)^{\beta}\right\} \tag{1.3}$$

with λ being the location parameter, α the scale parameter, and β the shape parameter.

The method used to estimate the parameters of the distribution is well explained in chapter 2, when it was firstly implemented. For the distribution of H_s in chapter 3, three versions were studied, but for this work, the results were computed using the standard 3-parameter distribution as it has been done traditionally for modelling the 3-hour significant wave heights. A comparison is shown further on.

1st variation: 2-paremeter distribution for $H_s - T$

The 2-paremeter Weibull distribution does not include a location parameter, so it's always zero. Here, the scale and shape parameters are obtained after the value of the threshold, T, is subtracted from every value of H_s and then the equation becomes

$$F(H_s) = 1 - exp\left\{-\left(\frac{H_s^* - T}{\alpha}\right)^{\beta}\right\} \tag{1.4}$$

where α and β are obtained for the 2-parameter distribution and $H_s^* = H_s - T$, for every value of H_s

2nd variation: 3-paremeter distribution with artificial λ

Here, α and β are estimated for the 3-parameter distribution and the location parameter is forced to be the threshold.

$$F(H_s) = 1 - exp\left\{-\left(\frac{H_s - T}{\alpha}\right)^{\beta}\right\} \tag{1.5}$$

1.2. Data manipulation

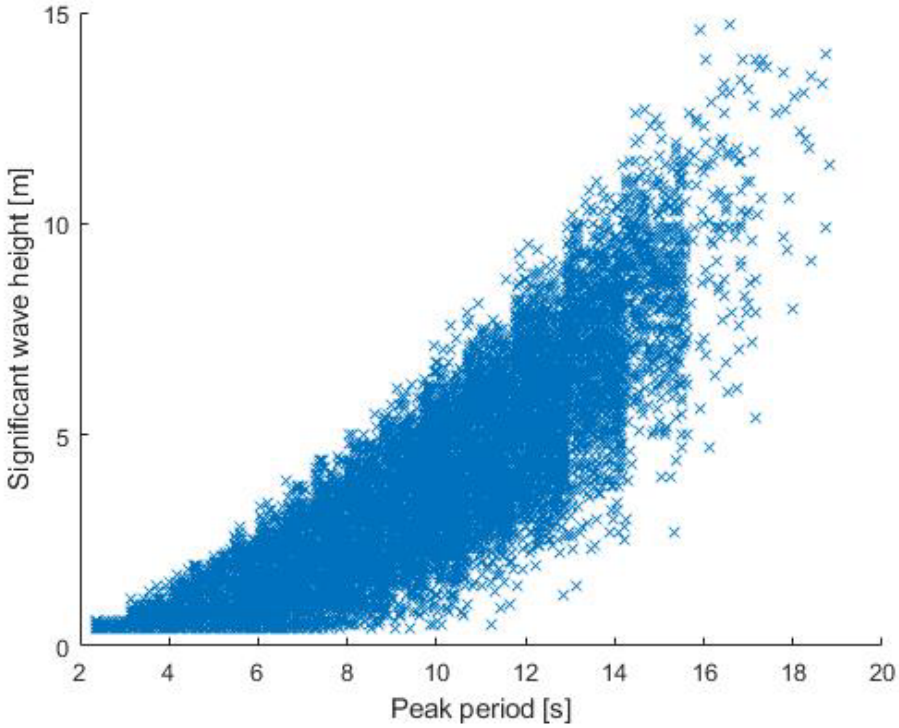

***Figure 1.3**: Scatter plot of H_s vs T_p after corrections*

Previously, many H_s values were very close to zero (see the empty gap in figure 1.3) and the values of T_p had a poor resolution. Additionally, the POT analysis considers a number of storms based on the threshold and the criterium for the tolerance of 12 hours in between -with the storms being merged in this case-. All the H_s in between that are lower than the threshold are left out.

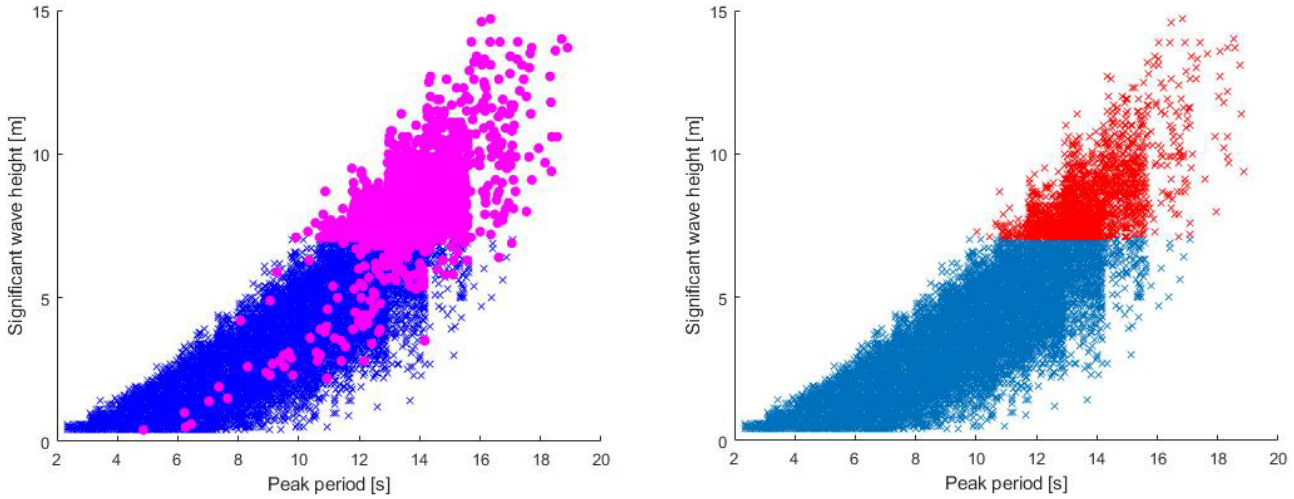

***Figure 1.4**: Storm (H_s, T_p) pairs with a threshold of 7 m.*
Before and after removing the values between the merged storms.

From setting the threshold and establishing the POT version (analysis of all storm steps vs analysis of the storm peaks) three matrices were created as inputs for the subsequent computations, where, for m storms and n steps, the indexes represent the i^{th} storm and the j^{th} step (with empty values where there are no j^{th} steps):

$$H_sH_s = \begin{bmatrix} H_s(i_1,j_1) & H_s(i_1,j_2) & \dots & H_s(i_1,j_n) \\ \vdots & \vdots & \vdots & \vdots \\ H_s(i_m,j_1) & \dots & \dots & H_s(i_m,j_n) \end{bmatrix} \tag{1.6}$$

$$T_pT_p = \begin{bmatrix} T_p(i_1,j_1) & T_p(i_1,j_2) & \dots & T_p(i_1,j_n) \\ \vdots & \vdots & \vdots & \vdots \\ T_p(i_m,j_1) & \dots & \dots & T_p(i_m,j_n) \end{bmatrix} \tag{1.7}$$

$$\theta_0 = \begin{bmatrix} \theta_0(i_1,j_1) & \theta_0(i_1,j_2) & \dots & \theta_0(i_1,j_n) \\ \vdots & \vdots & \vdots & \vdots \\ \theta_0(i_m,j_1) & \dots & \dots & \theta_0(i_m,j_n) \end{bmatrix} \tag{1.8}$$

with θ being the NORA10 direction and in the case analysing the storm peaks the number of steps becomes one. The NORA10 to WAMIT conversion is explained further on.

2. Minimum airgap with the Peak-Over-Threshold method

2.1. Directional transformation

NORA10 follows a meteorological convention where the directions represent where the waves come from. The response properties of the semisubmersible are given in a different format where the directions point to where the waves are going (WAMIT). Apart from this, the 0° direction is oriented differently in both cases. In the next page is a diagram (figure 2.1) illustrating the transformations: from the statistical analyses performed in chapter 2, to the response analyses performed in this chapter. According to the orientation of the platform discussed in the problem setup.

The transformation from NORA10 to WAMIT is as follows:

- The resolution of the NORA10 directions consists on 37 different directions, as shown with the small arrows in the diagram. And the number of directions for which the response properties of the floater were obtained is 16, these are multiples of 22.5°. Therefore, any direction of an incoming wave (WAMIT) could be rounded to the nearest multiple of 22.5° and all directions that would be rounded to that multiple would fit into the same sector. A WAMIT sector for that direction.
- Having oriented the platform in a way that the x axis (WAMIT) faces the worst storms (as in figure 10 of the problem setup) and looking at the NORA10 arrows at the same time, it was easy to assign a WAMIT direction to each NORA10 direction. The conversions are written in table 2.1

NORA10	WAMIT sector
350° 351° 6°	67.5°
20° 21°	45°
36° 50° 51°	22.5°
66°	0/360°
80° 81° 96°	337.5°
110° 111°	315°
126° 140° 141°	292.5°
156°	270°
170° 171° 186°	247.5
200° 201°	225°
216° 223° 230° 231°	202.5°
246°	180°
260° 261° 276°	157.5°
290° 291°	135°
306° 320° 321°	112.5°
336°	90°

Table 2.1

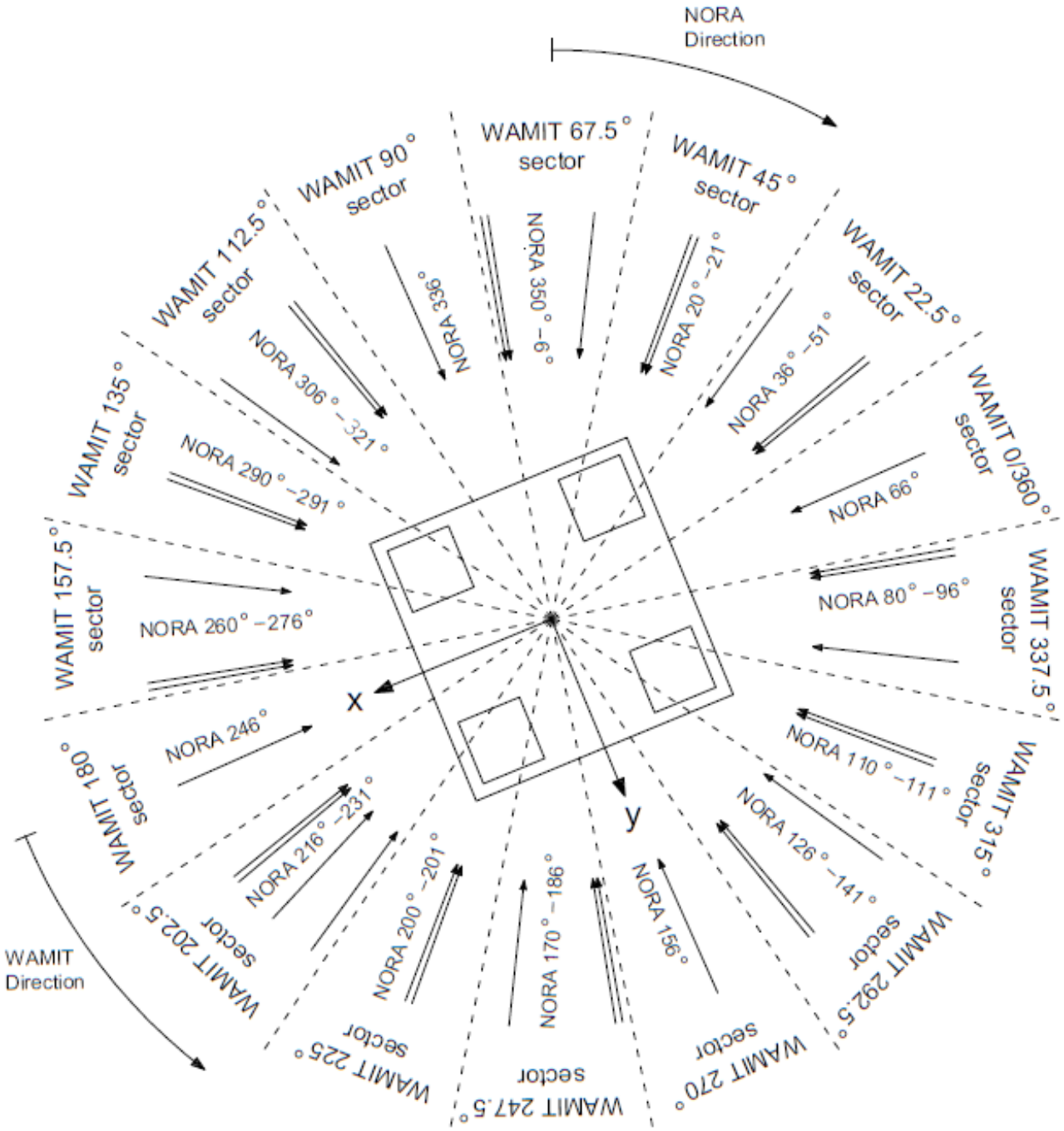

***Figure 2.1**: NORA10 to WAMIT*

2.2. The JONSWAP spectrum

Developed during the 70s, the JONSWAP spectrum was proposed by Hasselmann et al. as an extension of the Pierson-Moskowits spectrum -which considers a fully developed sea- with the idea of including a peak enhancement factor as a consideration of the developing sea. A wave spectrum represents the wave energy as a function of frequency, for a given sea state. For all combination of H_s and T_p with a significant wave height above the threshold, or for all storm peaks in the case of the analysis of the such only, the wave spectrum -which is the most suitable for the northern North Sea- reads

$$S_J(\omega) = A_\gamma S_{PM}(\omega)\gamma^{exp\left\{-0.5\left(\frac{\omega-\omega_p}{\sigma\omega_p}\right)^2\right\}} \tag{2.1}$$

with ω being the wave frequency, as a function of the wave period:

$$\omega = \frac{2\pi}{T} \tag{2.2}$$

thus, the peak frequency is $\omega_p = 2\pi/T_p$

γ is the non-dimensional peak shape parameter

σ is the spectral width parameter

$$\sigma = 0.07 \quad \text{for} \quad \omega \leq \omega_p$$

$$\sigma = 0.09 \quad \text{for} \quad \omega > \omega_p$$

$A_\gamma = 1 - 0.287\ln(\gamma)$ is a normalizing factor

and S_{PM} is the Pierson-Moskowits spectrum

$$S_{PM} = \frac{5}{16}H_s^2\omega_p^4\omega^{-5}exp\left\{-\frac{5}{4}\left(\frac{\omega}{\omega_p}\right)^{-4}\right\} \tag{2.3}$$

r every storm i and every step j, them, a JONSWAP spectrum was computed: $S_J(i,j)$

similarly, a peak shape parameter $\gamma(i,j)$:

being

$$\gamma = 5 \qquad \text{for} \qquad \frac{T_p}{\sqrt{H_s}} \leq 3.6$$

$$\gamma = exp\left\{5.75 - 1.15\frac{T_p}{\sqrt{H_s}}\right\} \qquad \text{for} \qquad 3.6 < \frac{T_p}{\sqrt{H_s}} < 5$$

$$\gamma = 1 \qquad \text{for} \qquad 5 \leq \frac{T_p}{\sqrt{H_s}}$$

Although swell waves are not considered, the wave spectra of wind and swell can be summed together to get the spectrum of the total sea.

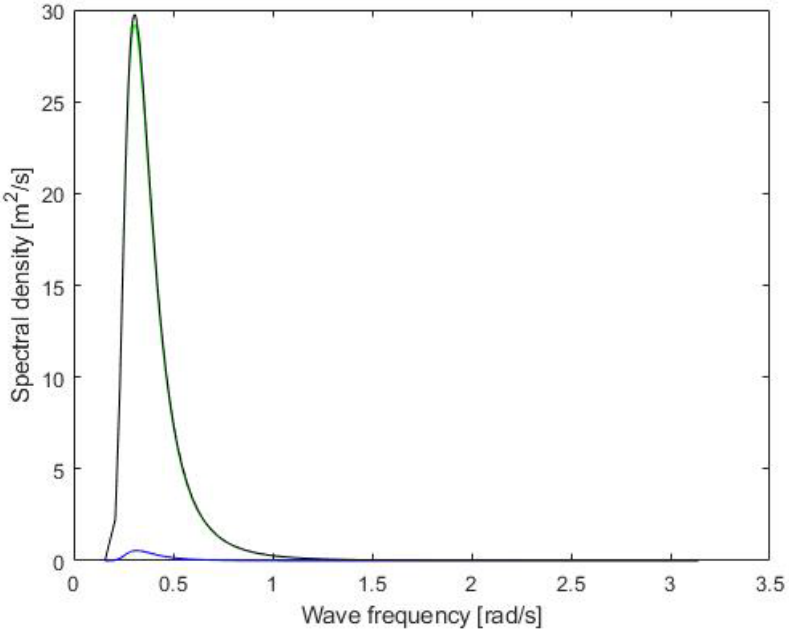

Figure 2.2: *JONSWAP spectrum for a wind sea with a significant wave height of 10 m and a peak period of 20.5 s and a swell sea with a significant wave height of 1.4 and a peak period of 19.8 s.*

2.3. Transfer functions: Rigid body and disturbed wave field

The rigid body transfer functions of the semisubmersible had been prepared before this work for the centre of the underside of the deck (for 57 values in the time domain). The Response Amplitude Operator (RAO) for a degree of freedom and a wave direction describes the magnitude of the amplitude of the floater motion in that degree of freedom and that direction compared to the amplitude of the incoming waves, for different wave periods/frequencies. For an airgap assessment, the surge, sway and yaw motions would not have a significant effect on the relative surface elevation, thus they are not analysed. For roll and pitch, the RAOs describe the ratio of angle or rotation to wave amplitude. Beside the RAOs, the phase angles are important. These are computed with the real and the imaginary part of the transfer functions:

For the heave motion, the rigid body transfer function at the centre of the deck is

$$h_z(\omega) = Re[h_z(\omega)] + Im[h_z(\omega)] \tag{2.4}$$

$Re[\ ]$ is the real part and $Im[\ ]$ the imaginary part

the RAO for this motion becomes

$$|h_z(\omega)| = \sqrt{(Re[h_z(\omega)])^2 + (Im[h_z(\omega)])^2} \tag{2.5}$$

the phase shift, in radians, is

$$\phi = \tan^{-1}\left(\frac{Im[h_z(\omega)]}{Re[h_z(\omega)]}\right) \tag{2.6}$$

and similarly for roll and pitch

Below, the transfer functions for the centre of the deck are shown. Plotted in the time domain (as they were given)

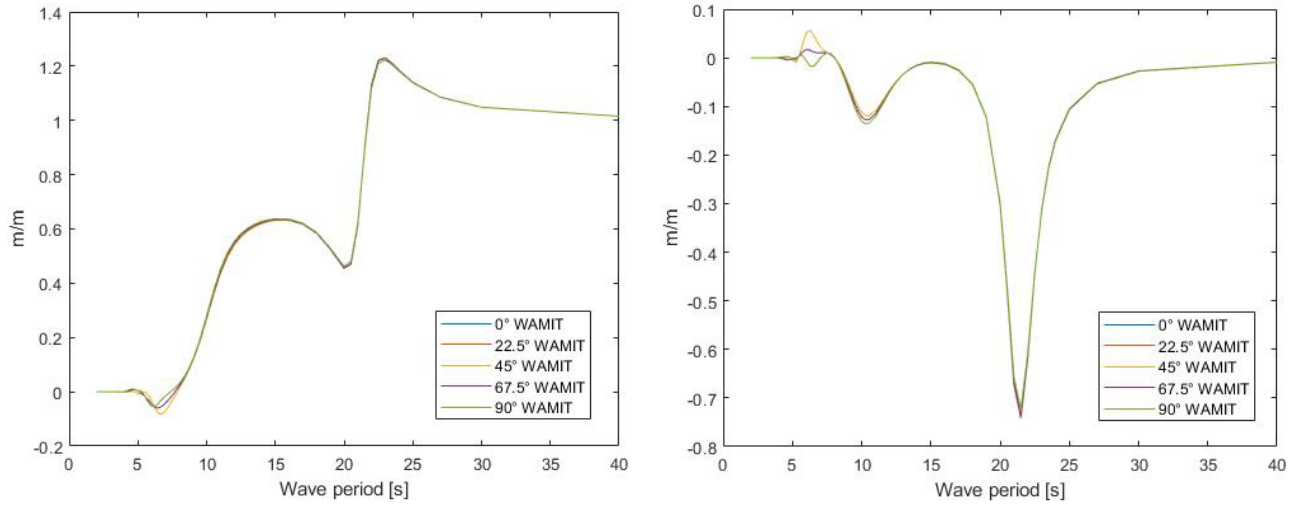

Figure 2.3: *Real and imaginary part of the rigid body transfer function for heave. (Plotted in time domain)*

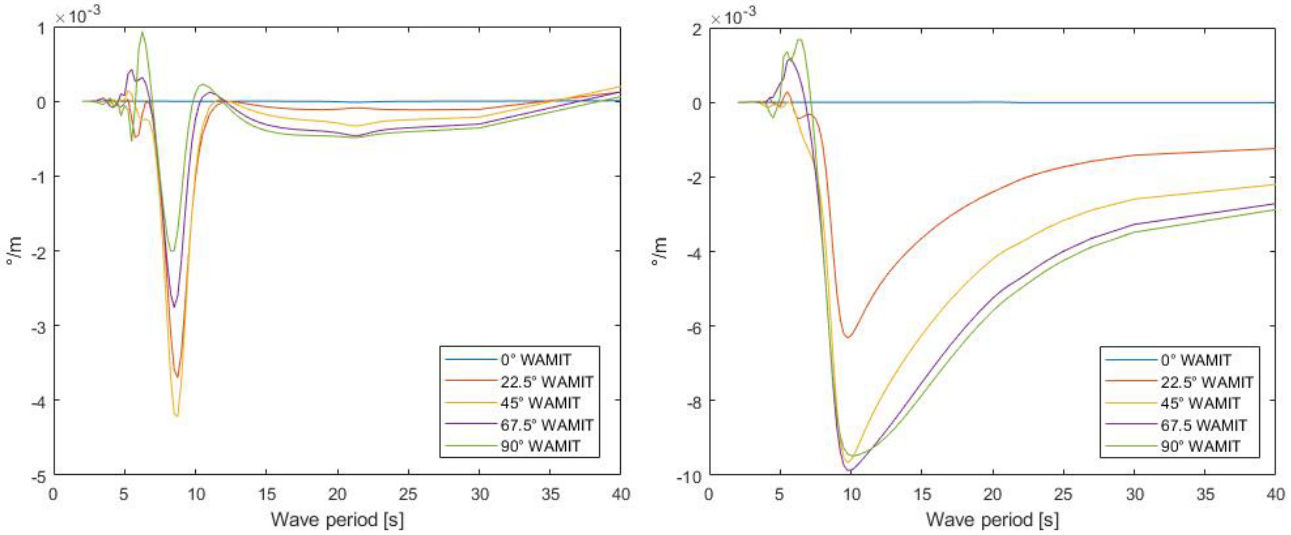

Figure 2.4: *Real and imaginary part of the rigid body transfer function for roll. (Plotted in time domain)*

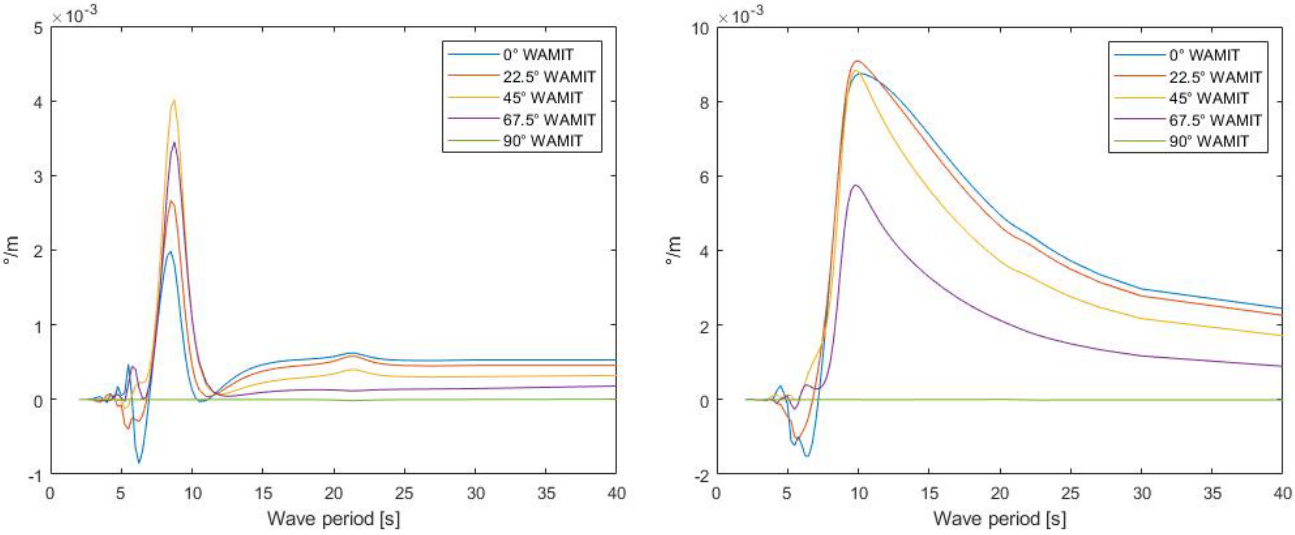

Figure 2.5: *Real and imaginary part of the rigid body transfer function for pitch. (Plotted in time domain)*

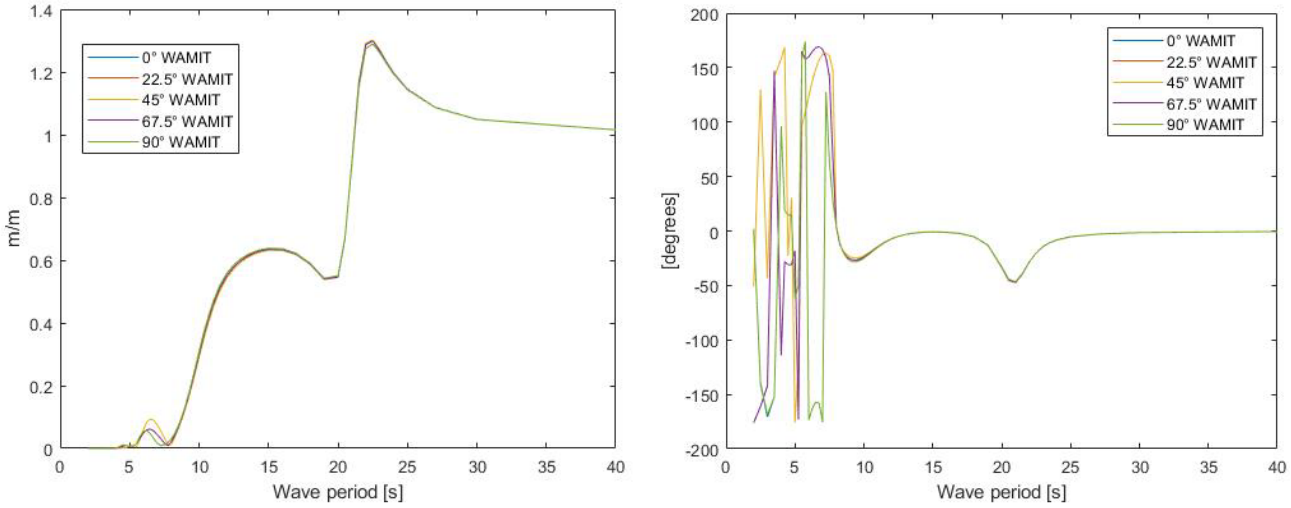

Figure 2.6: *Heave RAO and phase shift. (Plotted in time domain)*

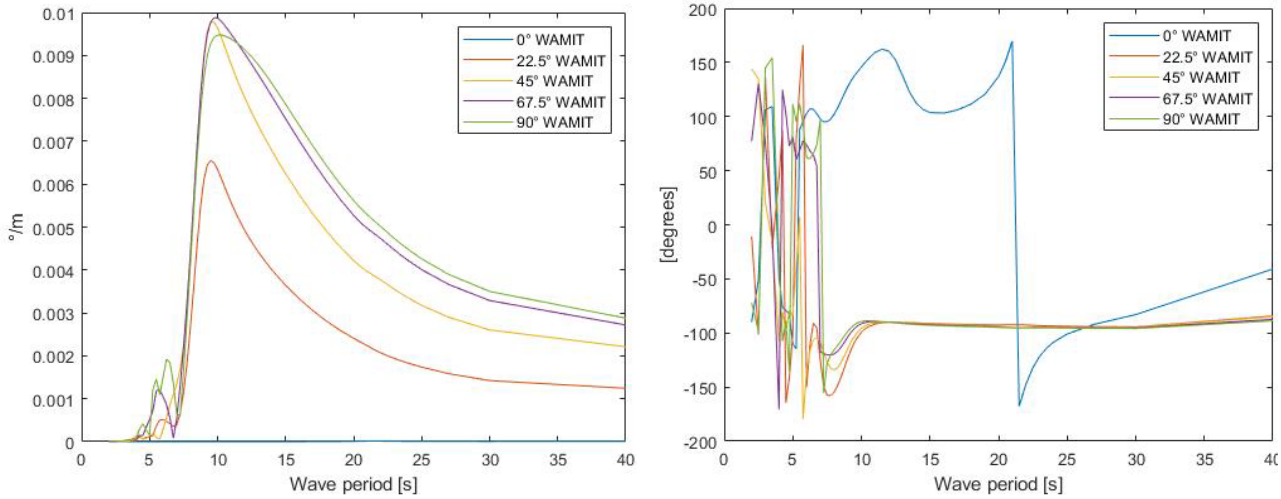

Figure 2.7: *Roll RAO and phase shift. (Plotted in time domain)*

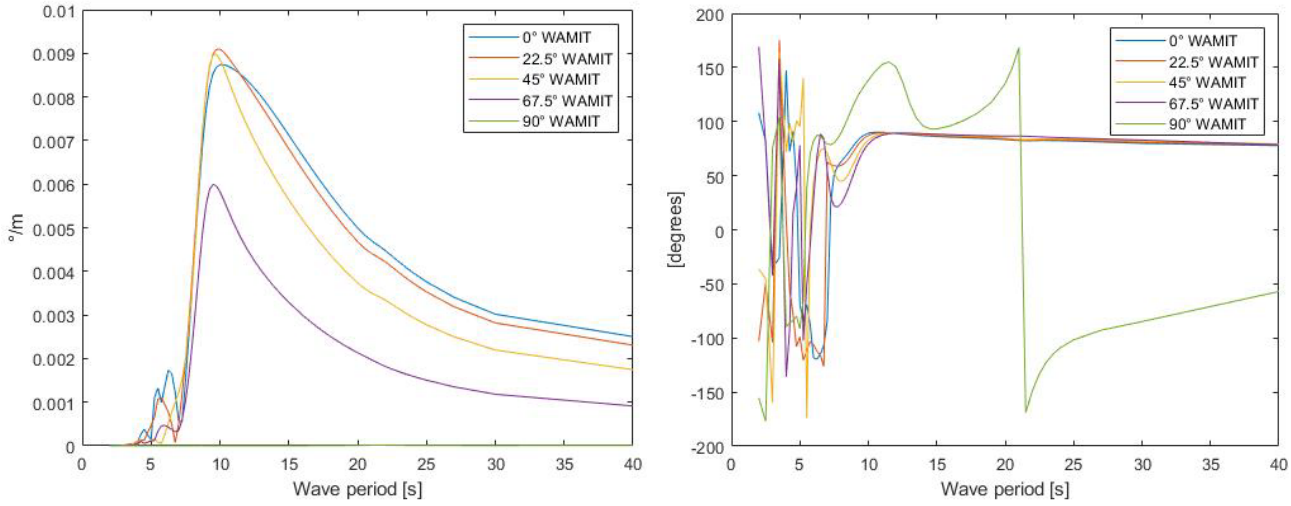

Figure 2.8: *Pitch RAO and phase shift. (Plotted in time domain)*

The heave displacements are affected by the roll and pitch motions and their influence increases outwards from the centre of the platform. By knowing the roll and pitch transfer functions and the coordinates x and y of each point p, it it possible to corrected RAOs accounting for these motions:

$$\left|h_{z,p}(\omega)\right| = \sqrt{\left(Re\left[h_{z,p}(\omega)\right]\right)^2 + \left(Im\left[h_{z,p}(\omega)\right]\right)^2} \tag{2.7}$$

where,

$$Re\left[h_{z,p}(\omega)\right] = Re[h_z(\omega)] + y\, Re\left[h_\phi(\omega)\right] - x\, Re[h_\theta(\omega)] \tag{2.7.1}$$

$$Im\left[h_{z,p}(\omega)\right] = Im[h_z(\omega)] + y\, Im\left[h_\phi(\omega)\right] - x\, Im[h_\theta(\omega)] \tag{2.7.2}$$

h_ϕ and h_θ denoting the roll and pitch transfer functions, respectively. And x and y being the distances from the centre, along those axes, to a particular point p.

Following are some examples of the corrected RAOs of the rigid body for points 115 and 431 with wave directions of 135° and 180° WAMIT plotted against the wave period, in seconds.

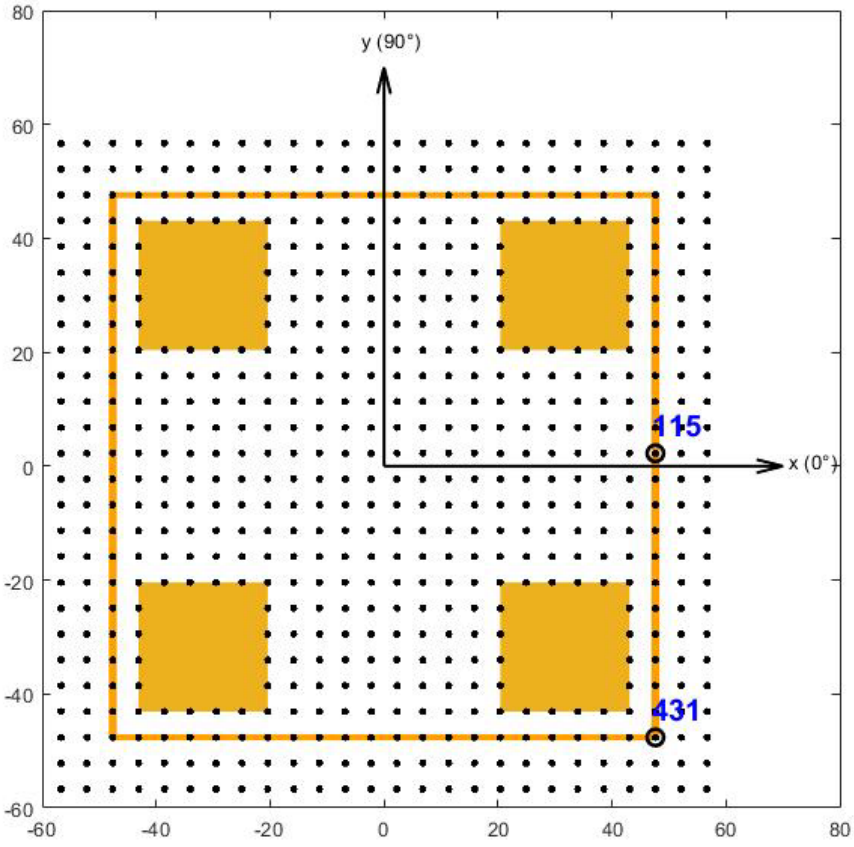

Figure 2.9: *Points 415 and 431*

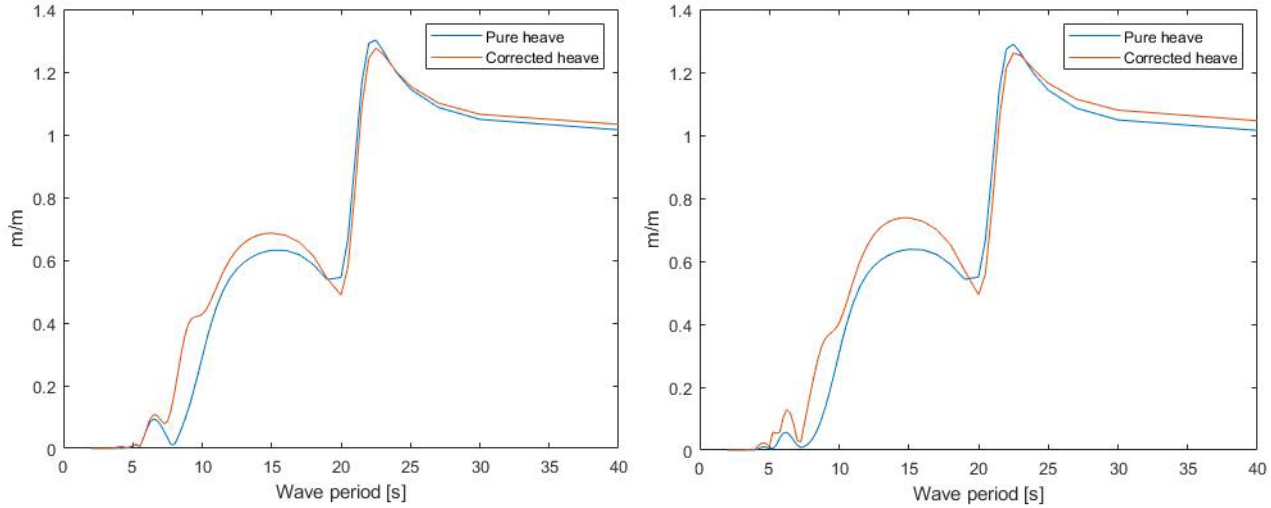

Figure 2.10: *Correction of heave RAO (accounting for roll and pitch) for point 115. On the left, for a wave direction of 135°. On the right, for a 180°. (Plotted in time domain)*

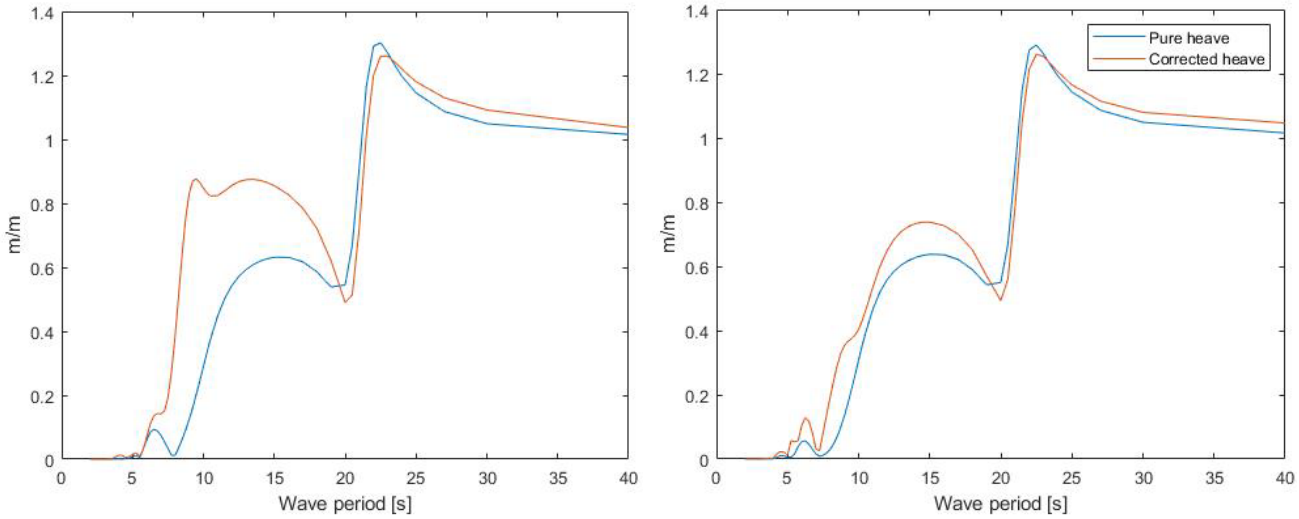

Figure 2.11: *Correction of heave RAO for point 431. On the left, for a wave direction of 135°. On the right, for a 180°. The RAO at 180° is virtually the same for as the corresponding RAO for point 115 in the image above. This is due to all pitch interaction and no roll interaction at 180° for both positions. (Plotted in time domain)*

The disturbances of the waves that occur under the deck due to the structure itself are as well dependent on both wave frequency and wave direction. Since this disturbances can be seen as changes in the surface elevation due to the structure they can as well be expressed as transfer functions where the RAOs are the ratios between the disturbed wave height to the undisturbed wave height (as if the structure was not there), but different -and computed- for each specific point under the deck.

$$h_{H,p}(\omega) = Re\left[h_{H,p}(\omega)\right] + Im\left[h_{H,p}(\omega)\right] \qquad 2.8$$

with the (wave) RAO for that specific point as

$$\left|h_{H,p}(\omega)\right| = \sqrt{\left(Re\left[h_{H,p}(\omega)\right]\right)^2 + \left(Im\left[h_{H,p}(\omega)\right]\right)^2} \qquad 2.9$$

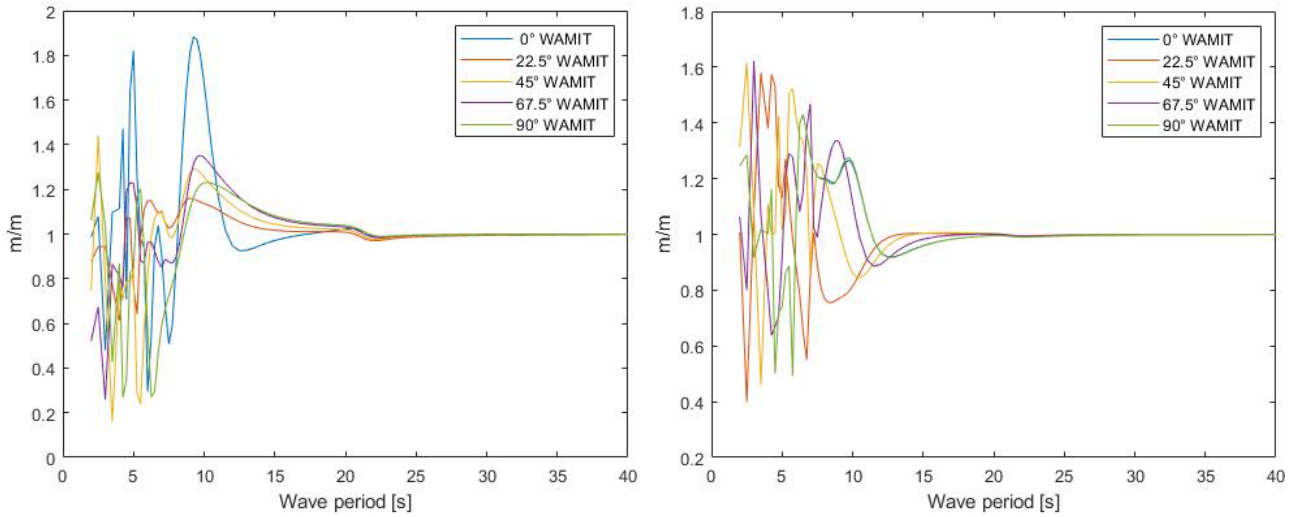

Figure 2.12: *Wave RAOs for different wave directions. On the left point for point 115, on the right for point 431. (Plotted in the time domain)*

2.3.1. RELATIVE SURFACE ELEVATION PROCESS

Por each point, the target function from the transfer functions is called the **Spectrum of the relative surface elevation process**, which is the product of the wave spectrum and the relative surface elevation process. It describes a measure, in the frequency domain, of how much the water surface moves vertically with respect to a point under the deck, for a given sea state. Like the wave spectra, the units are m^2/s and it can be superimposed for wind and swell seas.

$$\boldsymbol{S_{R,p} = \left|h_{R,p}(\omega)\right|^2 S_{\Xi}(\omega)} \qquad \boldsymbol{(2.10)}$$

where $S_{\Xi}(f)$ is the wave spectrum (the JONSWAP spectrum) and $h_{R,p}(f)$ is the Relative surface elevation process:

$$h_{R,p}(f) = Re\left[h_{R,p}(\omega)\right] + Im\left[h_{R,p}(\omega)\right] \qquad (2.11)$$

with

$$Re\left[h_{R,p}(\omega)\right] = \alpha\, Re\left[h_{H,p}(\omega)\right] - Re\left[h_{z,p}(\omega)\right] \qquad (2.11.1)$$

$$Im\left[h_{R,p}(\omega)\right] = \alpha\, Im\left[h_{H,p}(\omega)\right] - Im\left[h_{z,p}(\omega)\right] \qquad (2.11.2)$$

α is the asymmetry factor to correct for nonlinearities of the wave elevation. Taken as 1.2 for the whole platform[12] for the present assessment.

The modulus of the relative surface elevation process becomes

$$\left|h_{R,p}(\omega)\right| = \sqrt{\left(Re\left[h_{R,p}(\omega)\right]\right)^2 + \left(Im\left[h_{R,p}(\omega)\right]\right)^2} \tag{2.12}$$

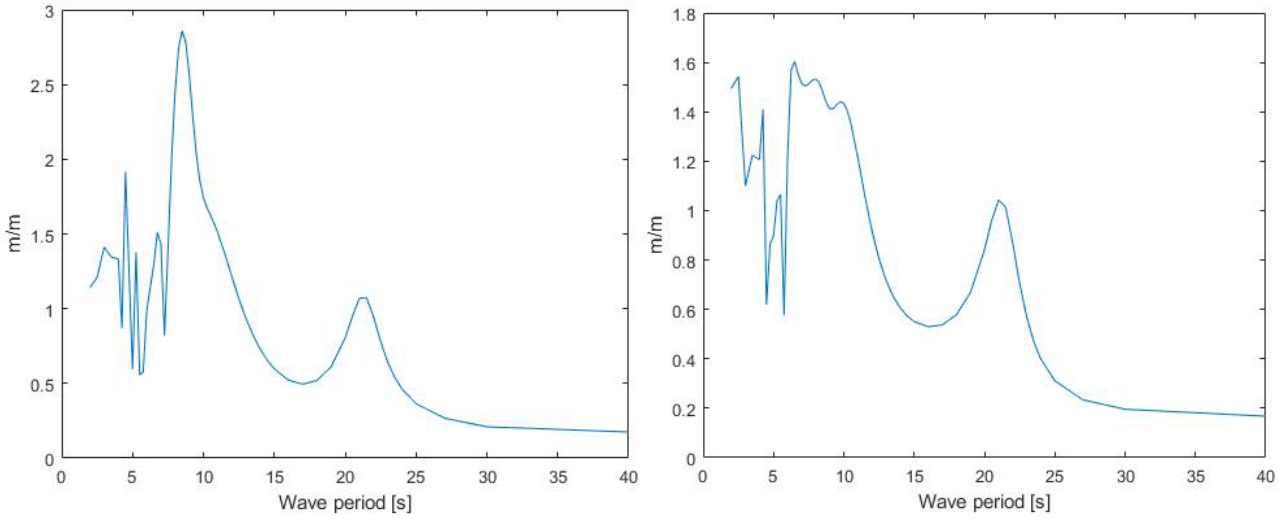

***Figure 2.13**: Relative surface elevation process for point 431. 135° and 180° WAMIT. (Plotted in the time domain)*

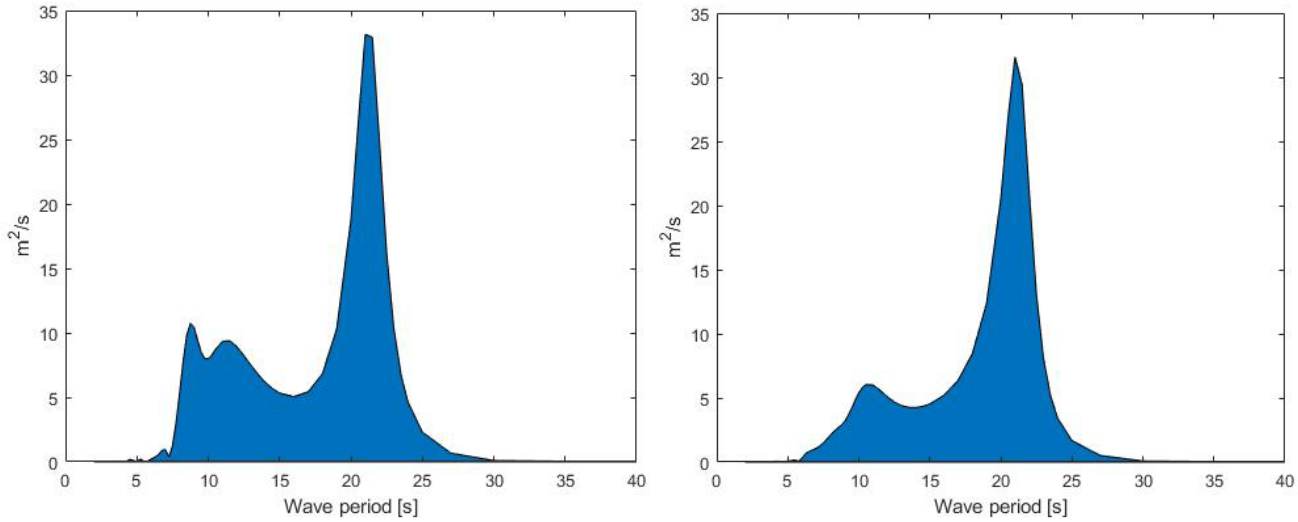

***Figure 2.14**: Spectrum of the relative surface elevation process. Point 431. For a sea with $H_s = 10\ m$ and $T_p = 20.5\ s$. 135° and 180° WAMIT. (Plotted in the time domain)*

[12] DNV GL: OTG-13 (2017)

The spectra of the relative surface elevation process was computed for 57 points in the time domain for all points under the deck, every storm step corresponding to each storm, and **the WAMIT direction of the corresponding 3-hour step**.

2.4. Exact distribution of the *storm maximum relative surface elevation* to get the *most probable maximum*

For a j^{th} 3-hour period within a storm, the maximum relative surface elevation under a point follows a probability density function. I.e. the maximum relative surface elevation in three hours. Its cumulative density function is the product of a Rayleigh distribution:

$$F_{R,j}(r) = \left[1 - exp\left\{-0.5\left(\frac{r}{\sigma_{R_p}}\right)^2\right\}\right]^{n_{3h}} \tag{2.13}$$

where the exponent n_{3h} is the expected number of zero up-crossings during the 3-hour event (the number of times that the surface moves vertically across the waterline). In other words, the Rayleigh distributions for each event where the relative surface is above the waterline are multiplied to obtain the cumulative density function of the maximum. σ_{R_p} is the variance of the spectrum of the relative surface elevation…

$$n_{3h} = \frac{10{,}800}{T_z} \tag{2.14}$$

T_z is the expected zero up-crossing period and it was computed for every step j of storm i and stored in the form

$$T_zT_z = \begin{bmatrix} T_z(i_1, j_1) & T_z(i_1, j_2) & \dots & T_z(i_1, j_n) \\ \vdots & \vdots & \vdots & \vdots \\ T_z(i_m, j_1) & \dots & \dots & T_z(i_m, j_n) \end{bmatrix} \tag{2.15}$$

Approximations were obtained from DNV-RP-C205: Environmental Conditions and Environmental Loads:

If

$$T_z = 2\pi\sqrt{\frac{M_0}{M_2}} \tag{2.16}$$

and

$$M_0 \cong \frac{1}{16}H_s^2 \tag{2.17}$$

$$M_2 \cong \frac{1}{16}H_s^2\omega_p^2\frac{11+\gamma}{5+\gamma} \tag{2.18}$$

with ω_p being the peak frequency, $\omega_p = 2\pi/T_p$, then

$$T_z(i,j) \cong \sqrt{\frac{[5+\gamma(i,j)]T_p^2(i,j)}{11+\gamma(i,j)}} \tag{2.19}$$

γ being peak shape parameter of the corresponding storm step and M_n the nth moment of the wave spectrum

$$M_n = \int_0^\infty \omega^n S_\Xi(\omega)d\omega \tag{2.10}$$

Knowing the distribution of the 3-hour maximum relative surface elevations for the steps, and following the same principle of multiplying the CDFs to obtain the distribution of the maximum, the distribution of the storm maximum relative surface elevation for storm i becomes the product of the distributions for maximum of the steps the steps:

$$F_{R,i}(r) = \prod_{j=1}^{n_j}\left[1 - exp\left\{-0.5\left(\frac{r}{\sigma_{R_{p,j}}}\right)^2\right\}\right]^{n_{3h,j}} \tag{2.20}$$

where n_j is the number of 3-hour steps

The variance of the spectrum of the relative surface elevation is the area under its curve and in order to calculate it exactly, the following numerical method was adopted:

$$\sigma_{R_p} = \sum_{n=1}^{56} E_n = \sum_{n=1}^{56} (\omega_{n+1} - \omega_n) \frac{S_R(\omega_n) + S_R(\omega_{n+1})}{2} \tag{2.21}$$

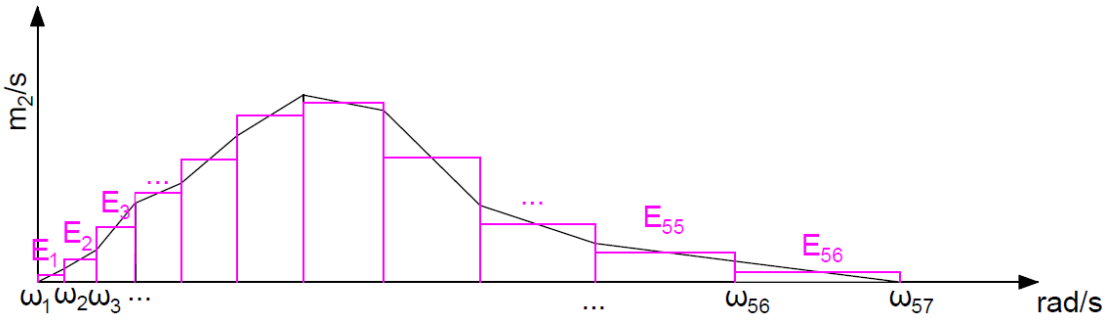

Figure 2.15: *Illustration the methodology to obtain the area under a spectrum*

The calculations are exact in the way the transfer functions are given (discrete and not strictly exact themselves, they were computed with a finite element analysis). At this point it is worth remembering that ω was used: $\omega = 2\pi/T$. Below, some examples of the variances for different sea states:

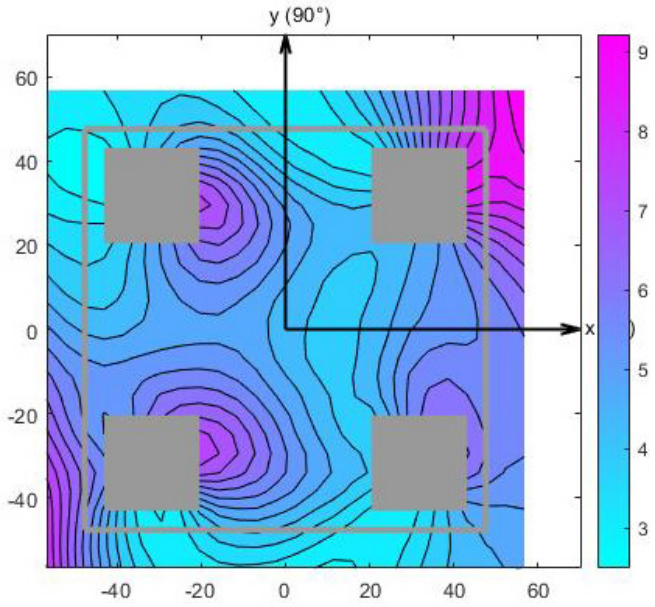

Figure 2.16: *Variance for H_s=8.1 m, T_p=13.3 s with 202.5°*

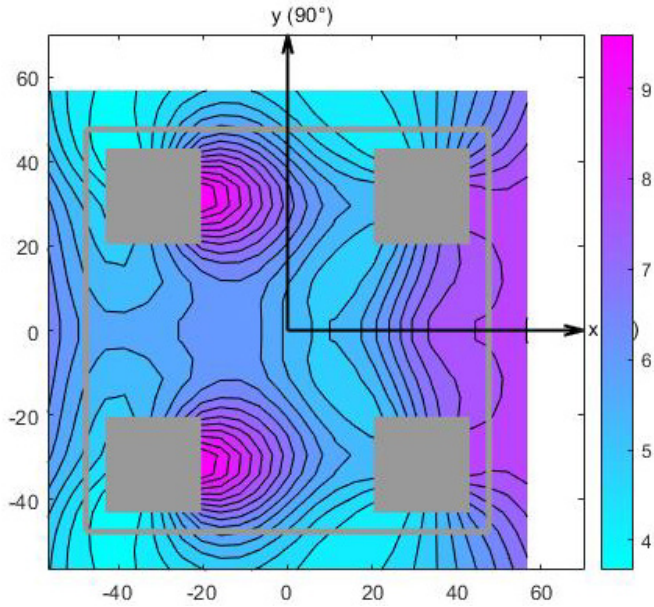

Figure 2.17: *Variance for H_s=11.5 m, T_p=16.1 s with 180°*

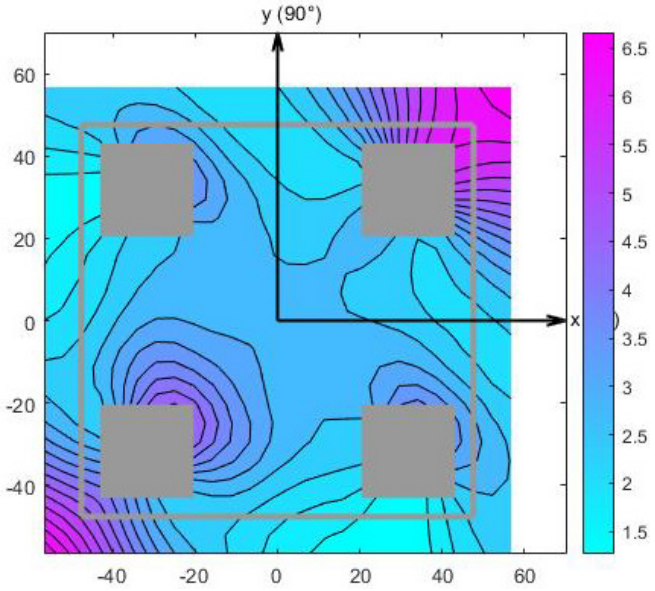

Figure 2.18: Variance for H_s=7 m, T_p=13.4 s with 222.5°

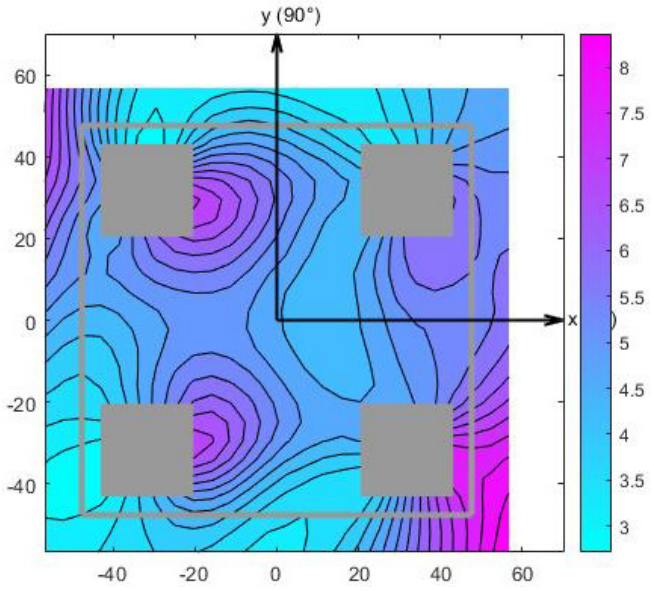

Figure 2.19: Variance for H_s=10.3 m, T_p=16.1 s with 157.5°

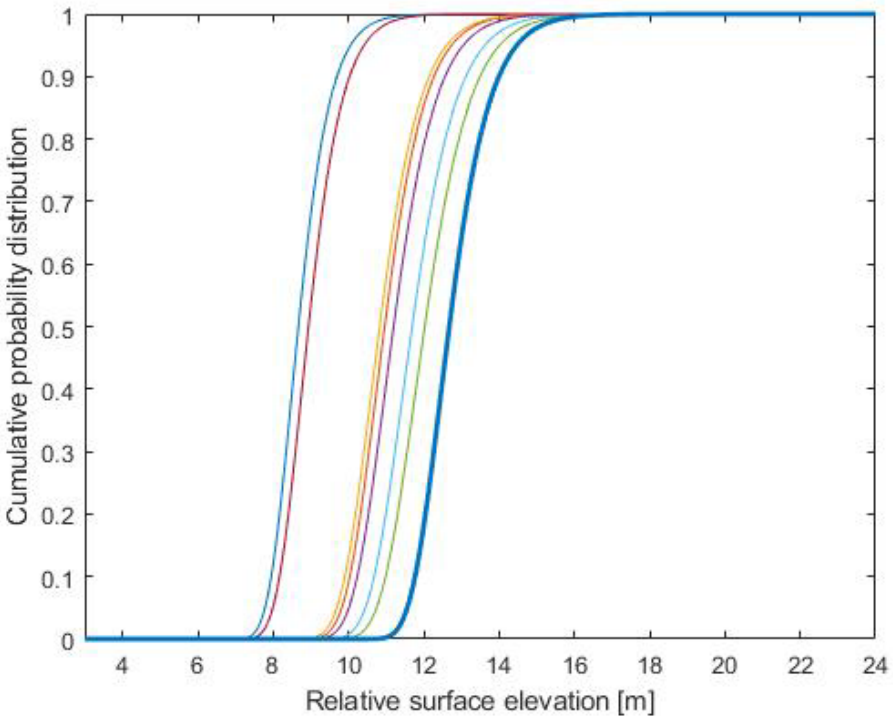

Figure 2.20: *Maximum of the relative surface elevation for a storm with 7 steps (point 431). From equation 2.20.*

Figure 2.20 illustrates a case of a storm with 7 steps, with the thick line being the product of all steps according to equation (2.20) The properties are shown in table 2.2.

Table 2.2: *Properties of each component of the distribution of the maximum relative surface elevation under point 431 for a storm with 7 steps. Direction in WAMIT convention*

Step	1	2	3	4	5	6	7
H_s	7.1	8.5	9.5	10.4	11.5	11.0	8.1
T_p	11.0	12.4	14.0	14.7	14.7	14.6	15.1
σ_{Rp}	5.0	8.1	8.0	8.6	9.9	9.4	5.5
T_z	8.3	9.2	10.2	10.7	10.8	10.7	10.7
θ	180	157.5	157.5	157.5	157.5	157.5	157.5

For every point p, storm i of m storms, and step j of n steps with its corresponding WAMIT direction, the variances of the spectra of the relative surface elevation were stored as

$$\sigma_{R_p,p}(i,j) = \begin{bmatrix} \sigma_{R_p,p}(i_1,j_1) & \sigma_{R_p,p}(i_1,j_2) & \dots & \sigma_{R_p,p}(i_1,j_n) \\ \vdots & \vdots & \vdots & \vdots \\ \sigma_{R_p,p}(i_m,j_1) & \dots & \dots & \sigma_{R_p,p}(i_m,j_n) \end{bmatrix} \tag{2.22}$$

Having the exact distributions for the maximum relative surface elevation, the next step was to find the values that would be considered for the design. Looking at figure 2.20 as an example, it can be seen that anywhere from 12 to 14 meters could be a likely maximum value for that storm. Tromans and Vanderschuren[13] have shown that the Most Probable Storm Maximum (MPSM) for storm i occurs when $F_{R,i} = 1/e$

$$F_{R,p,i}(MPSM_p(i)) = \frac{1}{e} \tag{2.23}$$

for point p and storm i

To solve equation (2.23), the following numerical approximation was performed:

1. First, a general initial value $MPSM^*$ of 11.5 m was set for all MPSMs and it was assumed that all MPSMs would be within the range R of 0.5 to 22.5 m (this range is somewhat arbitrary)
2. If $F_{R,p,i}(MPSM^*) < 1/e$, then $MPSM_p(i) = MPSM^* + c\,R$

   If $F_{R,p,i}(MPSM^*) > 1/e$, then $MPSM_p(i) = MPSM^* - c\,R$

Step 2 is repeated with $c = 1/4$, then $c = 1/8$, then $c = 1/16$, … until a high precision is achieved. The maximum error accepted was $0.01(1/e)$.

[13] Tromans, P.S., & Vanderschuren, L. (1995)

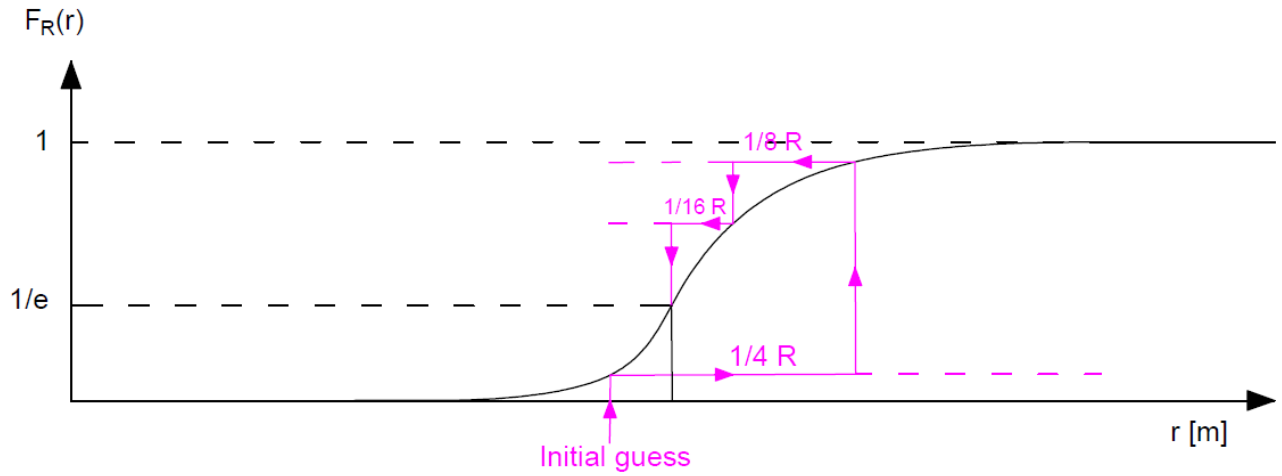

Figure 2.21: *Illustration of the methodology to obtain the most probable storm maxima*

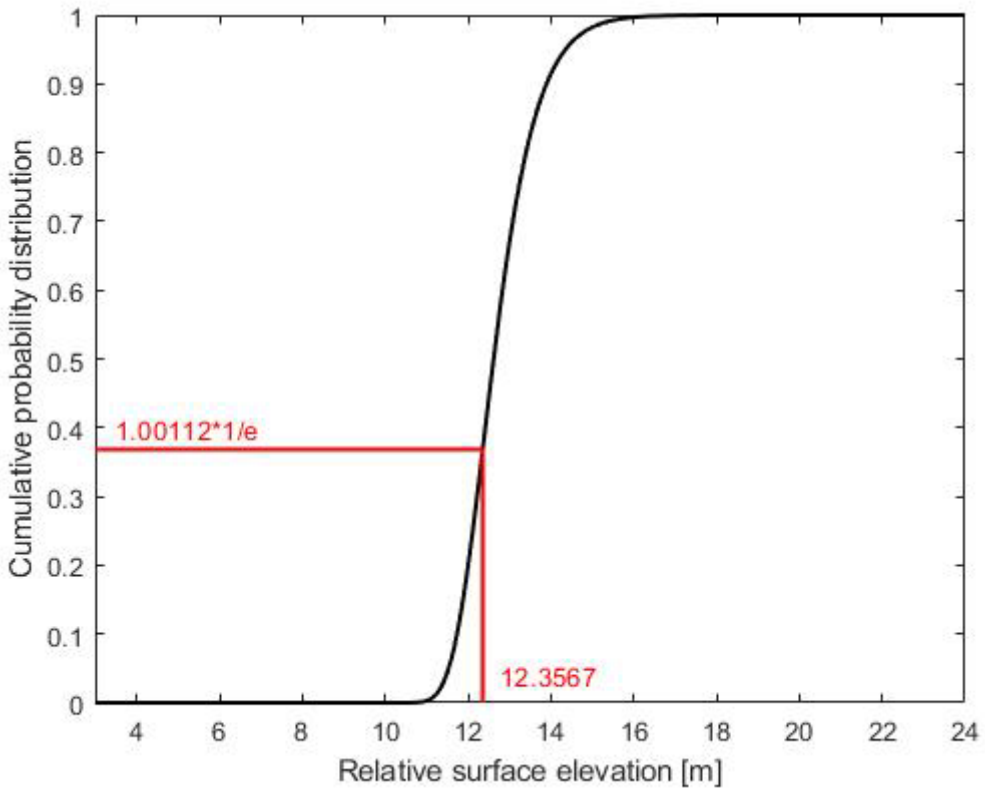

Figure 2.22: *Precision of the MPSM obtained for the same storm example (figure 2.10 and table 2.2)*

Although the directions of each 3-hour step were considered, the direction of the MPSMs for each storm was the direction of the peak of the storm as if only the peaks were analysed. With the direction of the step with the lowest T_p being the chosen one in case of multiple H_s peaks. Below, some examples.

Table 2.3: *Properties of each storm step for stroms 13 to 16 with a threshold of 7 m*

			3-hour storm step (WAMIT directiom))							Storm direction
			1	2	3	4	5	6	7	
Storm	13	Hs [m]	7.5	8.4	9.7	10.4	8.7	8.8	8.5	
		Tp [s]	11.8	13.0	14.3	14.5	16.0	14.8	14.9	
		θ	180°	157.5°	157.5°	157.5°	157.5°	180°	157.5°	157.5°
	14	Hs [m]	7.9	9.3	10.3	9.9	8.3			
		Tp [s]	13.6	14.5	15.4	17.2	16.0			
		θ	202.5°	180°	180°	180°	180°			180°
	15	Hs [m]	7.1	7.2						
		Tp [s]	12.3	12.7						
		θ	202.5°	180°						180°
	16	Hs [m]	7.1	8.1	9.1	9.8	10.3	9.3		
		Tp [s]	11.9	14.0	14.3	14.3	14.2	14.9		
		θ	225°	202.5°	202.5°	202.5°	202.5°	202.5°		202.5°

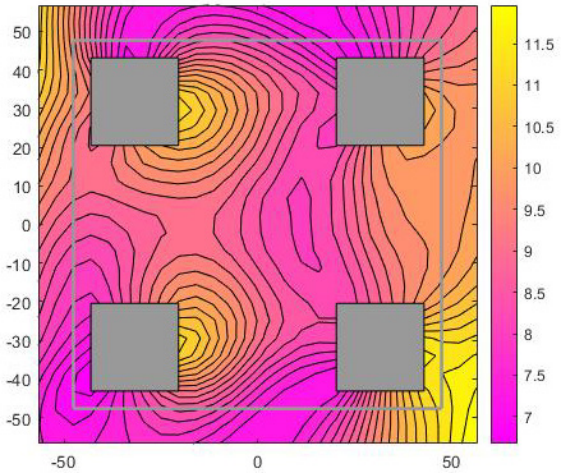

Figure 2.23: *MPSMs [m]. Storm 13/456. 157.5°.*

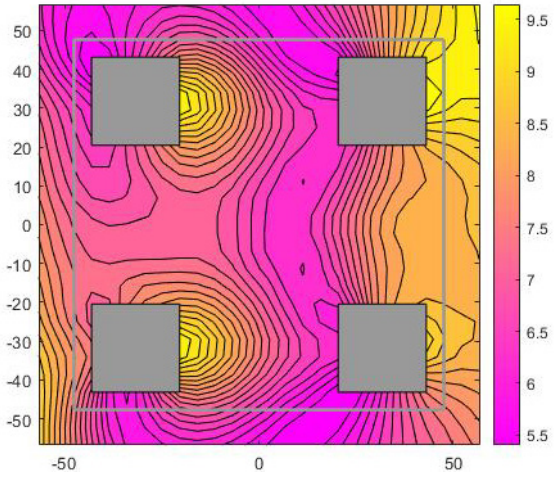

Figure 2.24: *MPSMs [m]. Storm 14/456. 180°.*

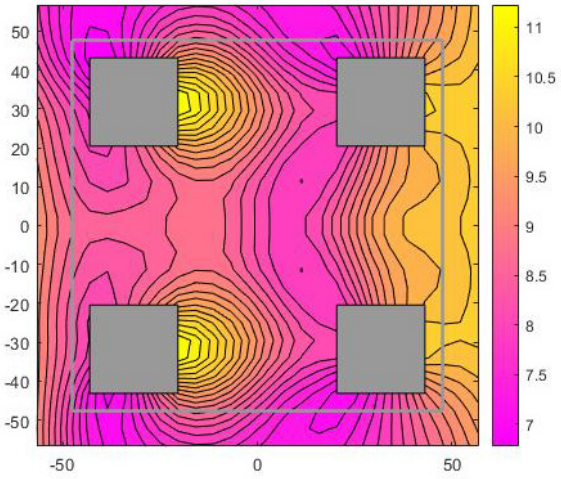

Figure 2.25: *MPSMs [m]. Storm 15/456. 180°.*

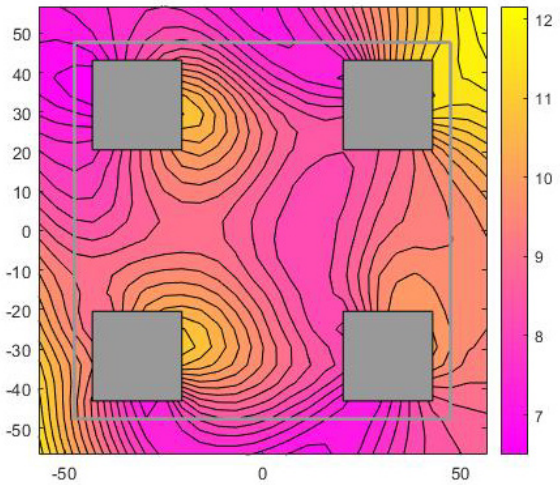

Figure 2.26: *MPSMs [m]. Storm 16/456. 180°.*

2.5. Distribution of the MPSMs and extreme values of the Long-term maxima without short term variability

For each point p, the most probable storm maxima are

$$MPSM_p(i) = \begin{bmatrix} MPSM_p(i_1) \\ MPSM_p(i_2) \\ \vdots \\ MPSM_p(i_m) \end{bmatrix} \tag{2.24}$$

where m is the number of storms, determined by the threshold.

As an example, for point 431 and a threshold of 7 m, the MPSM values are shown below

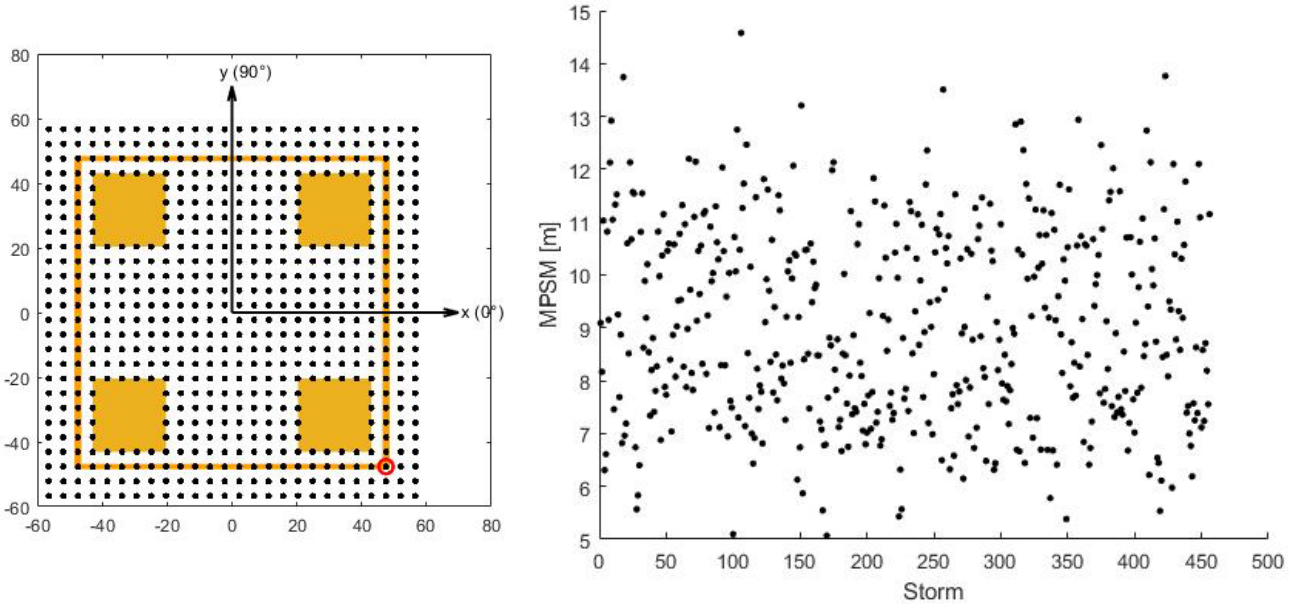

Figure 2.27: *MPSMs for all storms with a threshold of 7 m*

This is for the 61 years of data. To estimate the 100 and 10,000 year values corresponding to the ULS and ALS designs, for each point, a fit of the 3-parameter Weibull distribution was made (recall equation (1.3) from chapter 1). **Now denoting the MPSM domain as $\tilde{r}$:**

$$F_R(\tilde{r}) = 1 - exp\left\{-\left(\frac{\tilde{r} - \lambda}{\alpha}\right)^{\beta}\right\} \tag{2.25}$$

Introducing the method of moments, the parameters are estimated as follows:

$$\gamma_1 = \frac{\Gamma\left(1+\frac{3}{\beta}\right) - 3\Gamma\left(1+\frac{3}{\beta}\right)\Gamma\left(1+\frac{2}{\beta}\right) + 2\Gamma^3\left(1+\frac{1}{\beta}\right)}{\left[\Gamma\left(1+\frac{2}{\beta}\right) - \Gamma^2\left(1+\frac{1}{\beta}\right)\right]^{3/2}} \tag{2.26}$$

$$\sigma^2 = \alpha^2\left[\Gamma\left(1+\frac{2}{\beta}\right) - \Gamma^2\left(1+\frac{1}{\beta}\right)\right] \tag{2.27}$$

$$\mu = \lambda + \alpha\,\Gamma\left(1+\frac{1}{\beta}\right) \tag{2.28}$$

where γ_1, σ^2, and μ are the skewness, variance and mean of the MPSMs

γ_1 was computed by iteration until the β values reached a maximum error of 0.001.

The fit between the empirical MPSMs and the fitted distribution for point 431 is shown below, with the MPSMs in the plots sorted and binned into 100 intervals from the lowest to the highest value. The second subfigure is a probability plot to better appreciate the goodness of fit at the tail.

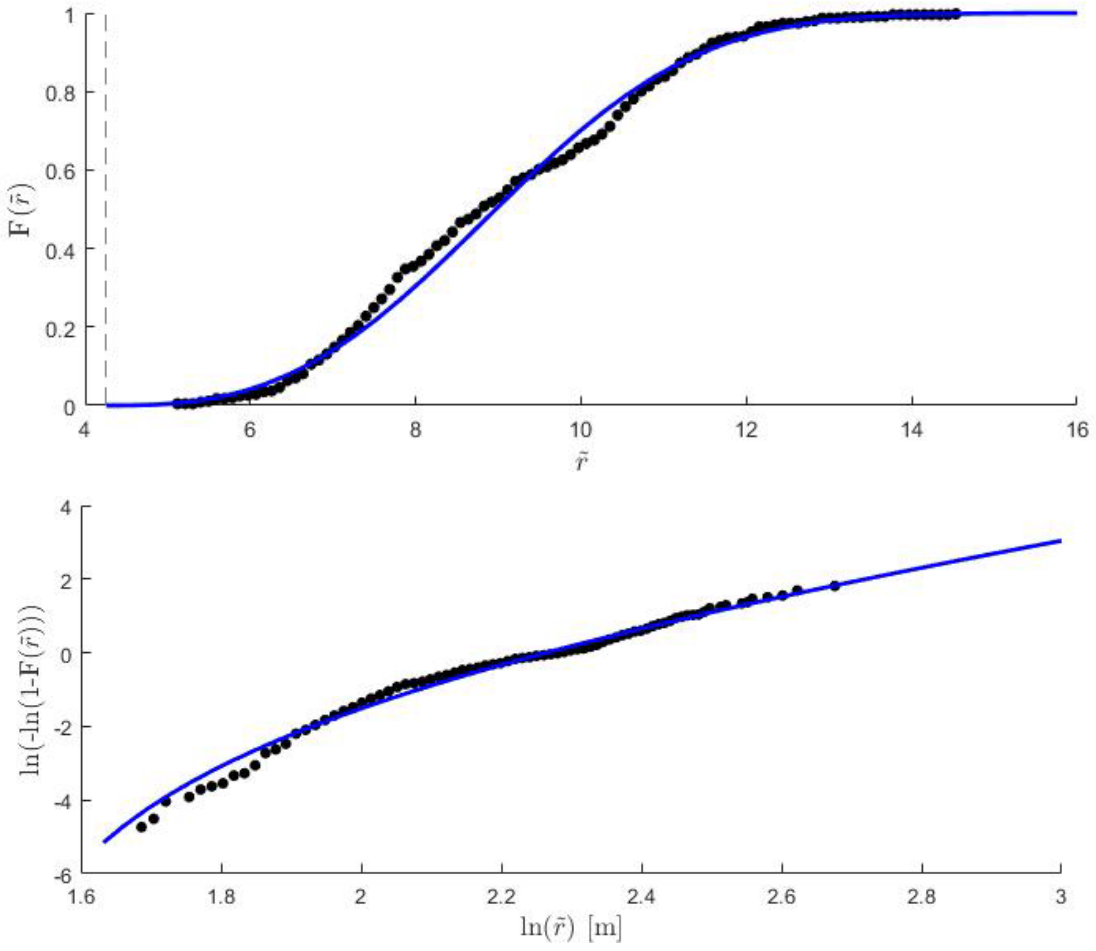

Figure 2.28: *Fitted vs empirical cumulative distribution of the MPSMs for point 431. Storms above 7 m.*

Solving the inverse of equation (2.25) with respect to $\tilde{r}$, for each point, it is then possible to find the extremes of $\tilde{r}$ (the most probable storm maximum relative elevation) with probabilities of exceedance of once every 100 and 10,000 years.

$$\tilde{r}^*_{100} = \lambda + \alpha \left[-ln\left(\frac{0.01}{N^*_{1y}}\right)\right]^{\beta} \tag{2.25}$$

$$\tilde{r}^*_{10K} = \lambda + \alpha \left[-ln\left(\frac{0.0001}{N^*_{1y}}\right)\right]^{\beta} \tag{2.26}$$

N^*_{1y} is, recalling (1.2) the average number of 3-hour events above the threshold per year and for the analysis of the storm peaks only, N^*_{1y} is the average number of annual storms.

Table 2.4: *N_{1y} **

		Analysis method	
		All storm steps	Storm peaks only
Threshold	6 m	61.6	13.0
	7 m	31.1	7.5
	8 m	15.3	4.2

Table 2.5: *Adjusted ULS probabilities of exceedance*

Originally 0.01		Analysis method	
		All storm steps	Storm peaks only
Threshold	6 m	0.0002	0.0008
	7 m	0.0003	0.0013
	8 m	0.0007	0.0024

Table 2.6: *Adjusted ALS probabilities of exceedance*

Originally 0.0001		Analysis method	
		All storm steps	Storm peaks only
Threshold	6 m	0.000002	0.000008
	7 m	0.000003	0.000013
	8 m	0.000007	0.000024

Solving for the two limit states, for each of the 612 points under the deck, the values of the relative surface elevation with probabilities of exceedance of once in 100 years and once in 10,000 years were computed. The contours below include the points outside the deck area, but the critical point is 431 on the north-western corner with the semisubmersible oriented to face the worst storms. These values were yet to be corrected to account for the 'short term variability'.

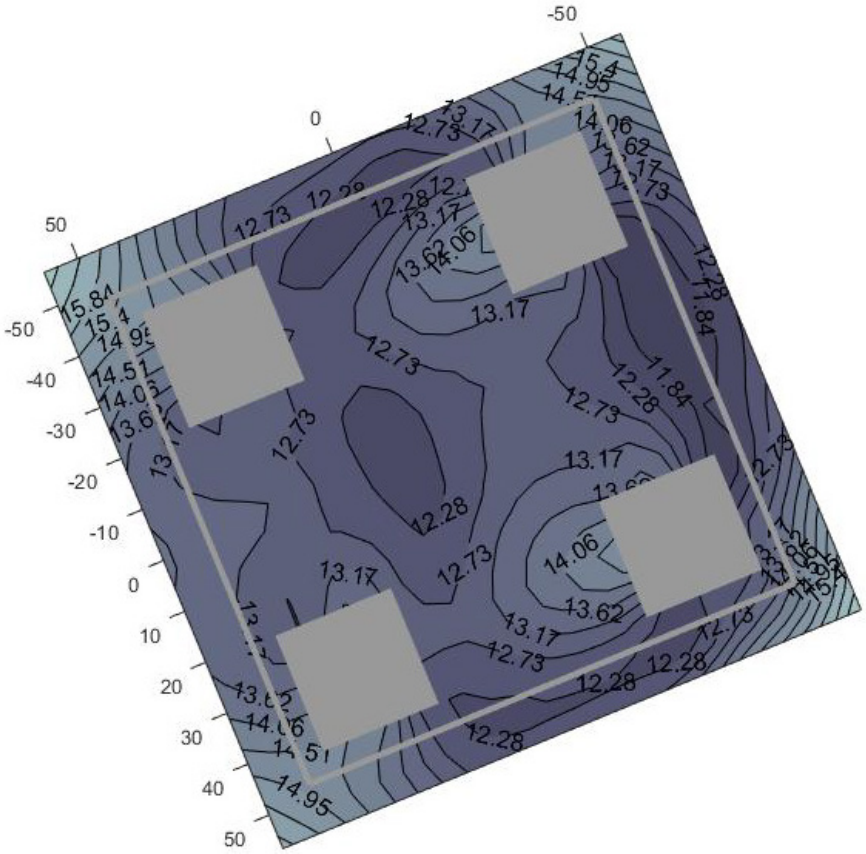

Figure 2.29: *100 years relative surface elevation without short-term variability. Storms with H_s >7 m.*

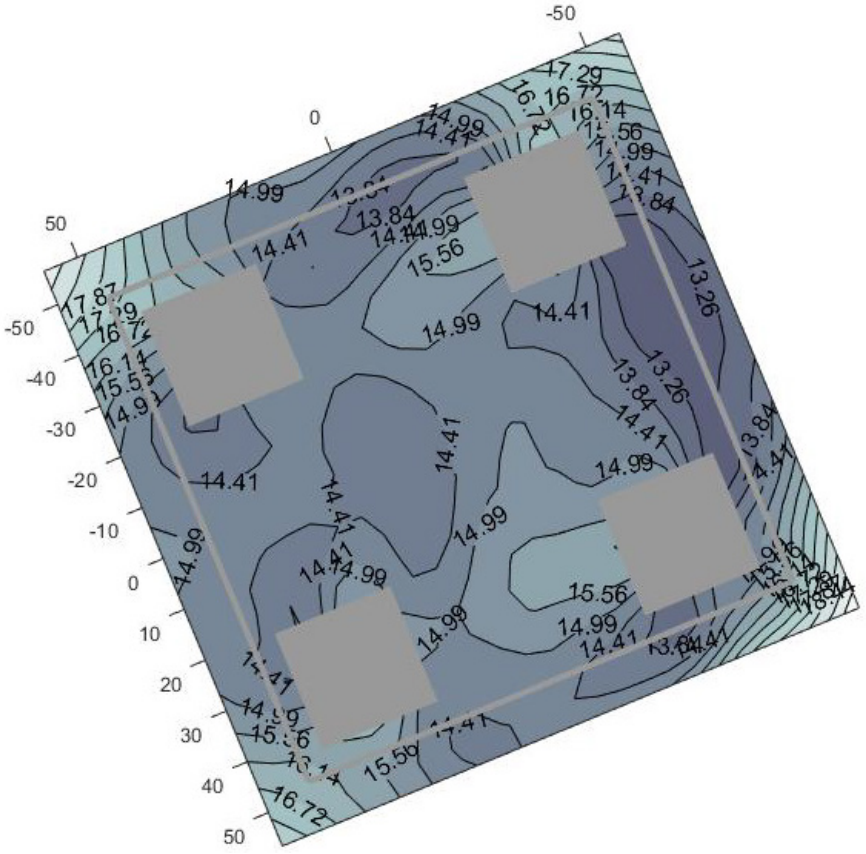

Figure 2.30: *10,000 years relative surface elevation without short-term variability. Storms with H_s >7 m.*

2.6. Introducing the short-term variability

When estimating the MPSM values of the distributions of the storm maximum relative surface elevation (2.20), it was properly established that they would occur when the cumulative distribution functions equal $1/e$. Although these values are indeed the most probable, it could well be the case that the storm maxima are significantly deviated from the most probable. It is therefore necessary to account for this, which would naturally increase the initial airgap requirement.

Recalling equation (2.20), for j being a storm step of storm i

$$F_{R,i}(r) = \prod_{j=1}^{n_j} \left[1 - exp\left\{ -0.5 \left(\frac{r}{\sigma_{R_{p,j}}} \right)^2 \right\} \right]^{n_{3h,j}} \tag{2.20}$$

It is known that this distribution can be approximated by the Gumbel distribution as a conditional distribution of the most probable storm maximum relative surface elevation when $n_{3h,j}$ -the expected number of zero up-crossings- tends to ∞:[14]

$$F_{R,i}(r) \approx exp\left\{ -exp\left\{ -\frac{r - \tilde{r}}{\beta_{G,i}\, \tilde{r}} \right\} \right\} \quad \leftrightarrow \quad F_{R,i}(r|\tilde{r}) \tag{2.27}$$

with r is the relative surface elevation under a point and $\tilde{r}$ a MPSM

For a point under the deck, and for each storm, the parameter β_G in the Gumbel distribution is obtained by requiring that the standard deviation of (2.20) equals that of (2.27). The variance of a random variable x with a probability density function f is

$$\sigma^2(x) = \int_{-\infty}^{\infty} x^2 f(x)\, dx - \mu^2 \tag{2.28}$$

with a mean, μ

$$\mu(x) = \int_{-\infty}^{\infty} x f(x)\, dx \tag{2.29}$$

[14] Naes, A. & Moan, T. (2005)

(2.28) was solved for the distribution of the storm maximum relative surface elevation (2.20) for each storm at each point with numerical integration (trapezoidal rule) of both $x^2 f(x)$ and $x f(x)$. I.e. for $r^2 f_{R,i}(r)$ and $r f_{R,i}(r)$. Where

$$f_{R,i}(r) = \frac{d}{dr} F_{R,i}(r) \tag{2.30}$$

is the probability density function of the storm maximum relative surface elevation. Which, with the following identity (for an arbitrary continuous function F)

$$\frac{d}{dx}\prod_{k=1}^{n} F_k(x) = \prod_{k=1}^{n} F_k(x) \sum_{k=1}^{n} \frac{F_k'(x)}{F_k(x)} \tag{2.31}$$

can be shown to become, with each 3-hour step j

$$f_{R,i}(r) = \prod_{j=1}^{n_j} \left[1 - exp\left\{-0.5\left(\frac{r}{\sigma_{R_{p,j}}}\right)^2\right\}\right]^{n_{3h,j}} \sum_{j=1}^{n_j} \frac{r\, n_{3h,j}}{\sigma_{R_{p,j}}^2 \left(exp\left\{0.5\left(\frac{r}{\sigma_{R_{p,j}}}\right)^2\right\} - 1\right)} \tag{2.32}$$

$\sigma_{R_{p,j}}$ is the standard deviation of the spectrum of the relative surface elevation under a particular point for step j of storm i.

And the β_G were obtained with the following characteristic of the Gumbel distribution:

$$\sigma^2_{f_{R,i}(r|\tilde{r})} = \frac{\pi^2}{6}\left(\beta_{G,i}\,\tilde{r}\right)^2 \quad \rightarrow \quad \beta_{G,i} = \frac{\sqrt{6\,\sigma^2_{f_{R,i}(r|\tilde{r})}}}{\pi\,\tilde{r}} \tag{2.33}$$

for each point and for the MPSM corresponding to each storm.

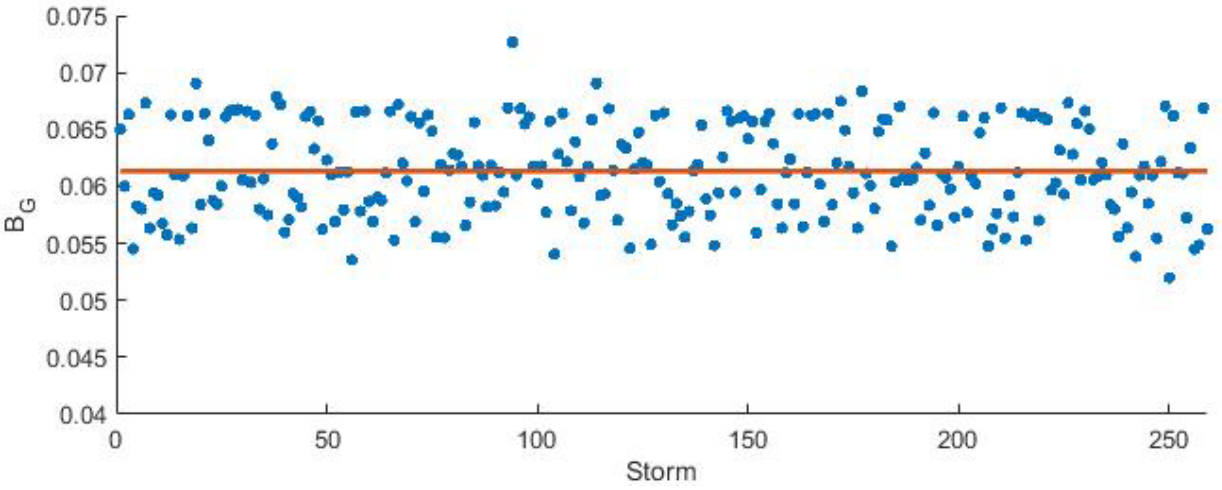

Figure 2.31: *Beta values for all storms with a threshold of 8 m under point 431*

Since the values of β_G for all storms tend to be very similar for all storms, the average of β_G of all storms i were used for each point. I.e. there was only one β_G for each point in equation (2.27). The averages tends to be around 0.061, generally.

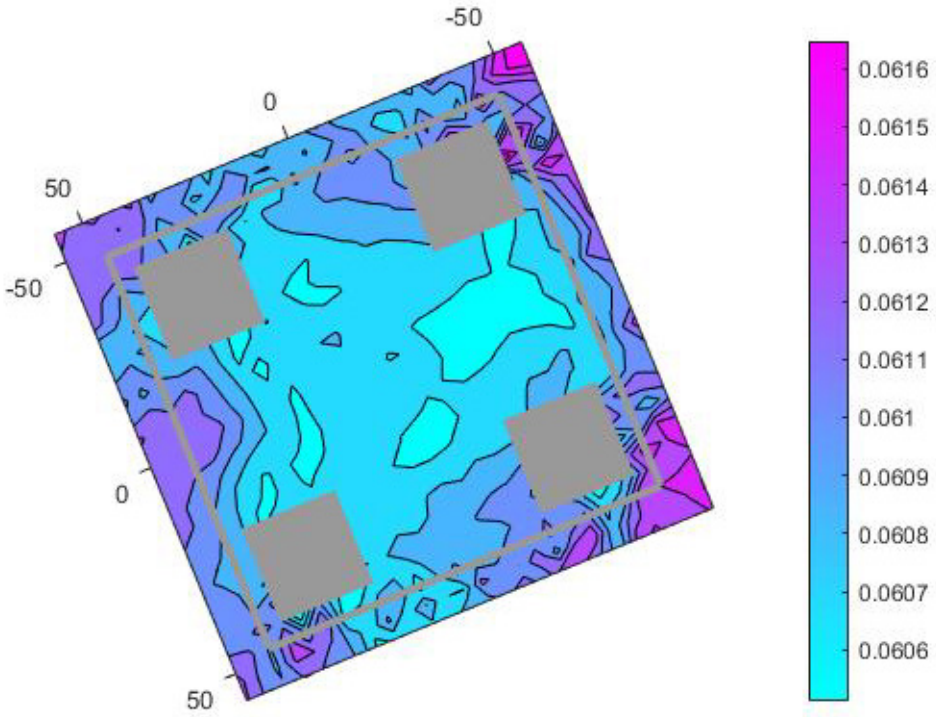

Figure 2.32: *Beta values for all storms with a threshold of 8 m*

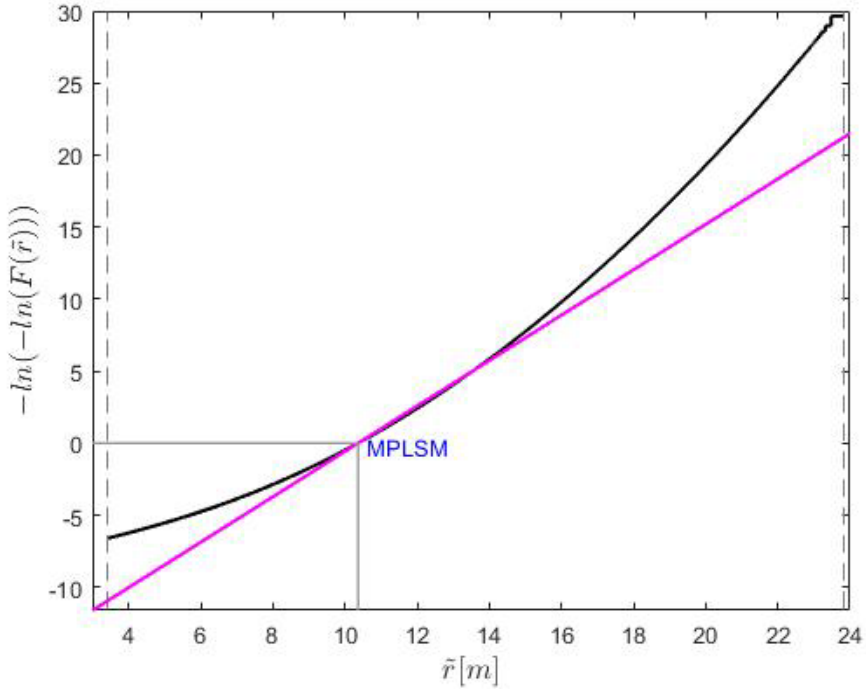

Figure 2.33: *Distribution of the storm maximum relative surface elevation under point 431 for a random storm from the analysis of all storms above 8 m. Rayleigh distribution plotted in black and Gumbel approximation in magenta. Plotted in a Gumbel probability paper.*

The long-term distribution of the maximum relative surface elevation accounting for the short-term variability becomes

$$\boldsymbol{F_R^*(r) = \int_{\tilde{r}} F_R(r|\tilde{r})\ f_R(\tilde{r})\ d\tilde{r}} \qquad \boldsymbol{(2.34)}$$

With $f_R(\tilde{r})$ being the fitted distribution (Weibull probability density function) of the MPSMs. The corresponding ULS and ALS probabilities are

$$F_{ULS} = 1 - \frac{0.01}{N_{1y}^*} \qquad (2.35)$$

and

$$F_{ALS} = 1 - \frac{0.0001}{N_{1y}^*} \qquad (2.36)$$

Technically, $F_R^*(r)$ is the area under the argument of (2.34) for a fixed r (the domain of the maximum relative surface elevation approximated with the Gumbel distribution). it was handy to visualize this argument; as r increases, the area under $F_R(r|\tilde{r})f_R(\tilde{r})$ tends to one.

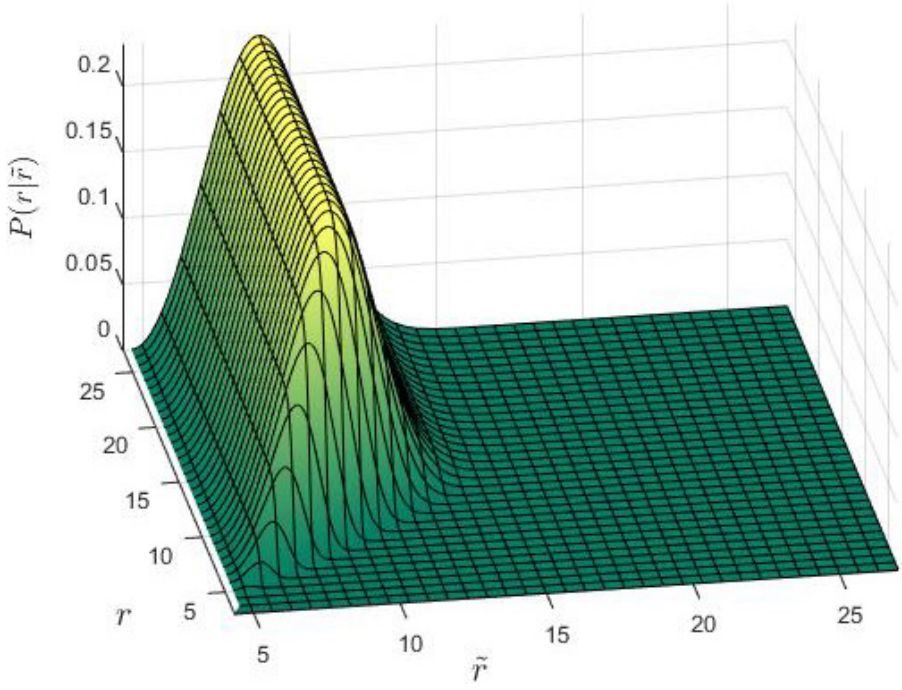

Figure 2.34: *$F_R(r|\tilde{r})f_R(\tilde{r})$. The long term distribution with short-term variability is computed by integrating along $\tilde{r}$, for every discrete r.*

To solve equation (2.34) exactly, there are not any analytical solutions for an exact inverse function, so it is necessary to perform the integral for discrete values of r, where the size of the increments is the precision of the end results. A precision of 10 cm was chosen in the present work. Then, the procedure to estimate r so that $F_R^*(r)$ takes the values of F_{ULS} and F_{ALS} was to find the r values that better made $F_R^*(r) = F_{ULS}$ and $F_R^*(r) = F_{ALS}$.

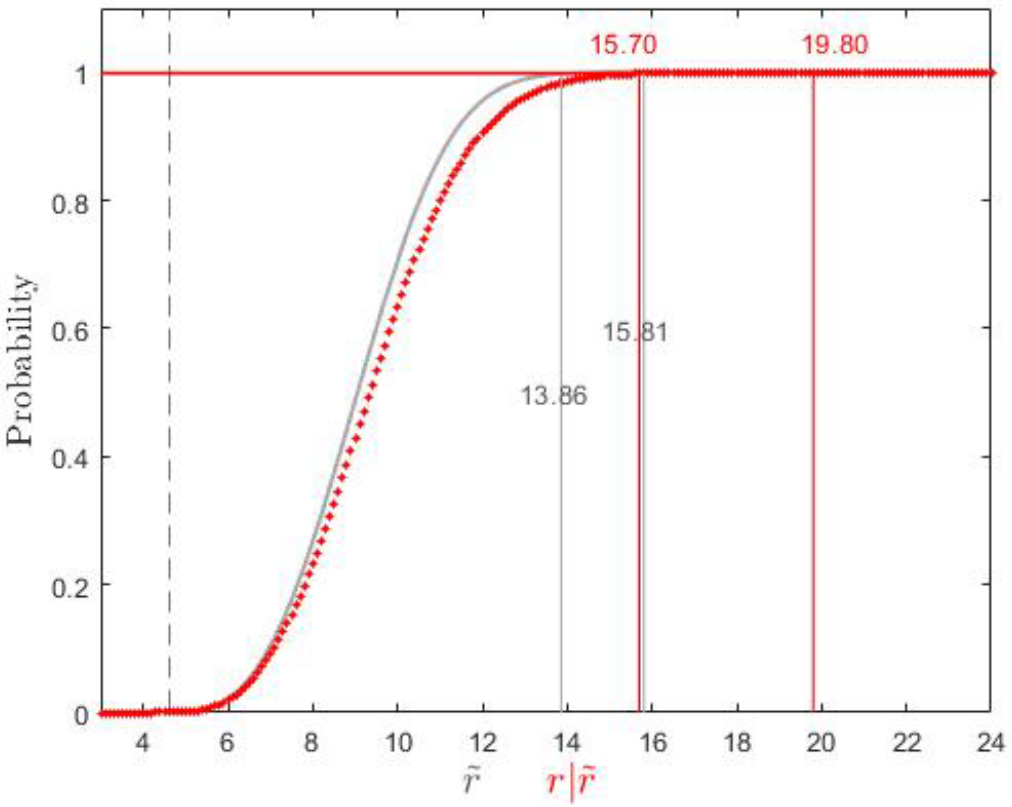

Figure 2.35: *Long-term distribution with and without short-term variability under point 431. Storm peaks with a threshold of 8 m.*

By doing this for all points, similar contours to those in figures 2.29 and 2.30 could be obtained, but with larger values due to the short-term variability. These are the correct results for 100 and 10,000 years relative surface elevation under the deck. Below are the contours for the same example as in section 2.5 (all storms above 7 m).

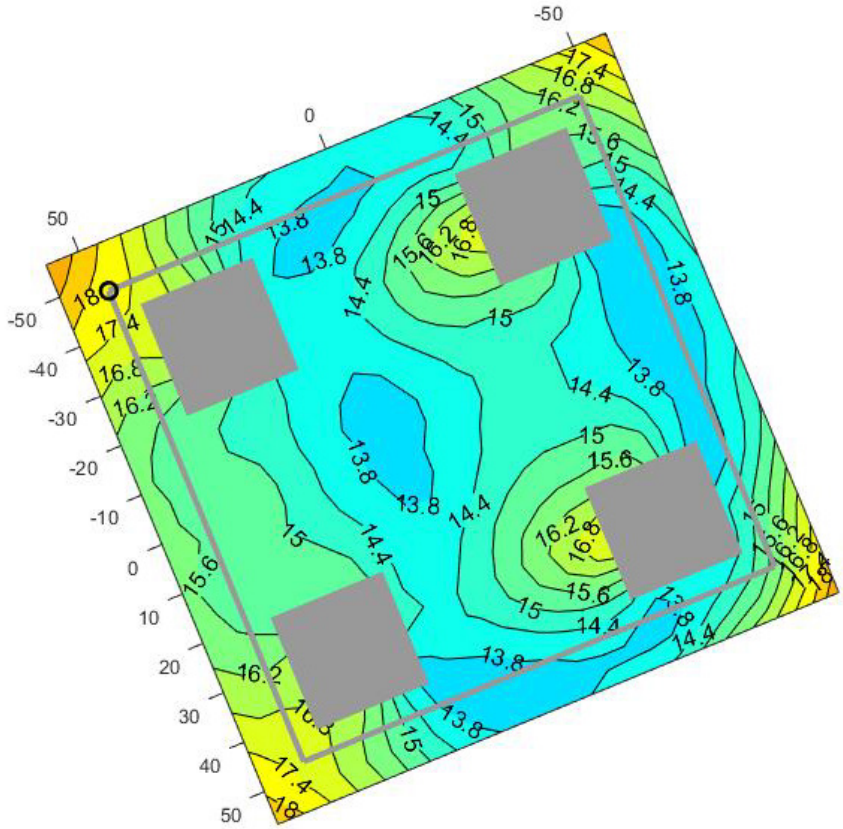

Figure 2.36: *100 years relative surface elevation. All storm steps with H_s >7 m.*

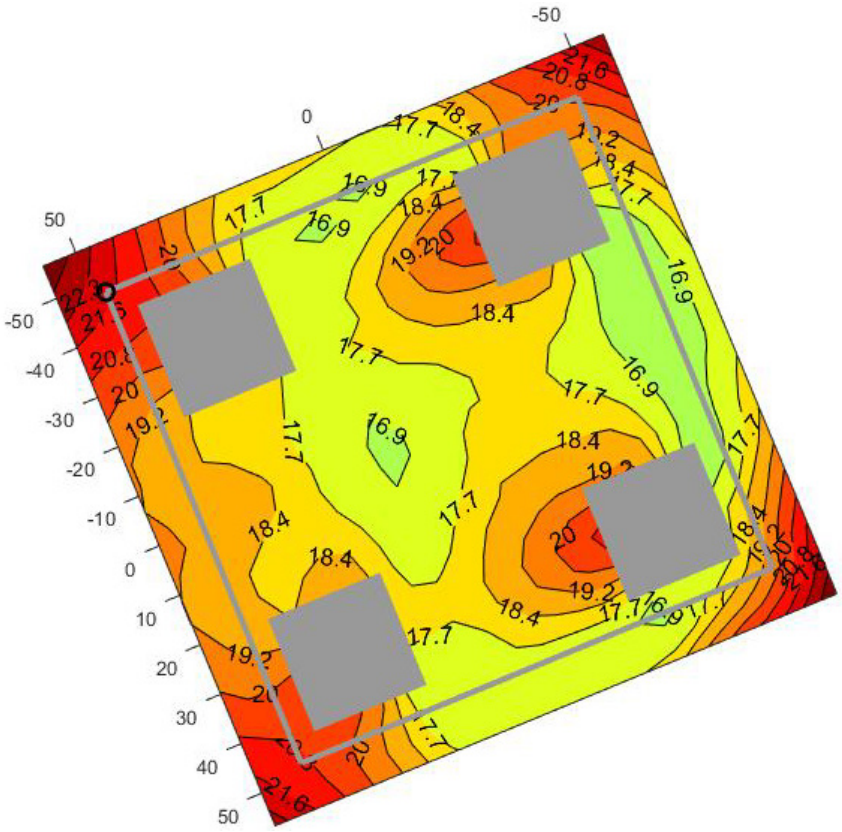

Figure 2.37: *10,000 years relative surface elevation. All storm steps with H_s >7 m.*

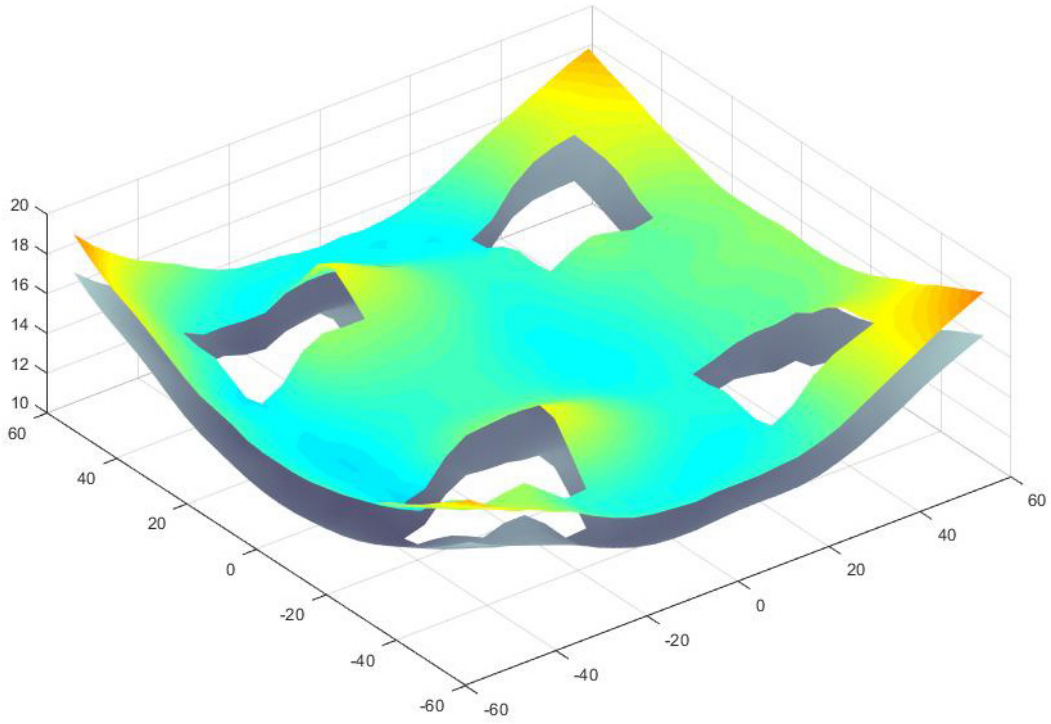

***Figure 2.38**: Comparison of 100 years relative surface elevation with and without short-term variability. All storm steps with H_s >7 m.*

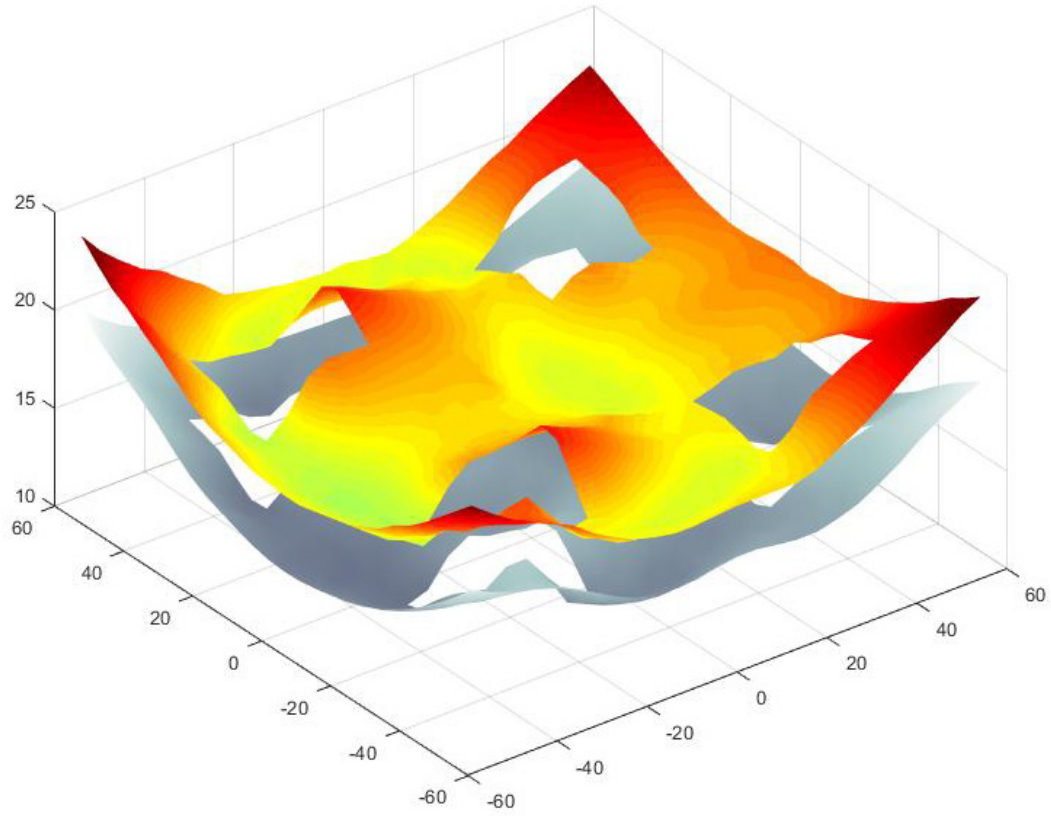

***Figure 2.39:** Comparison of 10,000 years relative surface elevation with and without short-term variability. All storm steps with H_s >7 m.*

2.7. Storm severity

It is possible to appreciate the severity of each particular storm by plotting a scatter diagram of H_s vs T_p with a colour code representing the MPSM that the particular H_s, T_p pair would result on, for a particular point under the deck. The way to approach this was to assign a H_s, T_p pair that represents each storm, and that was a point in the scatter plot (so a point per storm). Naturally, the H_s, T_p pairs that represent a storm were those corresponding to the storm peaks (taking the one with the lowest T_p in case of multiple H_s peaks). In other words, the storm severity scatter plots were done for the storm peaks only.

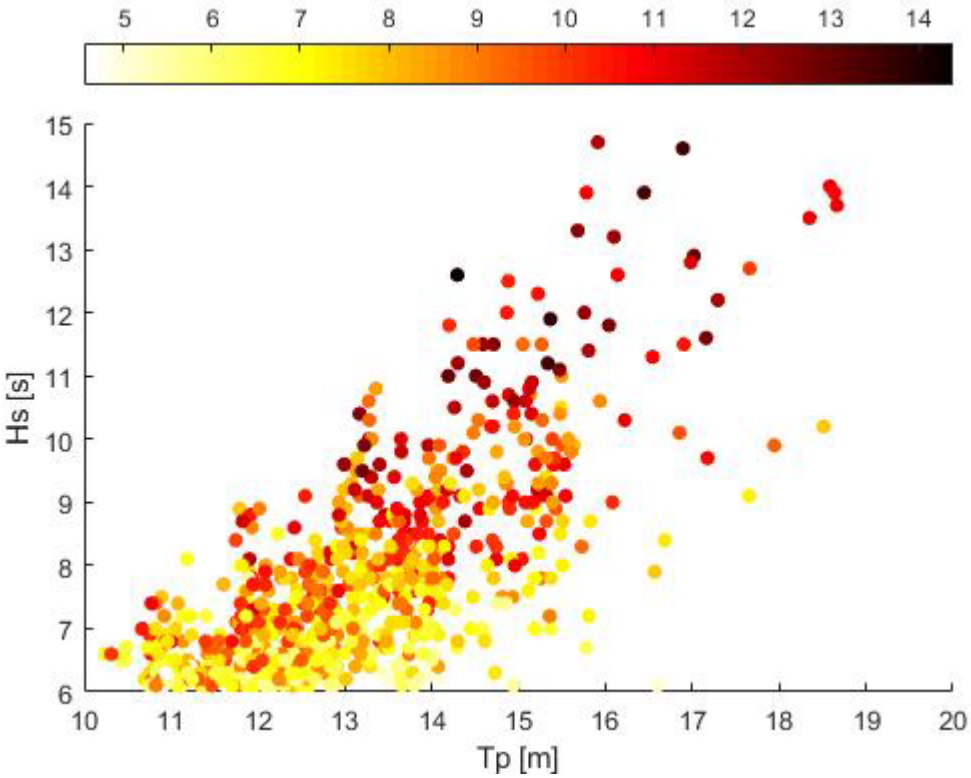

Figure 2.40: *Storm severity at point 431, all storm peaks with a threshold of 6 m.*

It is seen that the storm severity (the colour code), when plotted for all storms, does not show a very clear correlation with H_s/T_p (the steepness of the sea). Naturally, it is expected that the higher, steeper seas would account for higher relative surface elevations, the reason for this not strictly holding true is that the steepness of the seas can vary with respect to the direction where the waves come from. This can be seen with more clarity if the scatter plot is divided into directional sectors; which also allows to appreciate where the steepest seas come from.

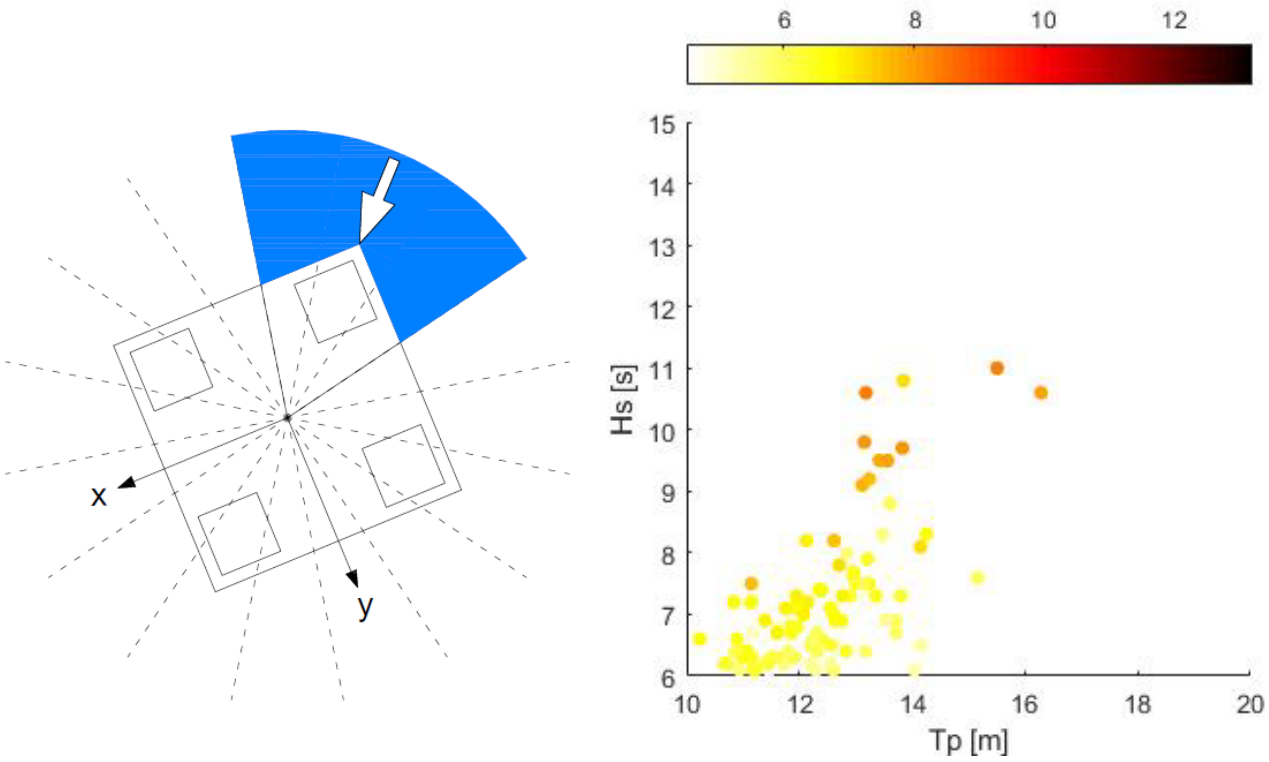

Figure 2.41: *Severity at point 431 for all storm peaks with a threshold of 6 m. 22.5° – 67.5° WAMIT.*

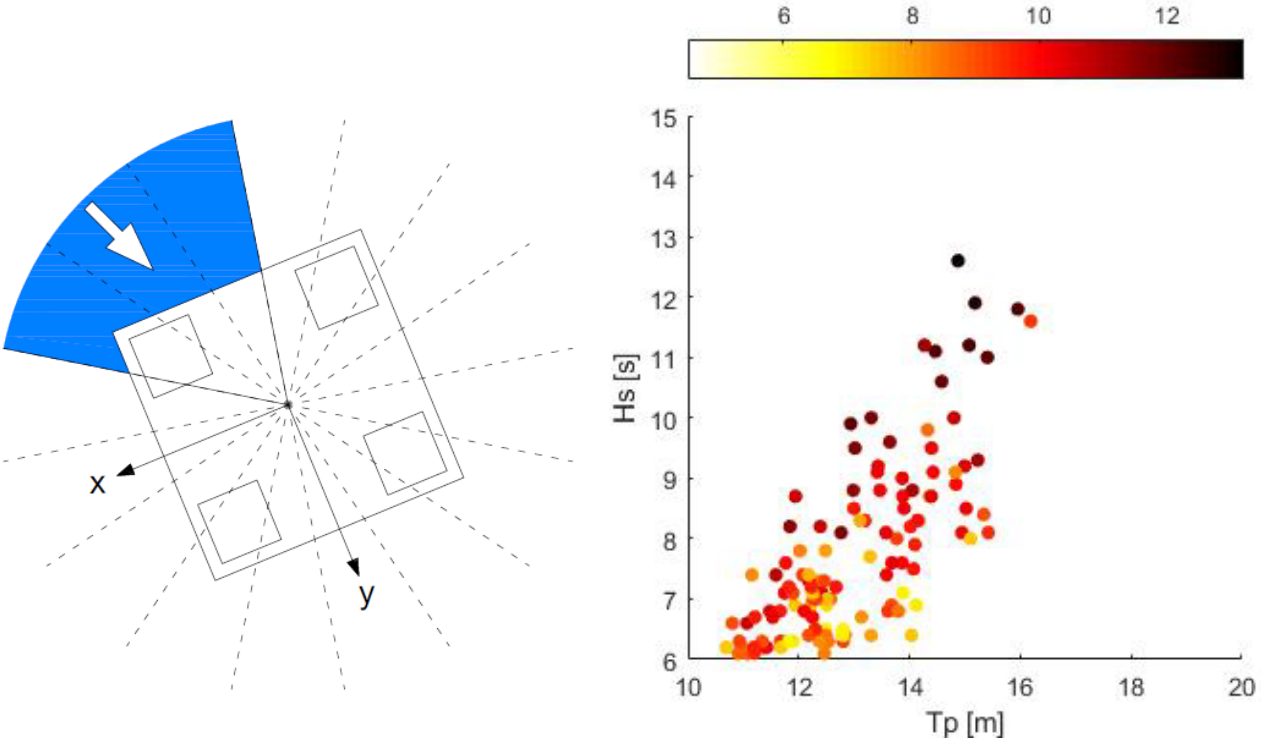

Figure 2.42: *Severity at point 431 for all storm peaks with a threshold of 6 m. 90° – 135° WAMIT.*

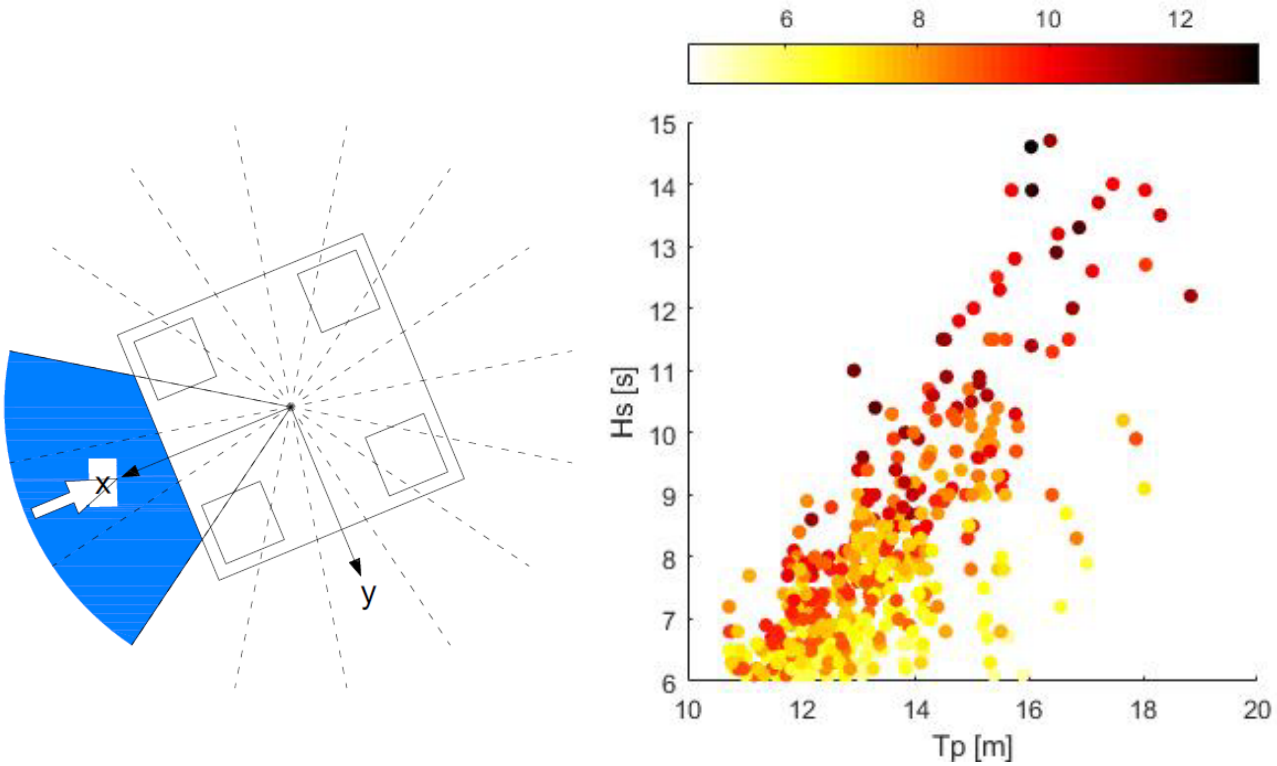

Figure 2.43: *Severity at point 431 for all storm peaks with a threshold of 6 m. 157.5° – 202.5° WAMIT.*

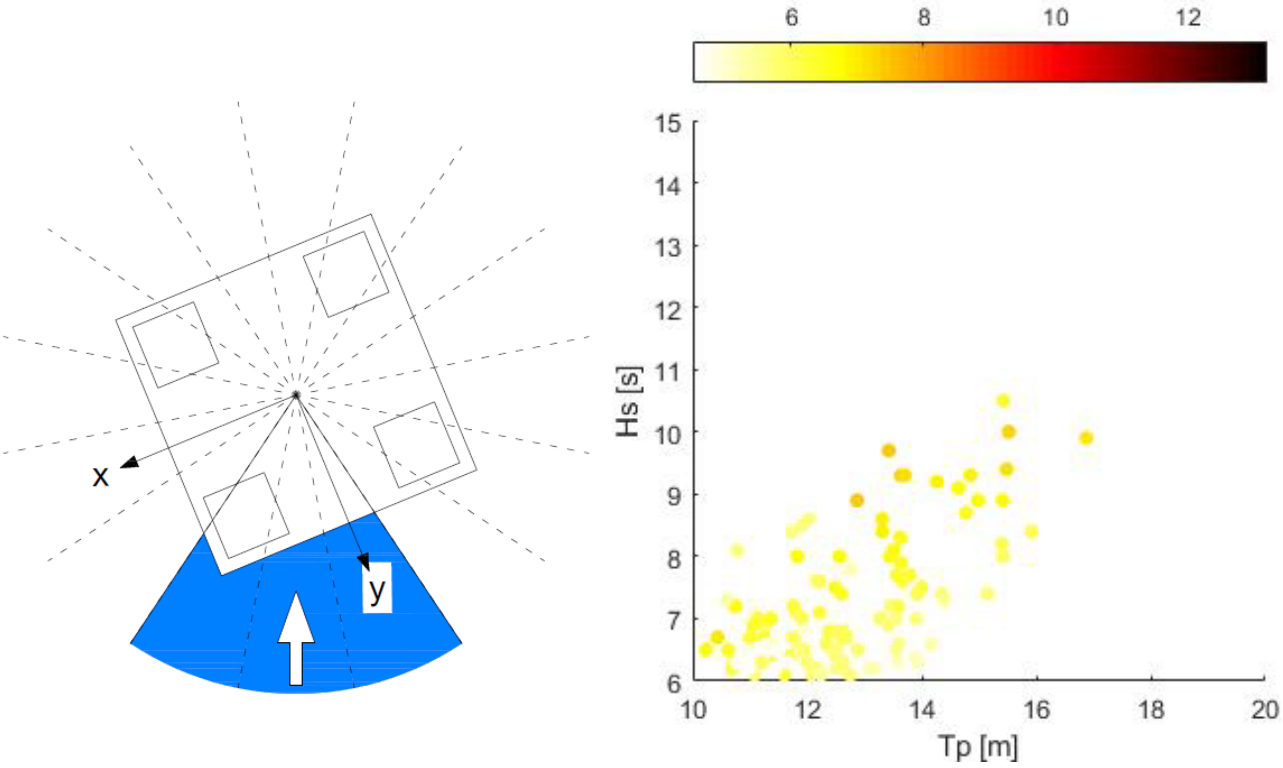

Figure 2.44: *Severity at point 431 for all storm peaks with a threshold of 6 m. 225° - 270° WAMIT.*

3. Statistical analysis to determine extreme sea states

At this point, it has been established that it's the wind seas that should be analysed and in order to estimate the maximum relative surface elevation, simple manipulations were made to the data according to the threshold and POT method. However, A more in-depth analysis was made to estimate extreme sea states; not only to have a broader understanding of the sea that the platform would deal with, but eventually to produce probability contours. These are explained in this chapter and implemented in chapter 4 as an alternative method to estimate extreme relative surface elevations.

3.1. Weibull analyses of the data

By setting a threshold and analysing the 3-hour sea states, fitting a Weibull distribution usually yields more reliable extremes than doing so for all sea states. The data studied were all 3-hour H_s values above the threshold. With the same definition of storm, so for each threshold there is the case of all H_s above it and also the case of the H_s peaks only. Recalling equations (2.26), (2.27) and (2.28), the parameters for a 3-parameter Weibull fit were obtained, but now for the values of the significant wave heights instead of the most probable storm maximum relative surface elevations. The method of moments has generally worked better than maximum likelihood estimators for this type of analyses.[15]

$$\gamma_1 = \frac{\Gamma\left(1+\frac{3}{\beta}\right) - 3\Gamma\left(1+\frac{3}{\beta}\right)\Gamma\left(1+\frac{2}{\beta}\right) + 2\Gamma^3\left(1+\frac{1}{\beta}\right)}{\left[\Gamma\left(1+\frac{2}{\beta}\right) - \Gamma^2\left(1+\frac{1}{\beta}\right)\right]^{3/2}} \tag{2.26}$$

$$\sigma^2 = \alpha^2\left[\Gamma\left(1+\frac{2}{\beta}\right) - \Gamma^2\left(1+\frac{1}{\beta}\right)\right] \tag{2.27}$$

$$\mu = \lambda + \alpha\,\Gamma\left(1+\frac{1}{\beta}\right) \tag{2.28}$$

[15] Bai, Y., & Lin, W. (2016)

where Γ denotes the gamma function.

The procedure to estimate β consists on iteration with a small enough initial value and small increments until the difference between the two sides of (2.26) does not exceed a certain precision (0.001). γ_1, σ^2, and μ are the skewness, variance, and mean of the data, respectively. Table 3.1 shows the statistical parameters and Weibull parameters for the different cases studied, where the main form of the 3-parameter Weibull distribution was used. From chapter 1:

$$F(H_s) = 1 - exp\left\{-\left(\frac{H_s - \lambda}{\alpha}\right)^{\beta}\right\} \tag{1.3}$$

***Table 3.1**: Statistical parameters and Weibull parameters*

	γ_1	σ^2	μ	β	α	λ
All Hs>6 m	1.621	1.743	7.46	1.151	1.593	5.944
All Hs>7 m	1.619	1.577	8.397	1.152	1.517	6.954
All Hs>8 m	1.605	1.423	9.328	1.158	1.45	7.95
Storm peaks with Hs>6 m	1.556	2.44	7.718	1.182	1.948	5.879
Storm peaks with Hs>7 m	1.531	2.194	8.657	1.195	1.872	6.894
Storm peaks with Hs>8 m	1.461	1.992	9.564	1.233	1.852	7.833
All sea states*	1.786	2.523	1.949	1.078	1.761	0.238

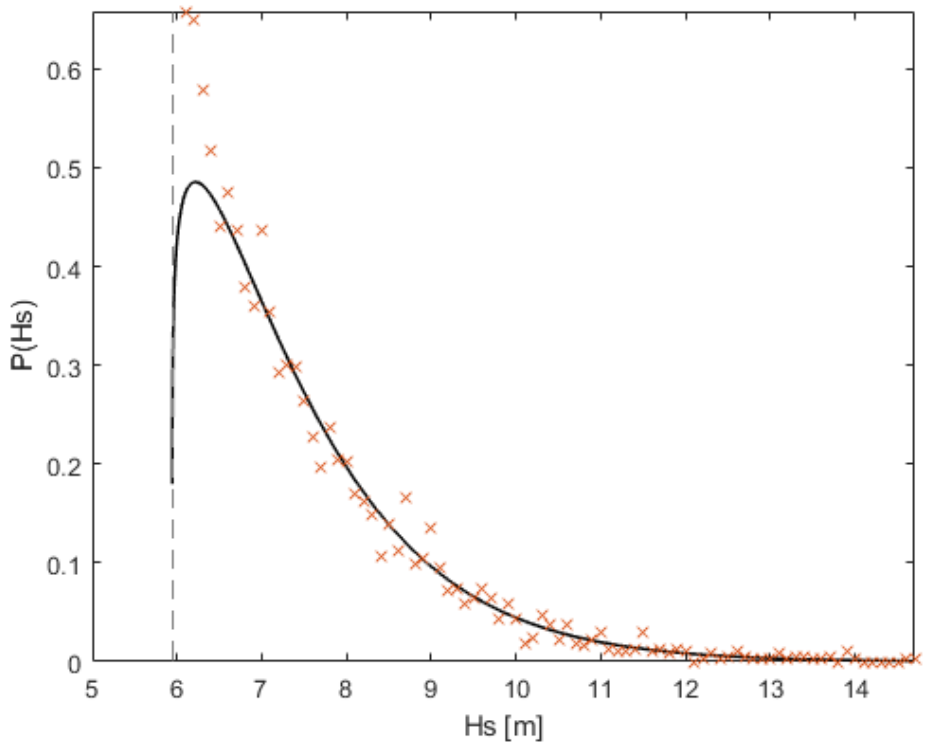

***Figure 3.1**: Fitted Weibull probability distribution compared to the empirical probability distribution. The sorted data points are scaled with a factor of 10 in the plot (because the H_s values have a precision of 0.1 m). Computed for all $H_s > 6$ m.*

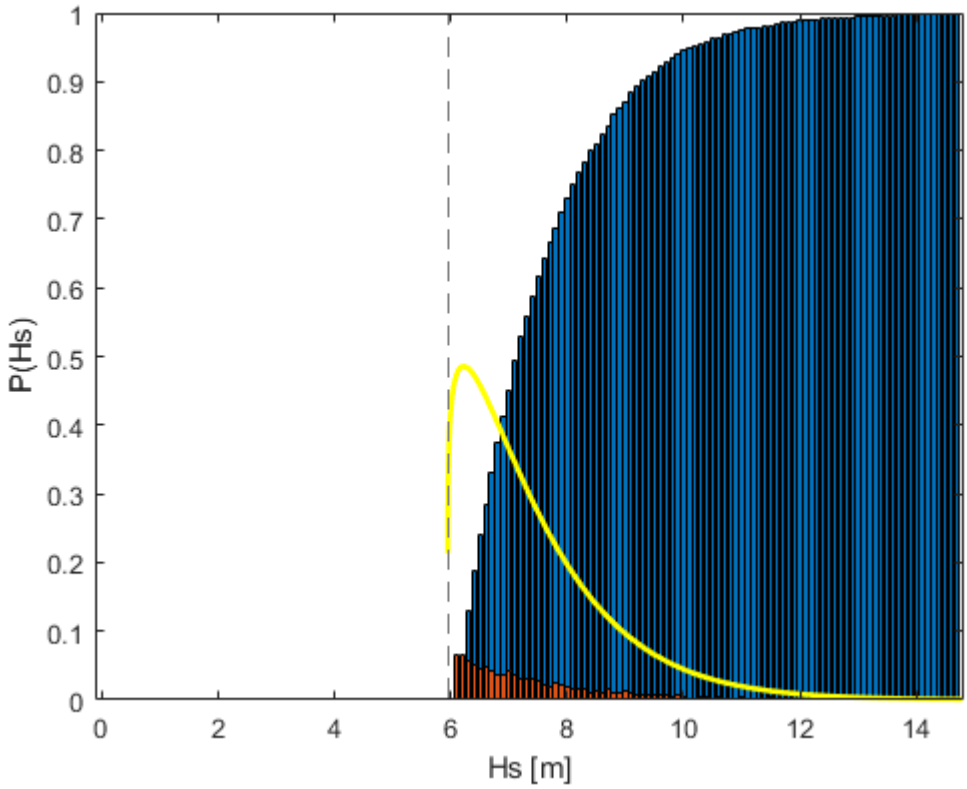

***Figure 3.2**: Fitted Weibull probability distribution compared to the empirical probability distribution and the empirical cumulative distribution. For all $H_s > 6$ m.*

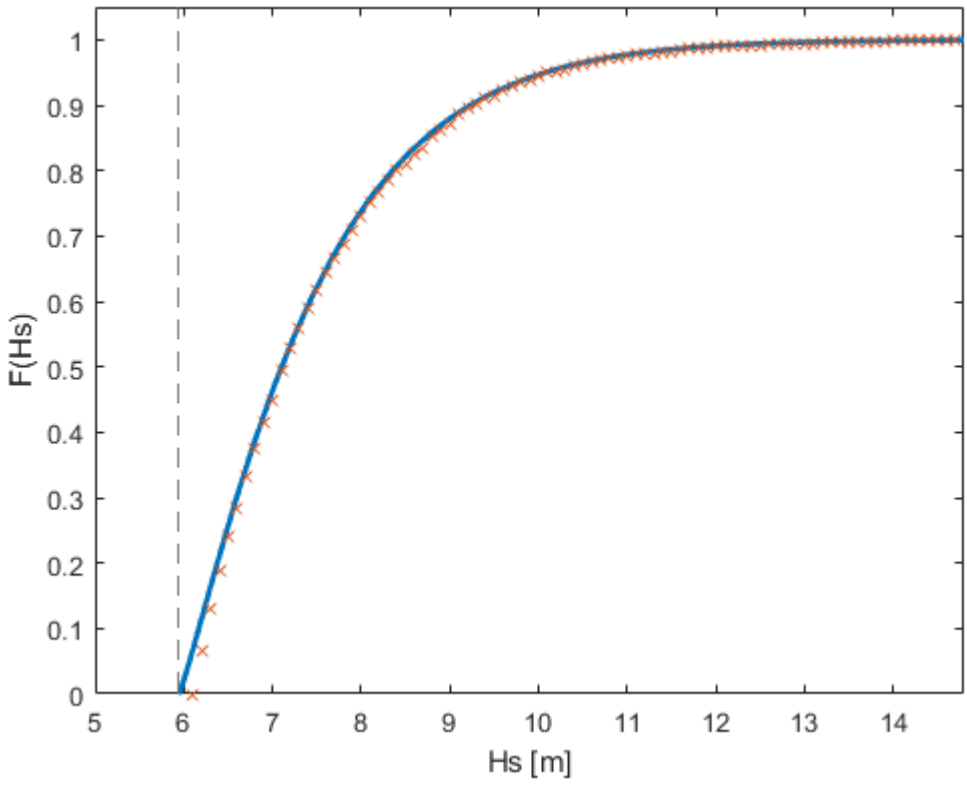

***Figure 3.3:** Fitted cumulative distribution vs empirical cumulative distribution for all H_s >6 m*

Probability plots help to better visualize the fits at the upper tail. The standard 3-parameter Weibull distribution (black in the figure below) was used, but a comparison in illustrated against the 2-parameter version (1.4) in green and the 3-parameter version with artificial λ (1.5), in cyan.

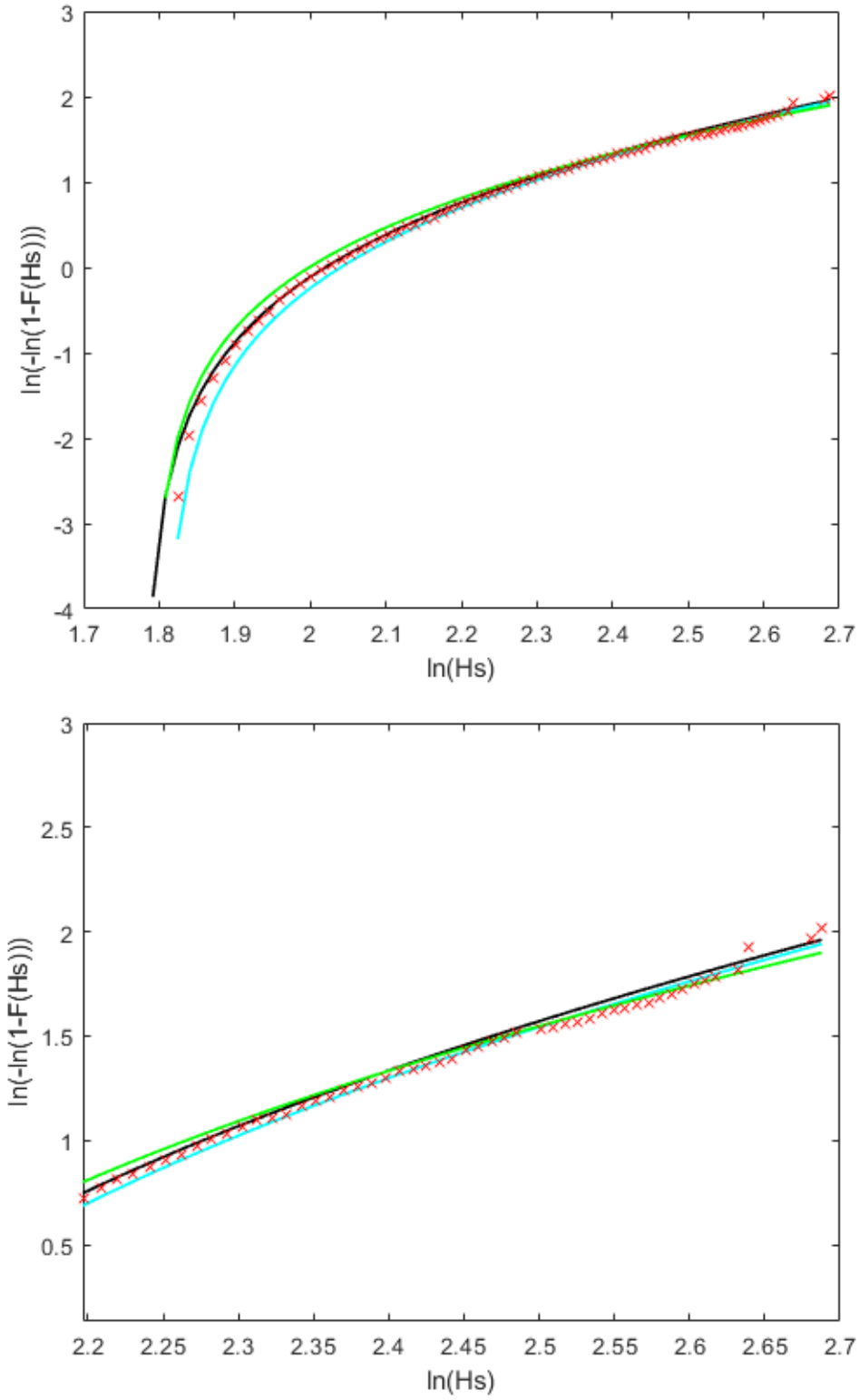

***Figure 3.4**: Cumulative distribution of all H_s >6 m plotted in a Weibull scale for three forms of the Weibull distribution. All 3 fits tend to the conservative side. The lines would be straight in the case of $\lambda = 0$.*

3.2. Extreme values of the significant wave height

With the fitted probability distributions of H_s it was then necessary to find the values that would have specific probabilities of exceedance. The cumulative distribution functions give probabilities of no-exceedance (or $1 - P(exceedance)$) for a certain value of the random variable they describe, however the Weibull model can be easily manipulated algebraically to obtain an inverse function that returns the H_s value for a given probability of exceedance. From (1.3), the values with probabilities of exceedance of 1 in 100 years and 1 in 10,000 years (corresponding to ULS and ALS limit state designs) are calculated by

$$H_s = \lambda + \alpha[-ln(1-F)]^{\beta} \tag{3.1}$$

where F is the probability of no exceedance

As seen in the previous chapters, the probabilities of exceedance must be corrected to account for only a fraction of the 3-hour sea states being taken for modelling. The H_s become

$$H_s = \lambda + \alpha\left[-ln\left(\frac{1-F}{N_{1y}^*}\right)\right]^{\beta} \tag{3.2}$$

Now denoting the H_s as $H_{s,ULS}$ for a 1 in 100 years probability of exceedance ($F = 0.99$) and $H_{s,ALS}$ for a 1 in 10,000 years probability of exceedance ($F = 0.99$)

The numbers of N_{1y}^* were previously shown in table 2.4

Table 2.4: *N1y **

		Analysis method	
		All storm steps	Storm peaks only
Threshold	6 m	61.6	13.0
	7 m	31.1	7.5
	8 m	15.3	4.2

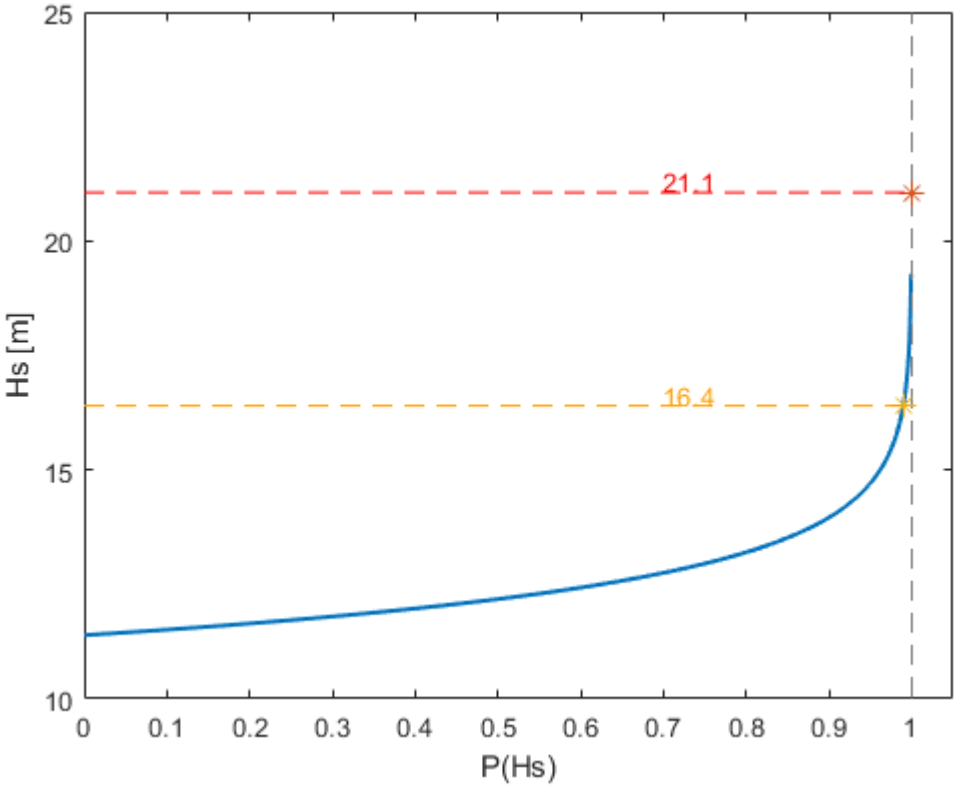

***Figure 3.5**: 100 years and 10,000 years significant wave height estimated from a 3-parameter Weibull fit of the data corresponding to H_s <6 m for the wind sea*

***Table 3.2** : ULS and ALS significant wave heights from a 3-parameter Weibull model. Wind sea*

	$Hs, ULS\ [m]$	$Hs, ALS\ [m]$
All Hs>6 m	16.4	21.1
All Hs>7 m	16.2	20.7
All Hs>8 m	16.1	20.3
Storm peaks with Hs>6 m	16.2	21.6
Storm peaks with Hs>7 m	16.0	21.0
Storm peaks with Hs>8 m	15.8	20.5
All sea states*	18.3	24.5

3.3. Peak period given a significant wave height

Estimating the extreme values of H_s is just a part of estimating the extreme sea states. By looking at the scatter plots of H_s and T_p it is not possible to determine with certainty which T_p would correspond to a given H_s, the uncertainties would be greater with the extremes of H_s, which are outside of the area encompassed by the scatter points. The approach to determine T_p given H_s was to model a probability function of T_p for each H_s and make it a continuous function in both domains. The procedure -from Haver, 2018 and somewhat simplified- is described below, considering an omnidirectional sector for the incoming waves. **This was done for all sea states.**

For a given significant wave height the peak periods follow a Log-Normal distribution:

$$\boldsymbol{f(T_p|H_s) = \frac{1}{\sqrt{2\pi}\,\sigma(H_s)[T_p]}\, exp\left\{-0.5\left(\frac{\ln(T_p)-\mu(H_s)}{\sigma(H_s)}\right)^2\right\}} \quad (3.3)$$

with

$$\mu(H_s) = E\left[ln(T_p)|H_s\right] \quad (3.4)$$

and

$$\sigma^2(H_s) = Var\left[ln(T_p)|H_s\right] \quad (3.5)$$

To make (3.4) and (3.5) continuous over the H_s domain, curve fits of $E\left[ln(T_p)|H_s\right]$ and $Var\left[ln(T_p)|H_s\right]$ were made. The values of $E\left[ln(T_p)|H_s\right]$ and $Var\left[ln(T_p)|H_s\right]$ were obtained not for each available value of H_s (with increments of 0.1 m), but for binned values of H_s. With 30 bins, ranges of close to 1/2 of a meter resulted (the largest H_s for wind seas registered is 14.7 m). Binning -dividing into classes- was made to smooth the functions. Details on how the continuous curve fits were obtained are not discussed here but the accuracy is seen in the figures below.

Remembering that all the H_s<0.4 m were sorted out of the data set, the solutions for (3.4) and (3.5) for all wind seas yielded the following expressions.

$$\mu(H_s) = 3.876\, {H_s}^{0.0966} - 2.148 \quad (3.6)$$

$$\sigma^2(H_s) = 0.02215\, e^{-0.1495\, x} \quad (3.7)$$

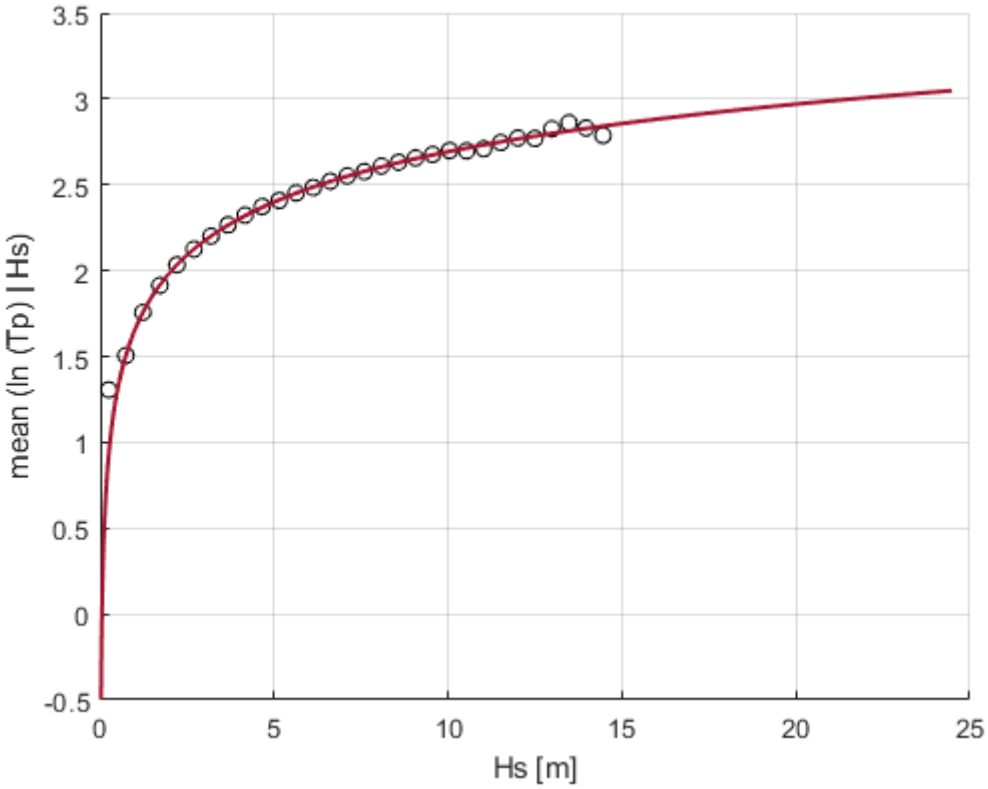

***Figure 3.6**: $E[ln(T_p)|H_s]$ for all directions of the wind seas of the specified NORA10 location with the H_s<0.4 m discarded.*

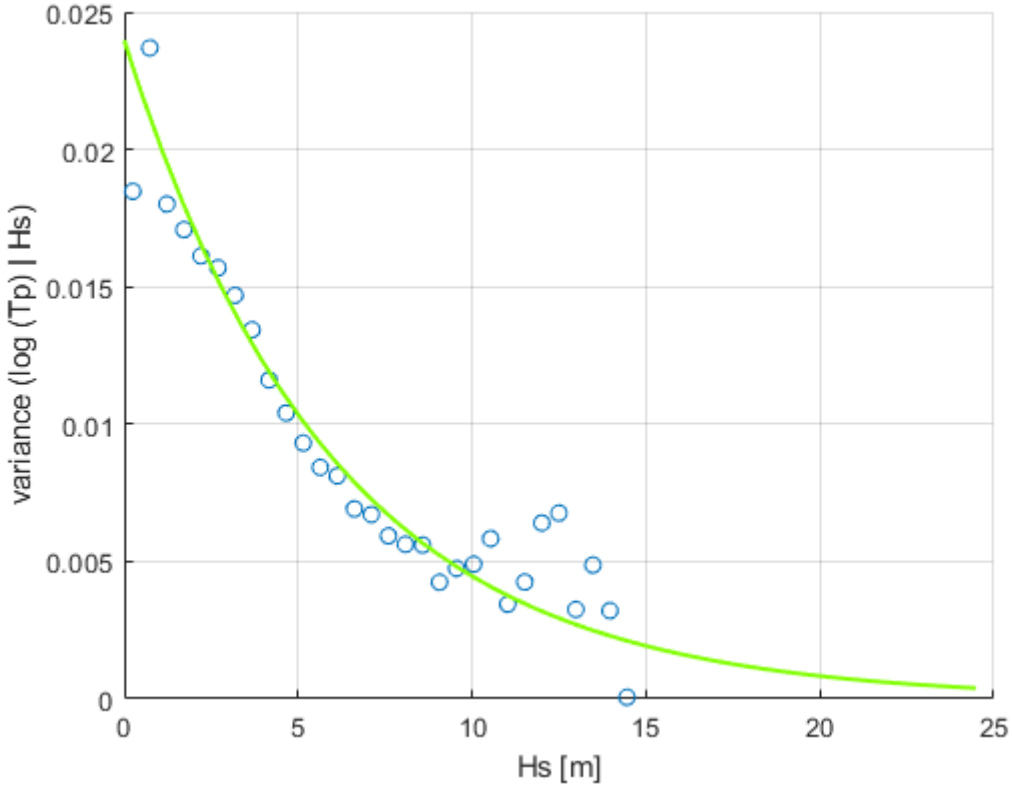

***Figure 3.7**: $Var[ln(T_p)|H_s]$ for all directions of the wind seas of the specified NORA10 location with the H_s<0.4 m discarded.*

The next plots are the conditional distribution of $T_p|H_s$ as a continuous surface over both T_p and H_s domains, and the function when H_s takes certain values:

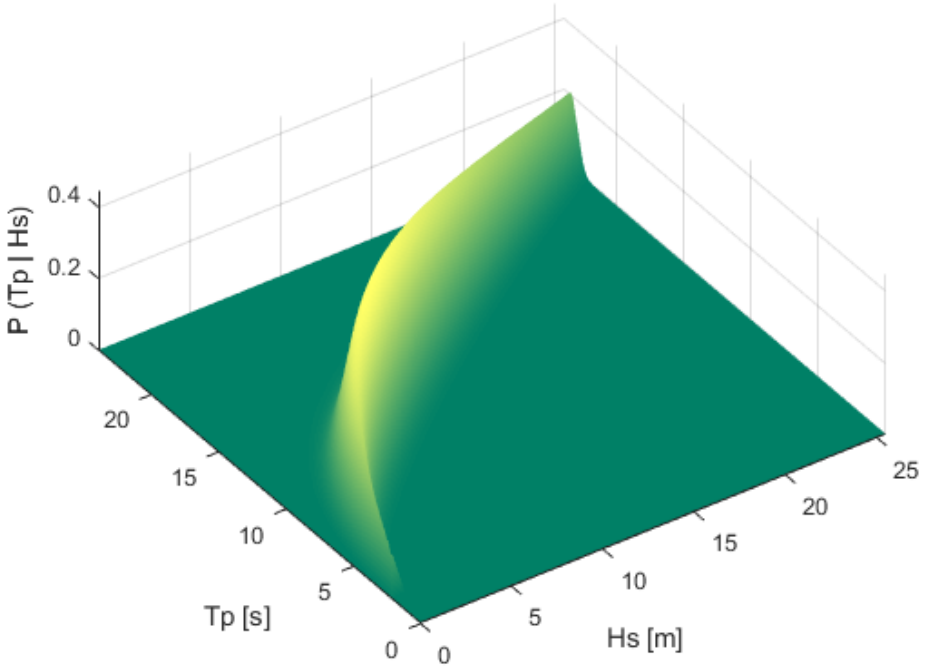

Figure 3.8: *Fitted continuous conditional probability distribution function of the 3-hour peak period given a significant wave height '$f(T_p|H_s)$' for all wind seas (except those corresponding to H_s<0.4 m)*

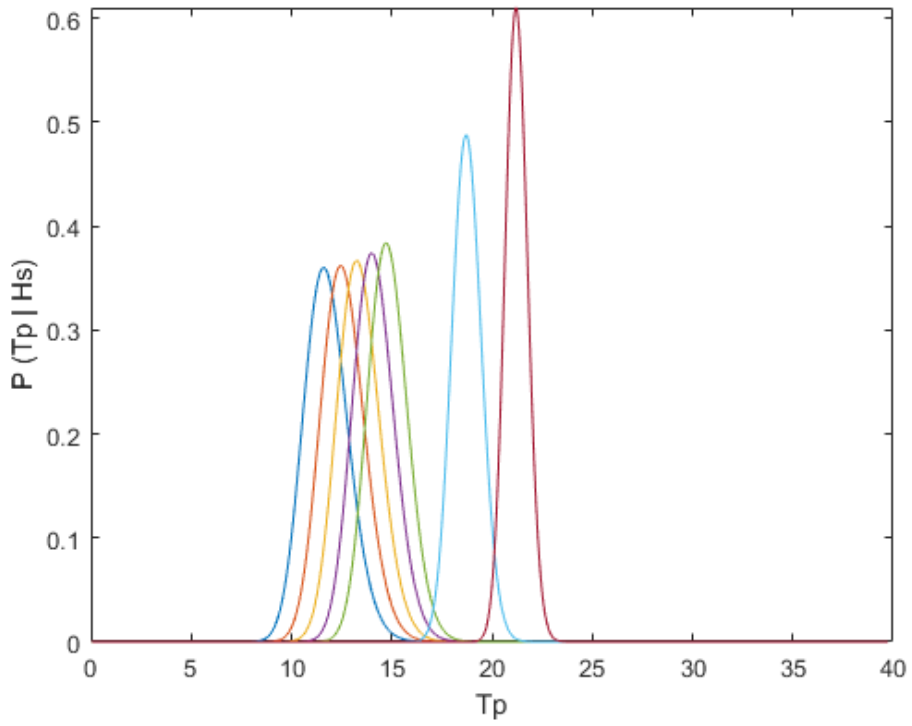

Figure 3.9: *'$f(T_p|H_s)$' follows a Log-Normal distribution. Here plotted for $H_s = 6\ m$, $H_s = 7\ m$, $H_s = 8\ m$, $H_s = 9\ m$, $H_s = 10\ m$, and $H_s = H_{s,ULS} = 18.3\ m$ and $H_s = H_{s,ALS} = 24.5\ m$*

The conditional probability distribution of T_p given H_s could be solved analytically for T_p; first, it can be shown that

$$\int f(T_p|H_s) = -0.5\, erf\left[\frac{\sqrt{0.5}\left(\mu(H_s) - ln(T_p)\right)}{\sigma(H_s)}\right] + c \qquad (3.8*)$$

where erf is the 'Gauss Error Function':

$$\text{erf}(x) = \frac{2}{\sqrt{\pi}}\int_0^x e^{-t^2}\, dt \qquad (3.8.1*)$$

In order to make (3.8*) a cumulative density function (make its image [0,1]), c must equal 0.5. Thus

$$F(T_p|H_s) = 0.5 - 0.5\, erf\left[\frac{\sqrt{0.5}\left(\mu(H_s) - ln(T_p)\right)}{\sigma(H_s)}\right] \qquad (3.8)$$

and $F \rightarrow [0,1]$. Then if $F(T_p|H_s)$ is to be solved with respect to T_p for a specific F, the resulting curve would be the $F \times 100$ percentile distribution of $T_p|H_s$; a curve describing $T_p|H_s$ with $P(T_p < T_p^*) = F$. (3.8) was solved in this way to produce

$$\boldsymbol{T_p^*(H_s, F) \approx exp\left\{\mu(H_s) - \frac{\sigma(H_s)\, erf^{-1}(1-2F)}{\sqrt{0.5}}\right\} \equiv T_p|H_s} \qquad (\mathbf{3.9})$$

erf^{-1} is the inverse of (3.8.1*) and F is the $F \times 100$ percentile distribution of the equation.

Traditionally, a 90 percentile band would be used to get the design sea states with this approach (figure 3.10)

Figure 3.10 below shows the scatter plot of all wind seas (except those with H_s<0.4 m) of the NORA10 data for the given location and the function of the peak period (equation 3.9) evaluated at $F = 0.05$ and $F = 0.95$ (dashed lines). The design peak periods with this approach correspond to such 5 and 95 percentile distributions evaluated at the extreme values of the significant wave heights obtained in section 3.2. For the airgap of a semisubmersible is can seem obvious that the steeper design sea states are the ones that would raise concern. Nevertheless, it is important not to discard that for certain type of structures it could be the higher periods that affect more for certain aspects of the design. The way of describing design sea states with this approach would be to indicate, for both $H_{s,ULS}$ and $H_{s,ALS}$, the low and the high peak periods. The figure shows $H_{s,ULS}$ and $H_{s,ALS}$ along the 50 percentile distribution -in the continuous line- as a reference. The design H_s, T_p pairs correspond to the red points, which are the 5 and 95 percentile distributions evaluated at $H_{s,ULS}$ and $H_{s,ALS}$. For this figure, although $T_p^*(H_s, F)$ is solved for all sea states, the points in this figure correspond to the extremes that were estimated for all (wind) seas with a significant wave height greater than 6 m.

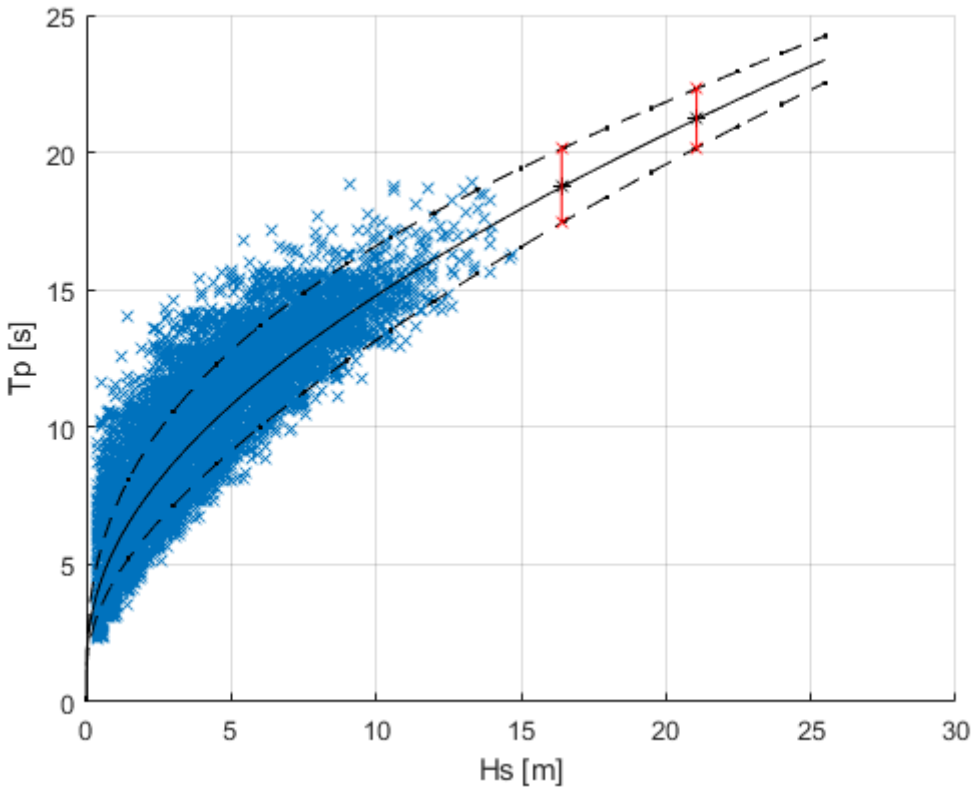

Figure 3.10: *90 percentile band of T_p^* showing the peak periods corresponding to the design significant wave heights. the extremes of H_s for this figure correspond to ULS and ALS design probabilities of exceedance and were estimated for all wind seas with H_s>6 m.*

3.4. Contour plots for estimating extreme sea states

Observing the H_s, T_p data on a scatter plot it is clear that due to the physics of the sea conditions they tend to follow a certain pattern; more precisely, given the how the scatter points have been distributed throughout the time of the observations, they follow a certain probability distribution of the location they 'land' on in this two dimensional space of H_s and T_p. Assuming that this probability distribution is constant over time requires the stationarity condition (described in the problem setup). This is fulfilled, as both H_s and T_p behave similarly over the years.

The idea of the probability contours is firstly, that the location of a point on the H_s, T_p plane follows a joint distribution that depends on both H_s and T_p; a distribution that should look like a 3-dimensional surface over the H_s, T_p space with the third axis -the 'elevation', or 'z' axis- representing the probability of a H_s, T_p pair landing on a specific location of the plane. Secondly, fixing a value for this joint distribution, i.e. fixing the 'z' axis in a specific value results in a contour with that probability of the H_s, T_p pair landing anywhere along that contour line. In this way, it was possible to produce contours for all possible sea states with ULS and ALS probabilities of occurrence. Sea states along the curves are possible 'design sea states' for the particular limit state design.

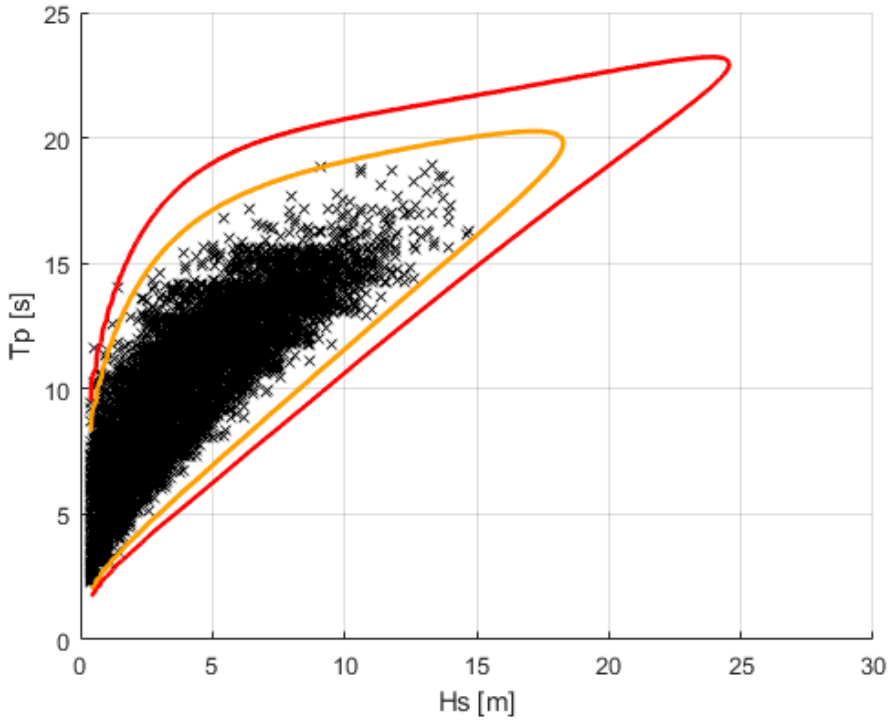

***Figure 3.11**: Contour plots for sea states with probabilities of exceedance of 1 in 100 years and 1 in 10,000 years. Produced for all sea states, where $H_{s,ULS} = 18.3\ m$ and $H_{s,ALS} = 24.5\ m$*

The method to create the contours in a simple way consisted on determining the joint probability distribution of H_s and T_p. Which can be either the product $f(H_s|T_p)f(T_p)$ or $f(T_p|H_s)f(H_s)$. Both alternatives would make the same 3D surface, but the conditional of the peak period given the significant wave height and the marginal distribution of the significant wave height were already determined in chapters 3.3 and 3.1, respectively. Thus

$$\boldsymbol{f(H_s, T_p) = f(T_p|H_s)\, f(H_s)} \qquad \textbf{(3.10)}$$

from equation (3.3):

$$f(T_p|H_s) = \frac{1}{\sqrt{2\pi}\,\sigma(H_s)[T_p]} exp\left\{-0.5\left(\frac{\ln(T_p) - \mu(H_s)}{\sigma(H_s)}\right)^2\right\}$$

and the derivation of (1.3) gives the density function of H_s with Weibull model:

$$f(H_s) = \frac{d}{dH_s}F(H_s) = \frac{d}{dH_s}\left[1 - exp\left\{-\left(\frac{H_s - \lambda}{\alpha}\right)^{\beta}\right\}\right]$$

$$f(H_s) = \frac{\beta}{\alpha} exp\left\{-\left(\frac{H_s - \lambda}{\alpha}\right)^{\beta}\right\}\left(\frac{H_s - \lambda}{\alpha}\right)^{\beta} \qquad (3.10.1)$$

Both $f(T_p|H_s)$ and $f(H_s)$ were solved for all sea states

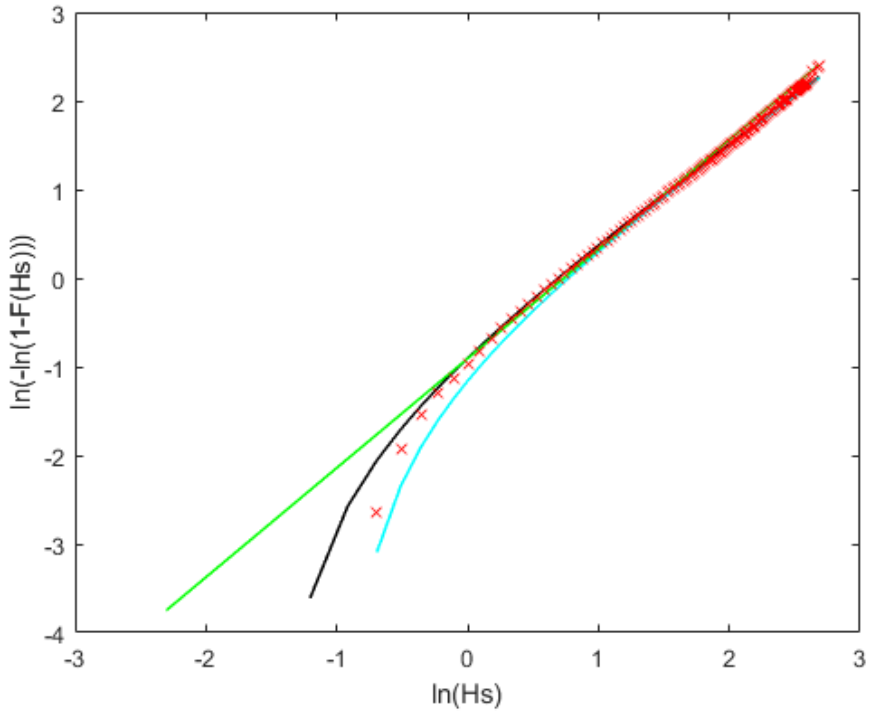

***Figure 3.12**: If a 2-parameter Weibull distribution (equation 1.4) without a threshold was used -for the case of all sea state-, $F(H_s)$ would result in a straight line on the Weibull scale ($\lambda = 0$).*

The values to fix $f(H_s, T_p)$ to to produce the contours can't be obtained from $1 - 0.01/N_{1y}^*$ and $1 - 0.0001/N_{1y}^*$, because the distribution is not the cumulative. While there may be many ways to obtain these numbers, a simple way was to try different values until the largest significant wave height in a contour met the significant wave height for the corresponding limit state design.

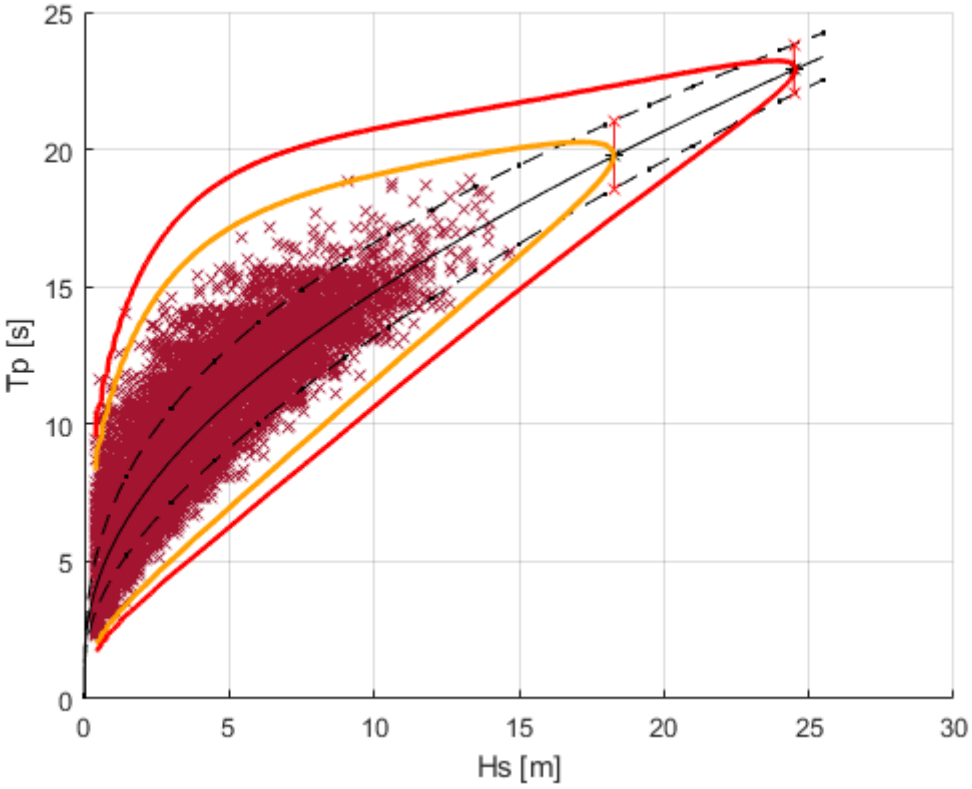

***Figure 3.13**: ULS and ALS sea states from contours vs from Weibull analysis and $T_p(H_s, F)$*

Figure 3.14 shows the contours that were produced by iterating values of $f(H_s, T_p)$ until the extreme values of H_s, met the extreme values of H_s obtained from the Weibull analysis. It should be noted that the extreme H_s from the contours occur by the 50 percentile distribution of T_p^*. With the contours correctly plotted, the figure shows how the contour method is superior than using 90 percentile band of T_p^* for estimating extreme sea states by not being unnecessarily conservative (Lower periods for a fixed H_s → steeper seas → higher relative surface elevations).

4. Extreme relative surface elevations with the contour method

Having obtained the contours for ULS and ALS design, it was possible to perform a response analysis analogous to the one in chapter 2 but with the use of the contour lines. The main idea is that the response analyses are not done for measured 3-hour sea states, but for design sea states with probabilities of occurrence of 1 in 100 years and 1 in 10,000 years corresponding to Ultimate Limit State an Accidental Limit State designs.

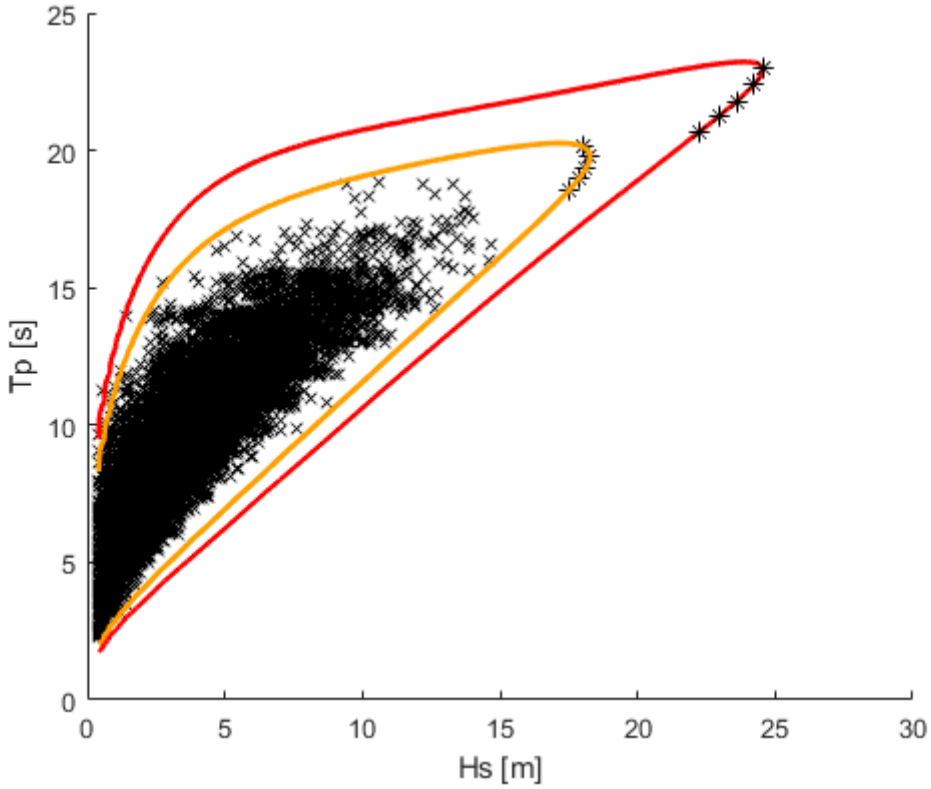

***Figure 4.1**: Contour lines for extreme sea states. Obtained from the all-wind-seas data*

Figure 4.1 shows the selected design sea states. It is common to do the screening for a few combinations along the curves where the significant wave heights reach their extremes and towards the steeper seas. When many combinations were analysed -moving towards even steeper seas- it was observing that the maximum relative surface elevations quickly decayed along the curve. But as expected, seas slightly steeper than those corresponding to the largest design H_s were the most severe.

Table 4.1: *Design sea states*

ULS	H_s [m]	18.02	18.27	18.12	17.90	17.50
	T_p [m]	20.14	19.80	19.35	19.02	18.54
ALS	H_s [m]	24.56	24.22	23.61	22.96	22.23
	T_p [m]	22.96	22.38	21.79	21.25	20.66

The methodology to obtain the results with this approach is explained below. Most parts had at least partially been carried out before.

a) 5 extreme sea states for each limit state design were determined form the contour plots. Table 4.1 shows combinations along the curves that were the closest to produce the largest relative surface elevations.

b) The extreme sea states obtained with the contours do not have associated directions. Looking at the storm severities (end of chapter 2) with respect to different sectors is useful to have an idea of where the most severe storms come from, but there are big uncertainties and it was only smart to direct the extreme sea states not to a particular direction but to a sector.

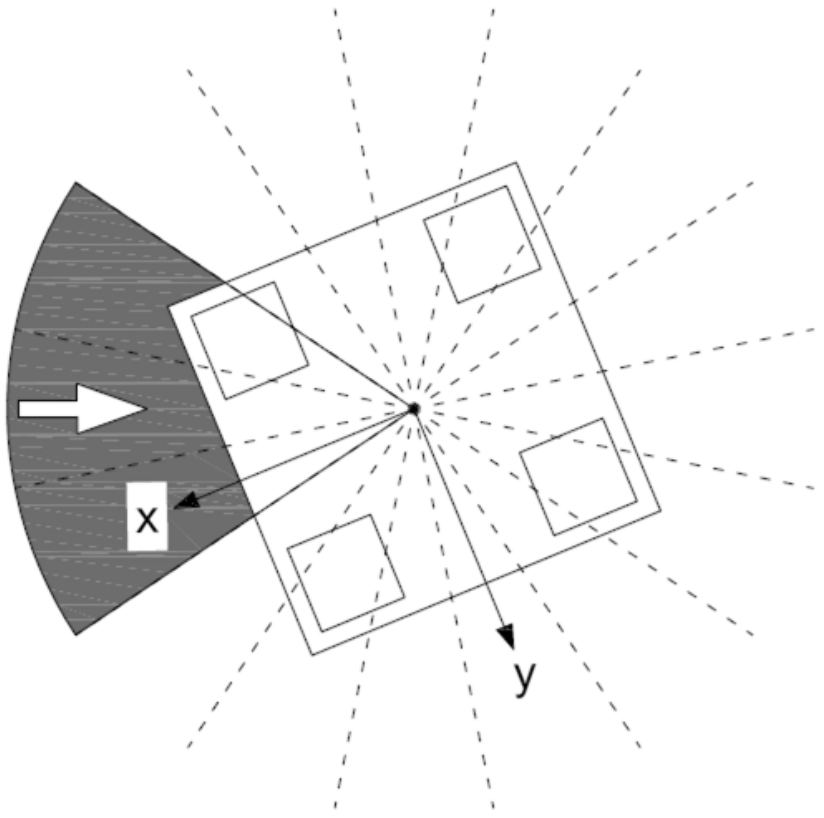

Figure 4.2*: Design sea states were applied from a 67.5°-wide sector coming from the West. Corresponding to the WAMIT 135°, 157.5° and 180° sectors.*

c) The response analysis (explained in chapter 2) was performed until getting the variances of the spectra of the relative surface elevations. For each limit state these were stored as

$$\sigma_{R_p,p}(k,l) = \begin{bmatrix} \sigma_{R_p,p}(k_1,l_1) & \sigma_{R_p,p}(k_1,l_2) & \sigma_{R_p,p}(k_1,l_3) & \sigma_{R_p,p}(k_1,l_4) & \sigma_{R_p,p}(k_1,l_5) \\ \sigma_{R_p,p}(k_2,l_1) & \sigma_{R_p,p}(k_2,l_2) & \sigma_{R_p,p}(k_2,l_3) & \sigma_{R_p,p}(k_2,l_4) & \sigma_{R_p,p}(k_2,l_5) \\ \sigma_{R_p,p}(k_3,l_1) & \sigma_{R_p,p}(k_3,l_2) & \sigma_{R_p,p}(k_3,l_3) & \sigma_{R_p,p}(k_3,l_4) & \sigma_{R_p,p}(k_3,l_5) \end{bmatrix} \quad (3.1)$$

with direction k and sea state l

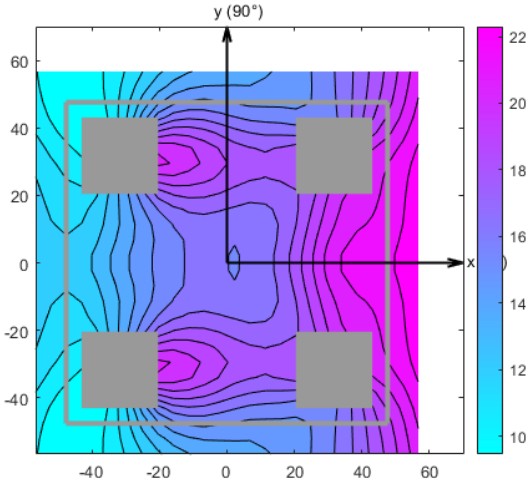

***Figure 4.3**: ALS sea state with $H_s = 24.56\ m$ and $T_p = 22.96$ at 180°*

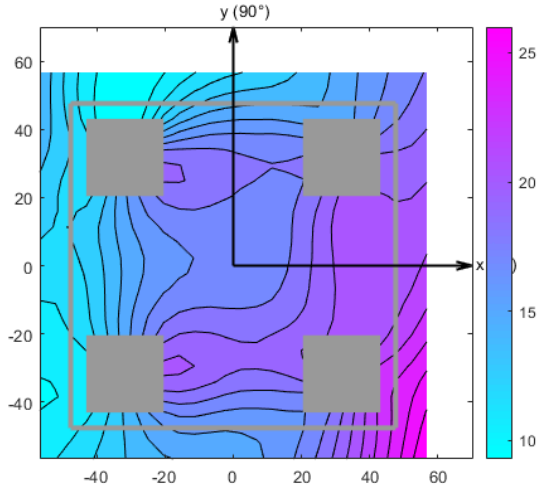

***Figure 4.4**: ALS sea state with $H_s = 24.22\ m$ and $T_p = 22.38\ m$ at 157.5°*

d) In chapter 2 the following formula (from the Rayleigh distribution) was used to describe the distribution of the maximum relative surface elevation for a storm step j.

$$F_{R,j}(r) = \left[1 - exp\left\{-0.5\left(\frac{r}{\sigma_{R_p}}\right)^2\right\}\right]^{n_{3h}} \quad (2.13)$$

Now, instead of a 3-hour storm step, it was used to describe the maximum relative surface elevation for an extreme 3-hour sea state. And instead of computing the MPSMs from solving $F_{R,j}(r) = 1/e$, the **sea-state maximum expected relative surface elevations**, denoted here by $\tilde{z}$, were solved for $F_{R,l}(r) = 0.9$ (0.9 turned out to yield the best results compared to the POT method). For each point under the deck

$$F_{R,l}(\tilde{z}) = 0.9 \quad (3.2)$$

e) The sea-state maximum expected relative surface elevations were filtered so that for each point and for each extreme sea state l, only the largest $\tilde{z}$ -the largest from the three WAMIT sectors- was kept and those were the results for the contour method before determining the worst sea state. For each limit state design

$$\tilde{z}_p(k,l) = \begin{bmatrix} \tilde{z}_p(k_1,l_1) & \tilde{z}_p(k_1,l_2) & \tilde{z}_p(k_1,l_3) & \tilde{z}_p(k_1,l_4) & \tilde{z}_p(k_1,l_5) \\ \tilde{z}_p(k_2,l_1) & \tilde{z}_p(k_2,l_2) & \tilde{z}_p(k_2,l_3) & \tilde{z}_p(k_2,l_4) & \tilde{z}_p(k_2,l_5) \\ \tilde{z}_p(k_3,l_1) & \tilde{z}_p(k_3,l_2) & \tilde{z}_p(k_3,l_3) & \tilde{z}_p(k_3,l_4) & \tilde{z}_p(k_3,l_5) \end{bmatrix} \quad (3.3*)$$

$$\downarrow$$

$$\tilde{z}_p(k,l) = [\tilde{z}_{p,max}(l_1) \quad \tilde{z}_{p,max}(l_2) \quad \tilde{z}_{p,max}(l_3) \quad \tilde{z}_{p,max}(l_4) \quad \tilde{z}_{p,max}(l_5)] \quad (3.3)$$

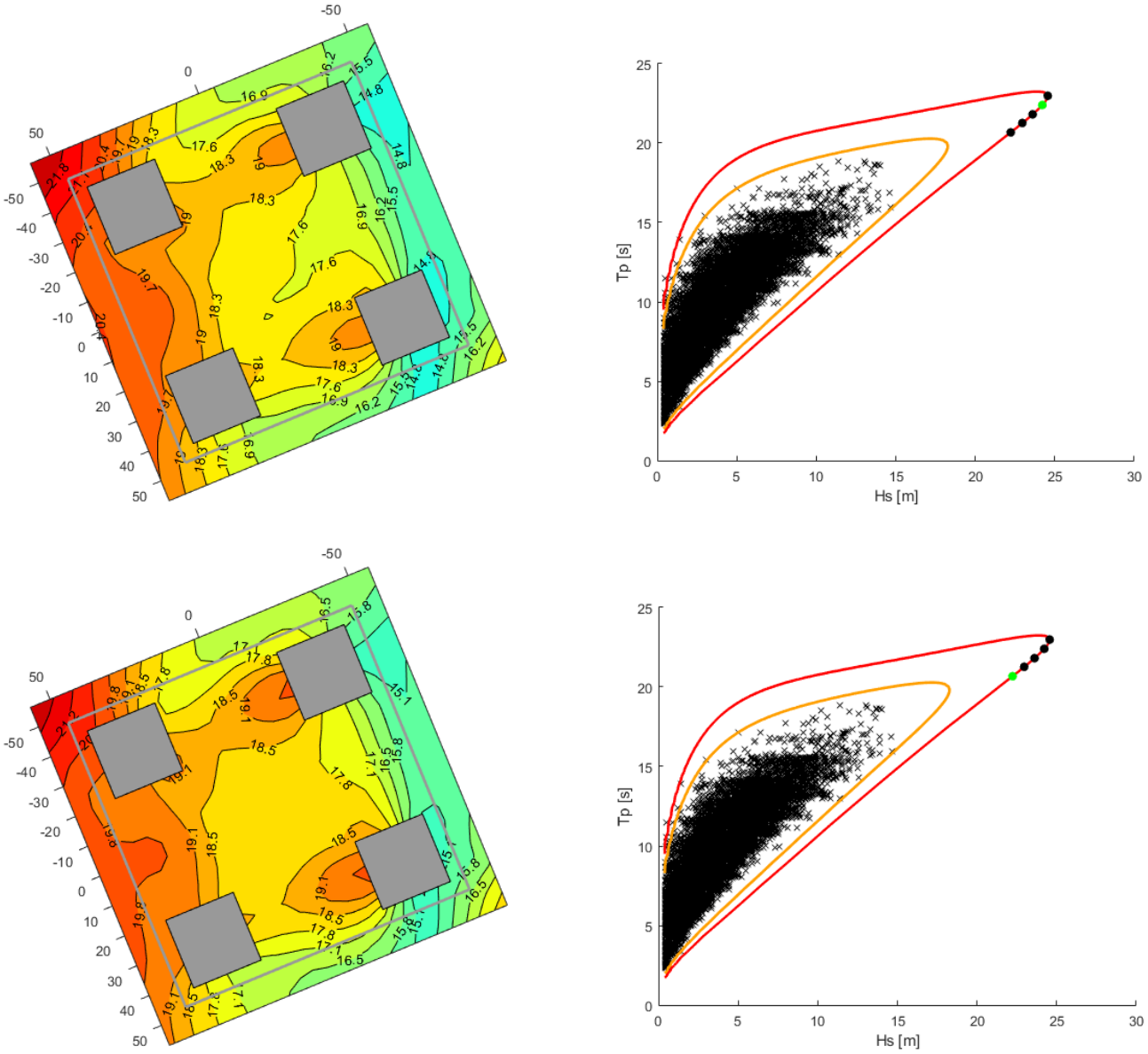

***Figure 4.5**: Two examples of the maximum expected sea-state relative surface elevations for ALS design*

f) The final results for the sea-state maximum expected relative surface elevations required to find the worst of the selected sea states along the contour lines. Since corner 431 was still the critical, a simple storm severity check was made oven this point to find what would be the approximate design sea state.

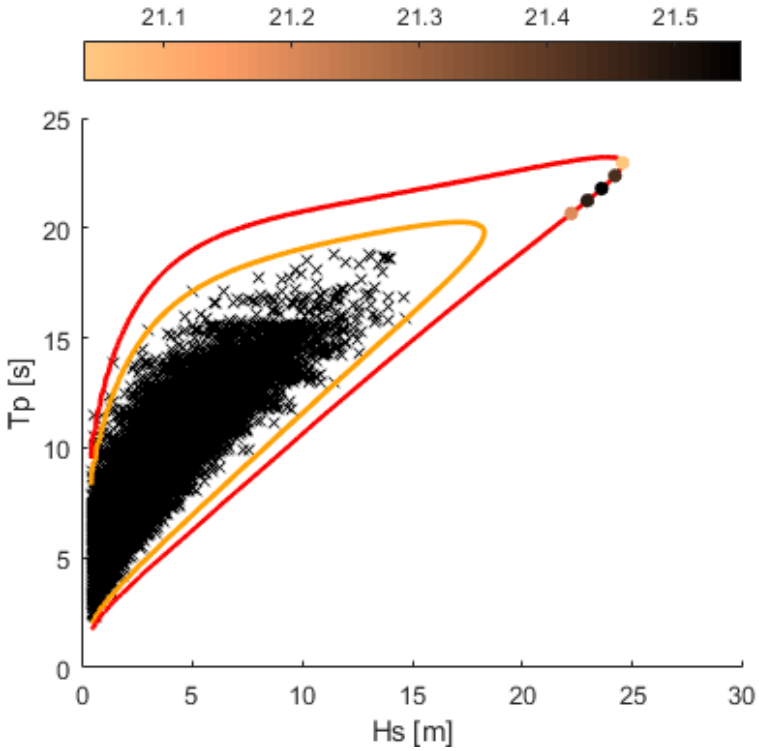

Figure 4.6: *Storm severity on corner 431 under the deck compared from 5 different sea states. The worst sea state in the ALS case turned to be $H_s = 22.96\ m$, $T_p = 21.25\ s$ (Second from the left).*

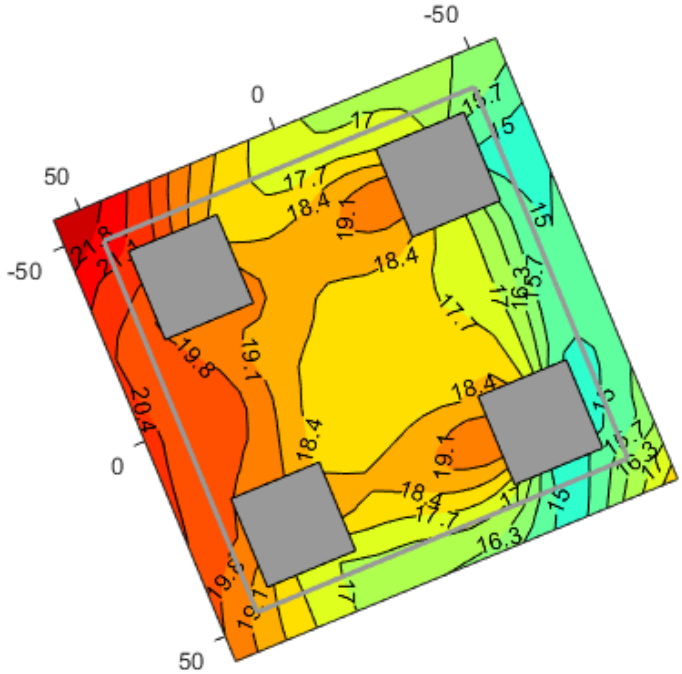

Figure 4.7: Maximum expected relative surface elevations for ALS design

RESULTS

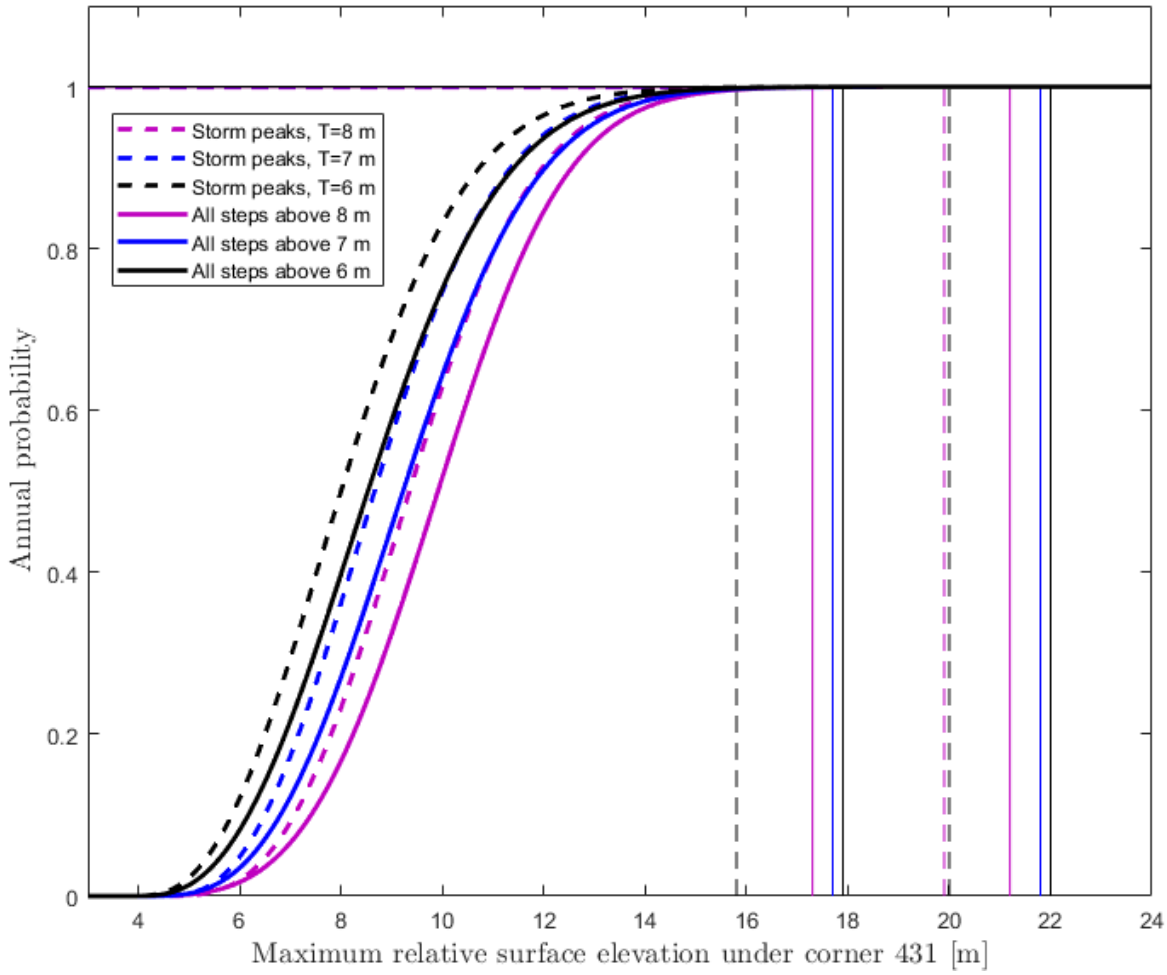

***Figure 15**: Long term distributions of the maximum relative surface elevations under point 431 with short-term variability*

***Table 1** : Minimum required distance from still water lever to underside of the deck (general wave asymmetry factor of 1.2)*

Distance in meters			Limit state		Adjusted annual probability	
			ULS	ALS	ULS	ALS
Method	POT	All storm steps above 6 m	**17.9**	**22**	0.0002	0.000002
		All storm steps above 7 m	**17.7**	**21.8**	0.0003	0.000003
		All storm steps above 8 m	**17.3**	**21.2**	0.0007	0.000007
		Storm peaks with threshold of 6 m	**15.8**	**20**	0.0008	0.000008
		Storm peaks with threshold of 7 m	**15.8**	**20**	0.0013	0.000013
		Storm peaks with threshold of 8 m	**15.8**	**19.9**	0.0024	0.000024
	Contour lines		**18.1**	**21.6**		

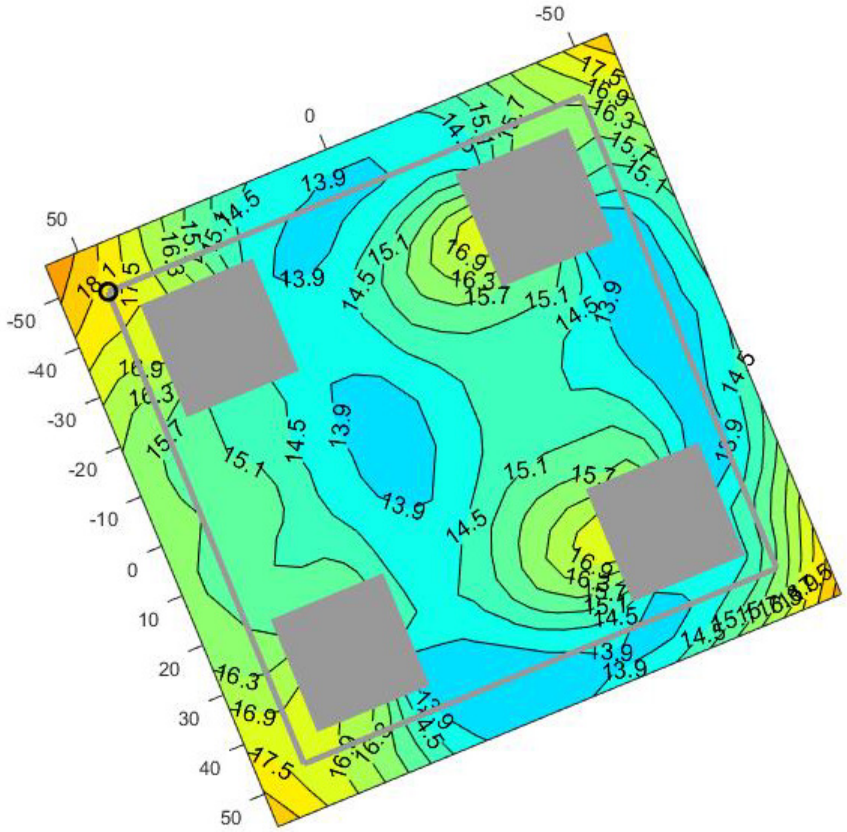

***Figure 16**: ULS minimum airgap from analysis of all storm steps above 6 m*

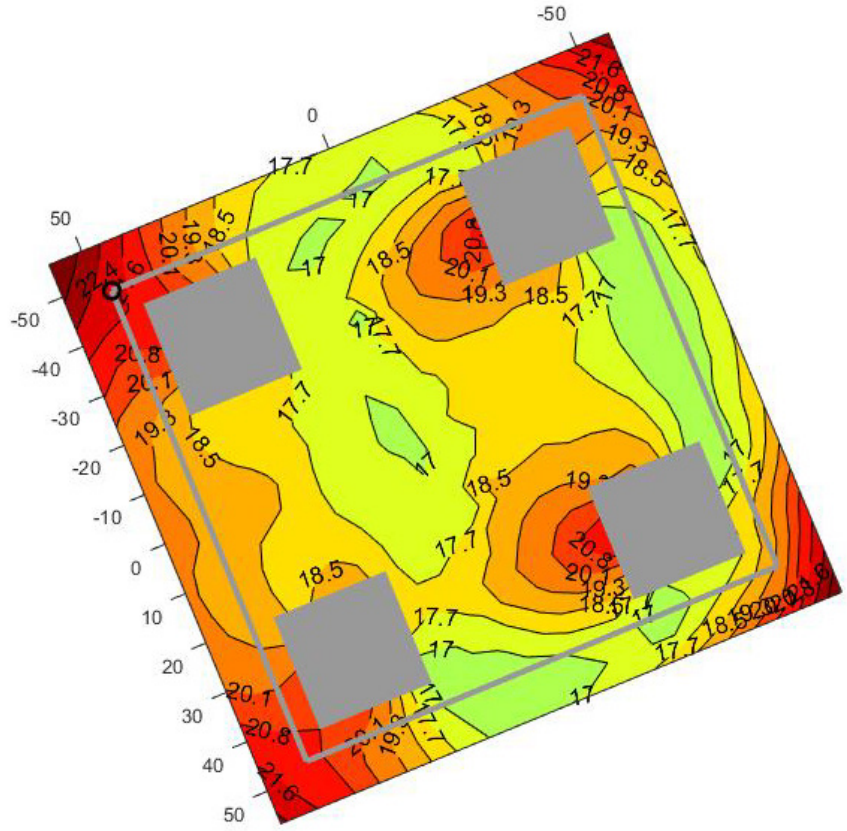

***Figure 17**: ALS minimum airgap from analysis of all storm steps above 6 m*

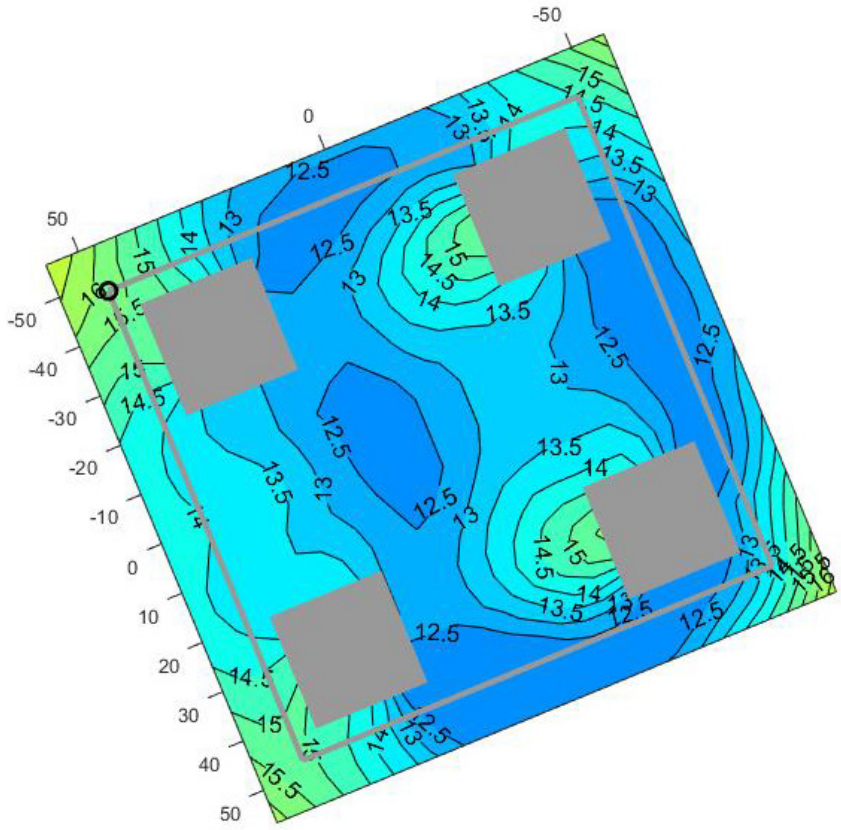

***Figure 18**: ULS minimum airgap from analysis of storm peaks with a threshold of 6 m*

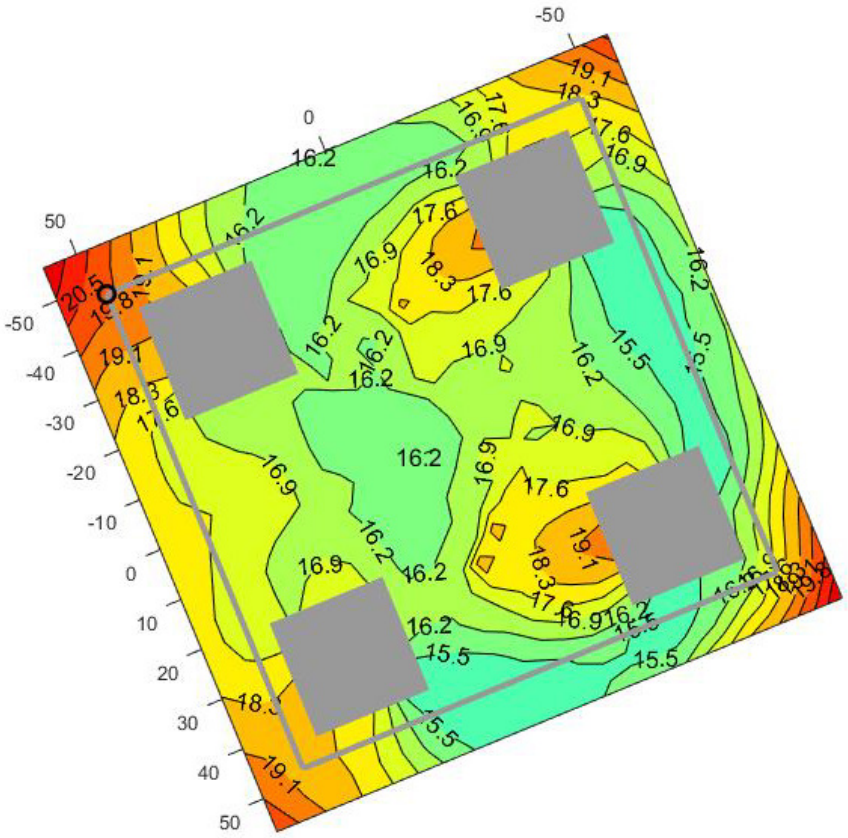

***Figure 19**: ALS minimum airgap from analysis of storm peaks with a threshold of 6 m*

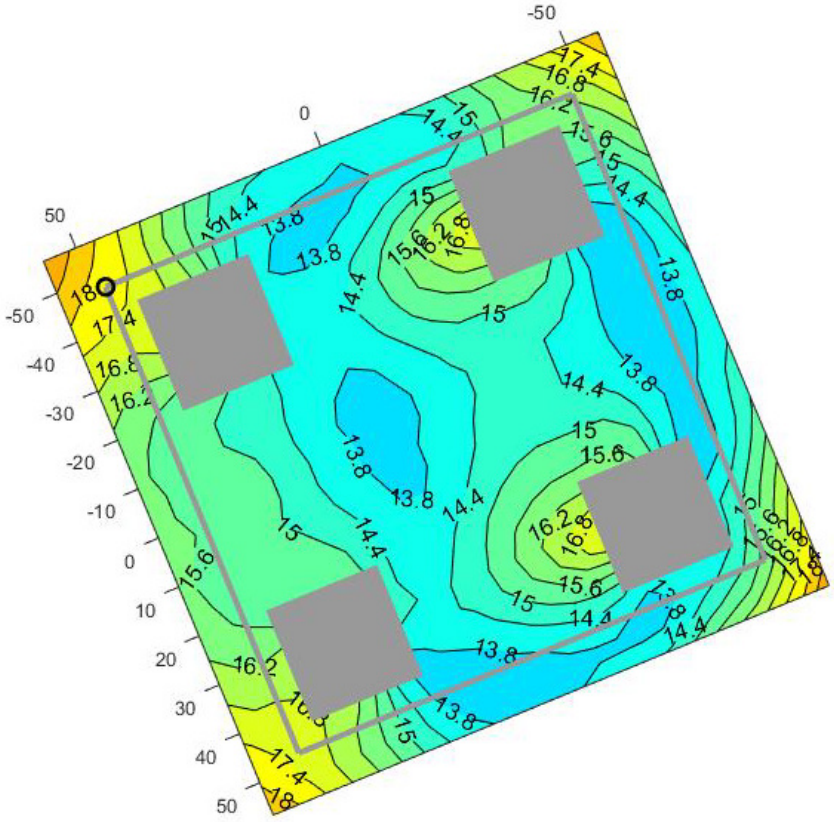

***Figure 20**: ULS minimum airgap from analysis of all storm steps above 7 m*

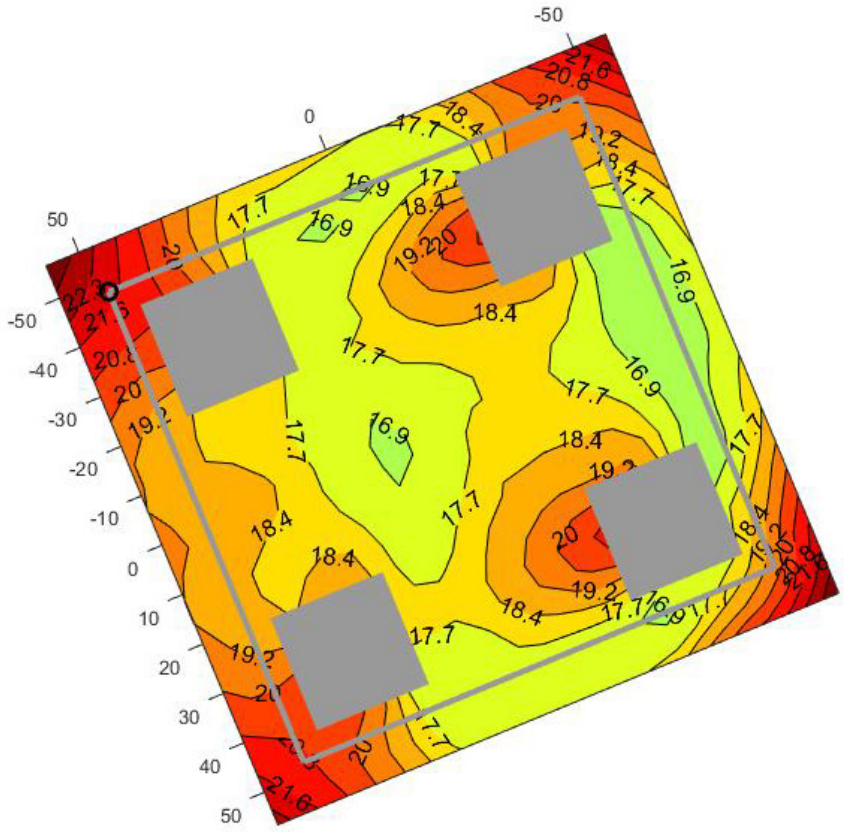

***Figure 21**: ALS minimum airgap from analysis of all storm steps above 7 m*

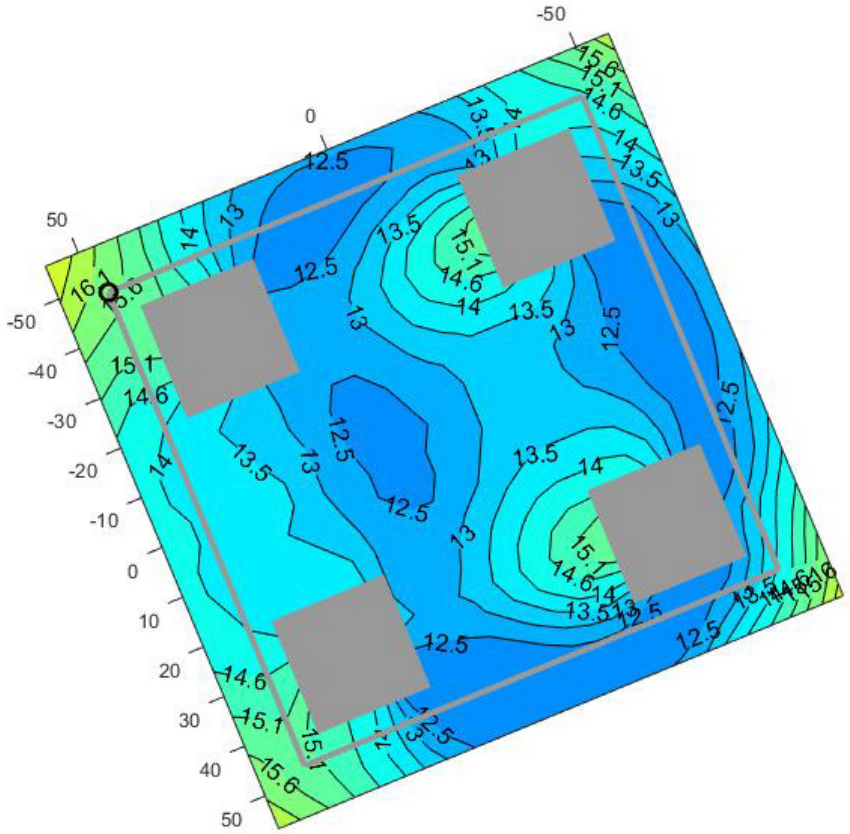

***Figure 22**: ULS minimum airgap from analysis of storm peaks with a threshold of 7 m*

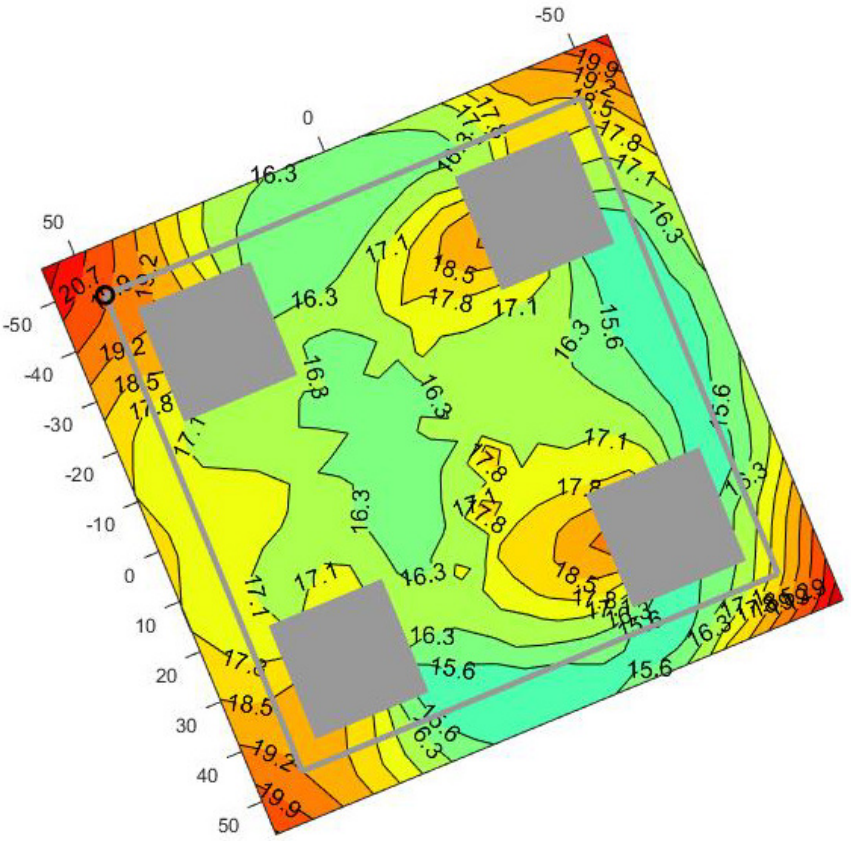

***Figure 23**: ALS minimum airgap from analysis of storm peaks with a threshold of 7 m*

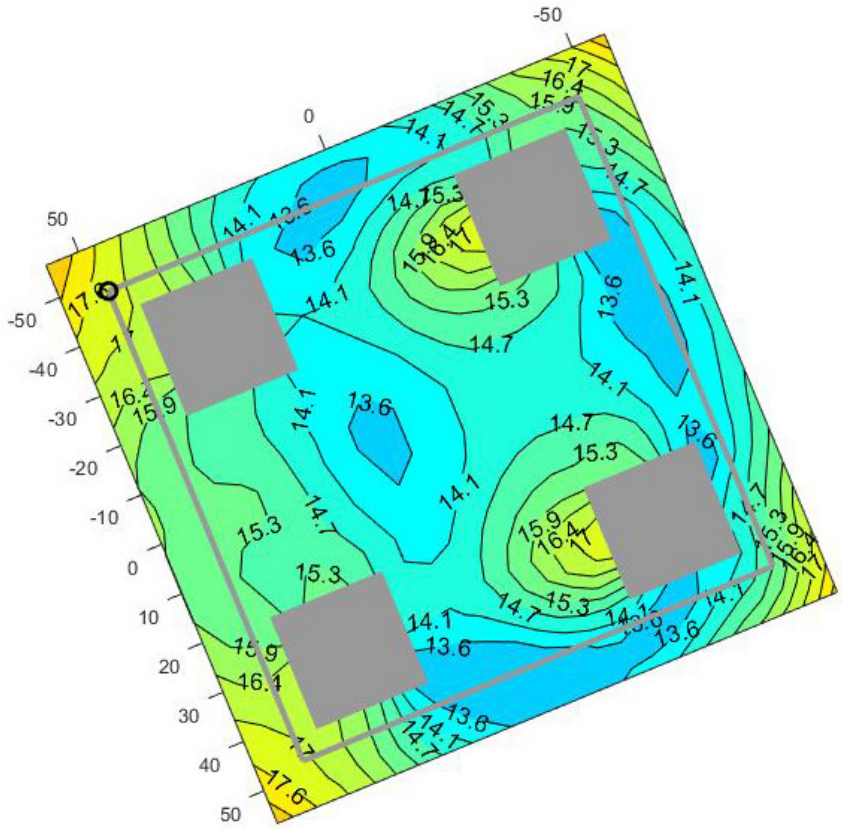

***Figure 24**: ULS minimum airgap from analysis of all storm steps above 8 m*

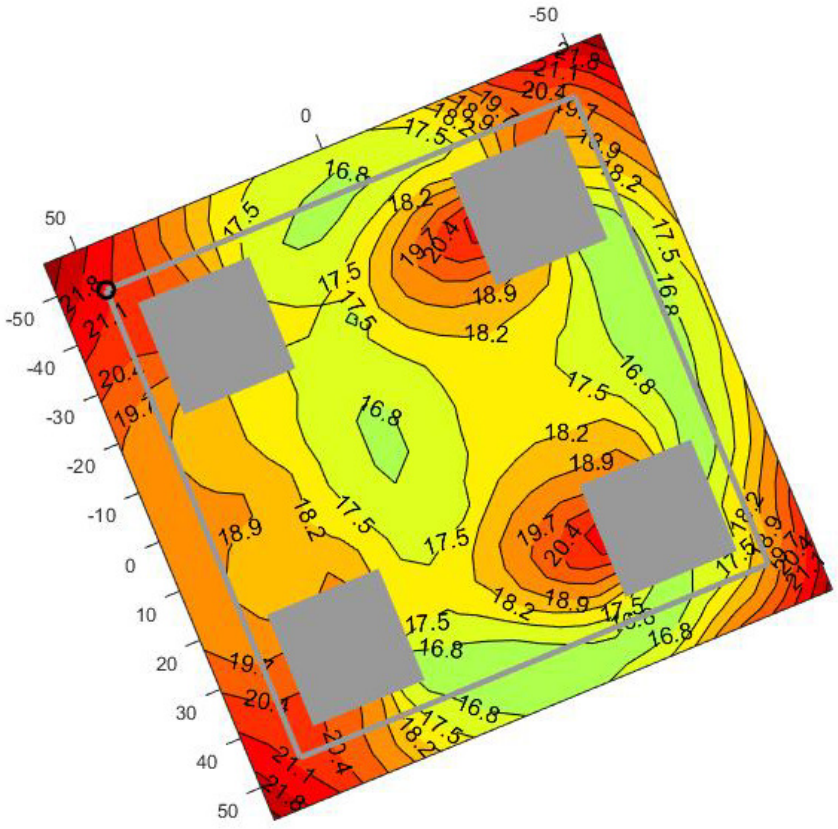

***Figure 25**: ALS minimum airgap from analysis of all storm steps above 8 m*

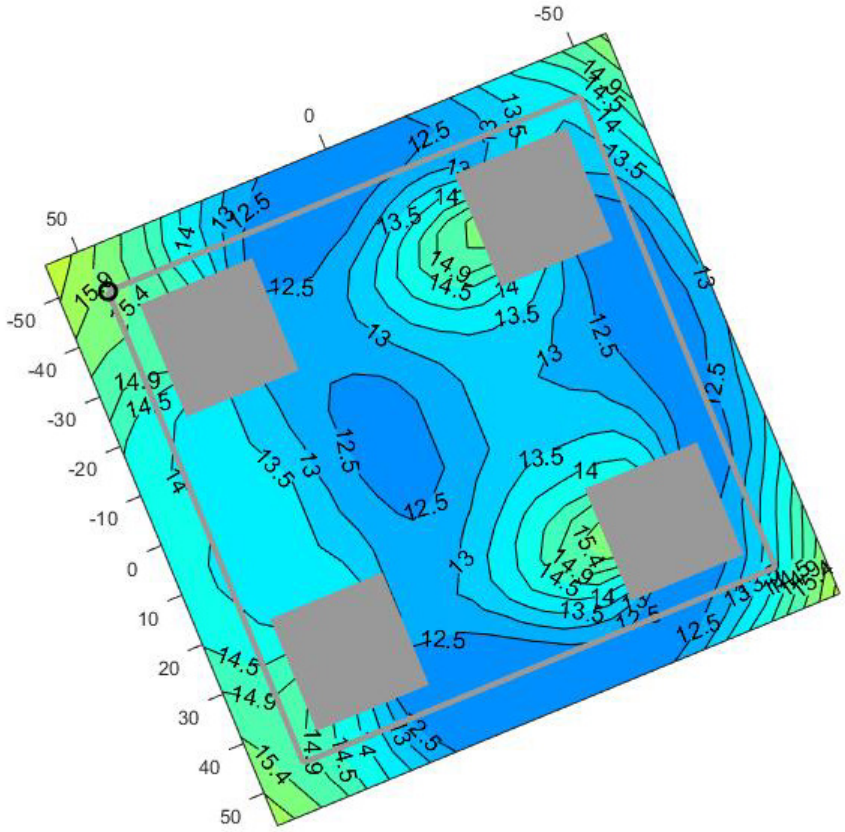

***Figure 26**: ULS minimum airgap from analysis of storm peaks with a threshold of 8 m*

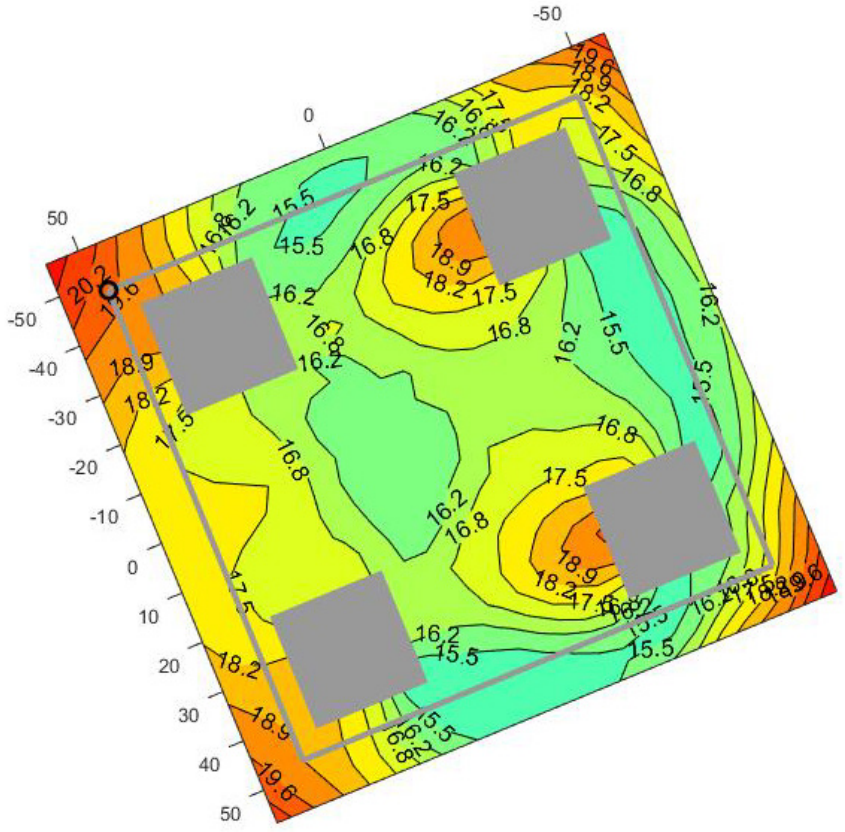

***Figure 27**: ALS minimum airgap from analysis of storm peaks with a threshold of 8 m*

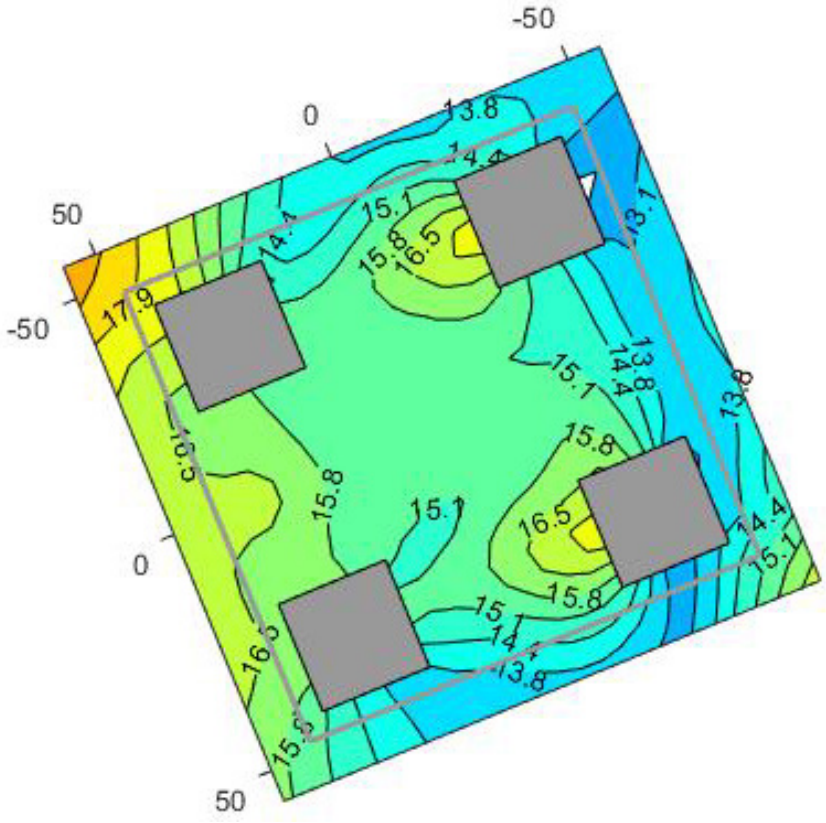

***Figure 28**: ALS minimum airgap **from contour plots** of extreme sea states*

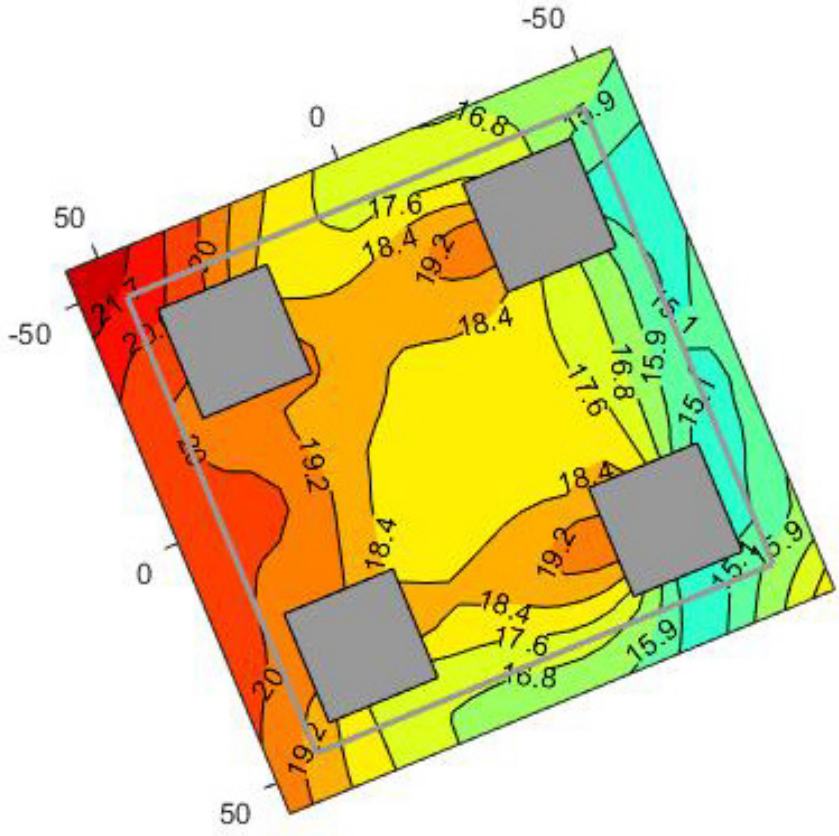

***Figure 29**: ULS minimum airgap **from contour plots** of extreme sea states*

Storm severity: Threshold = 7 m

(Severity for 6 m is in section 2.7)

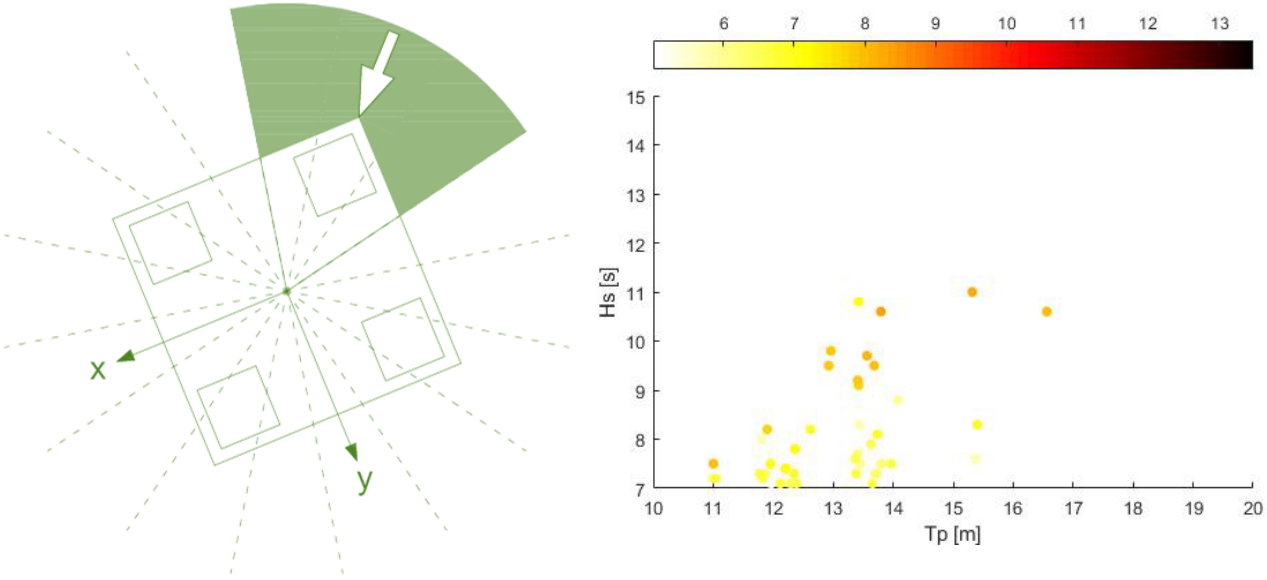

Figure 30: *MPSM at point 431 for all storm peaks with a threshold of 7* ***m****. 22.5° – 67.5° WAMIT.*

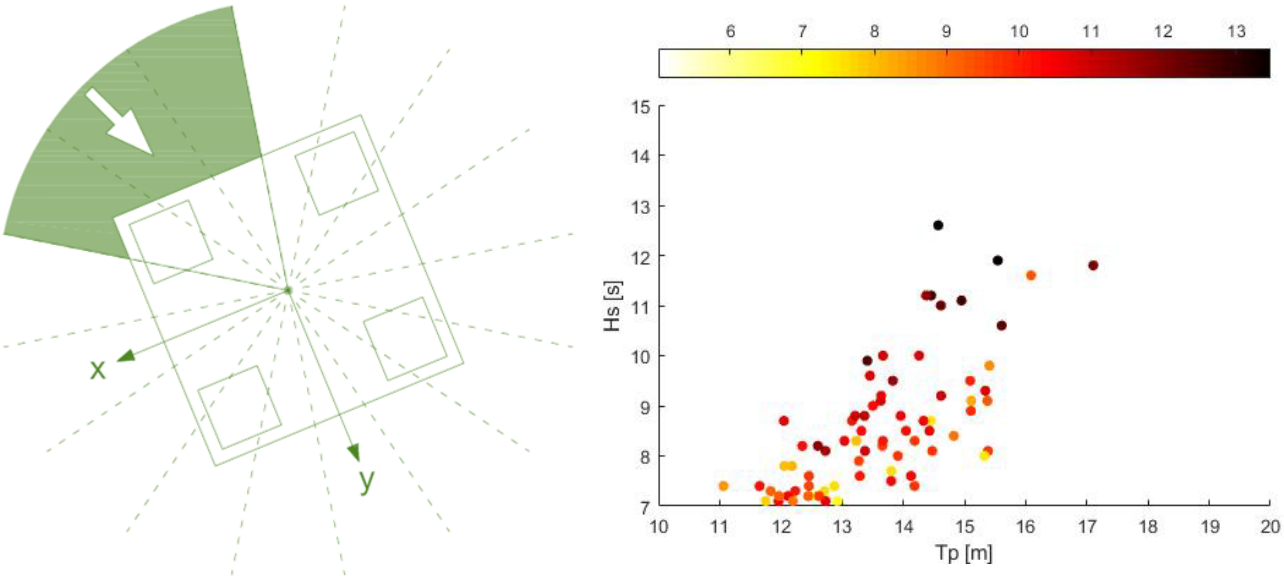

Figure 31: *MPSM at point 431 for all storm peaks with a threshold of 7* ***m****. 90° – 135° WAMIT.*

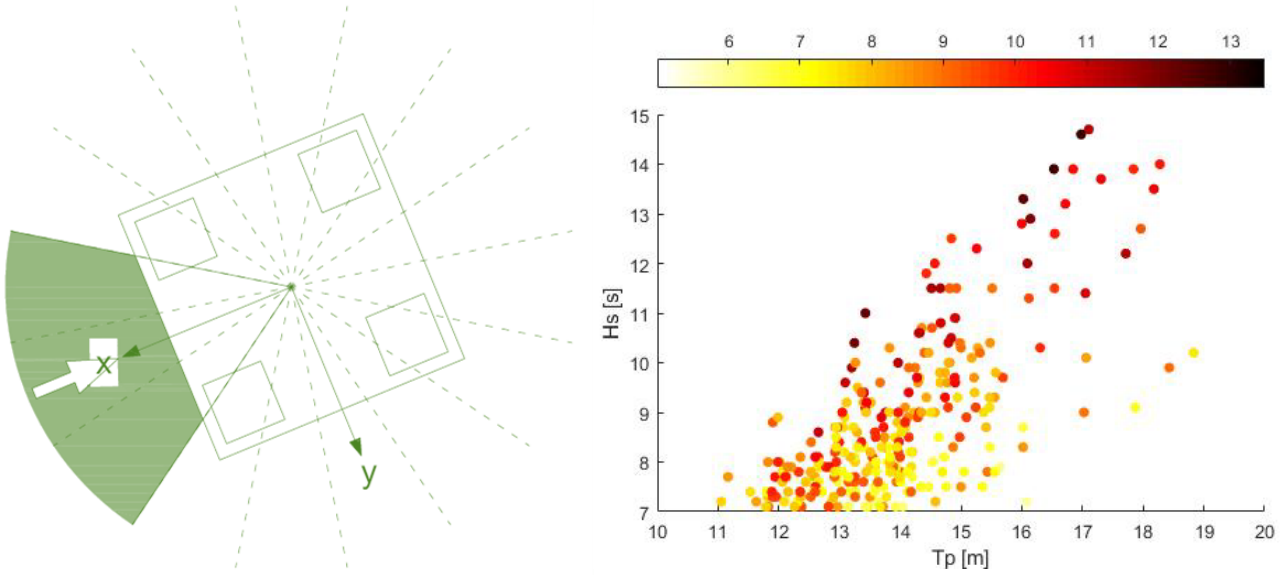

Figure 32: *MPSM at point 431 for all storm peaks with a threshold of* ***7 m****. 157.5° – 202.5° WAMIT.*

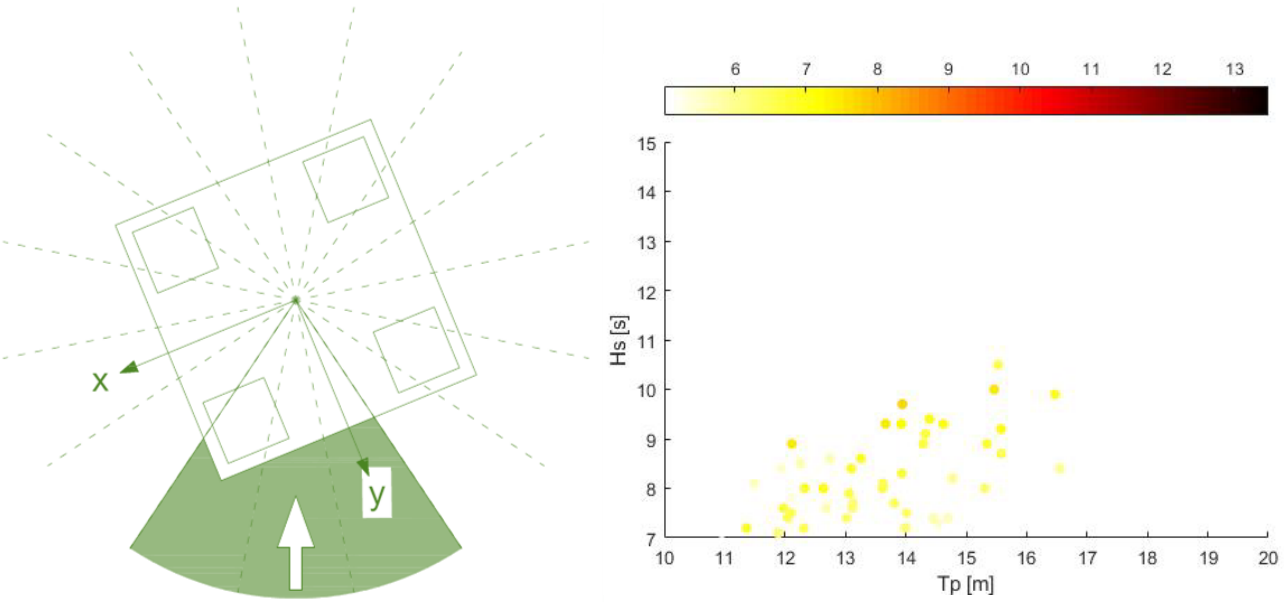

Figure 33: *MPSM at point 431 for all storm peaks with a threshold of* ***7 m****. 225° - 270° WAMIT.*

Storm severity: Threshold = 8 m

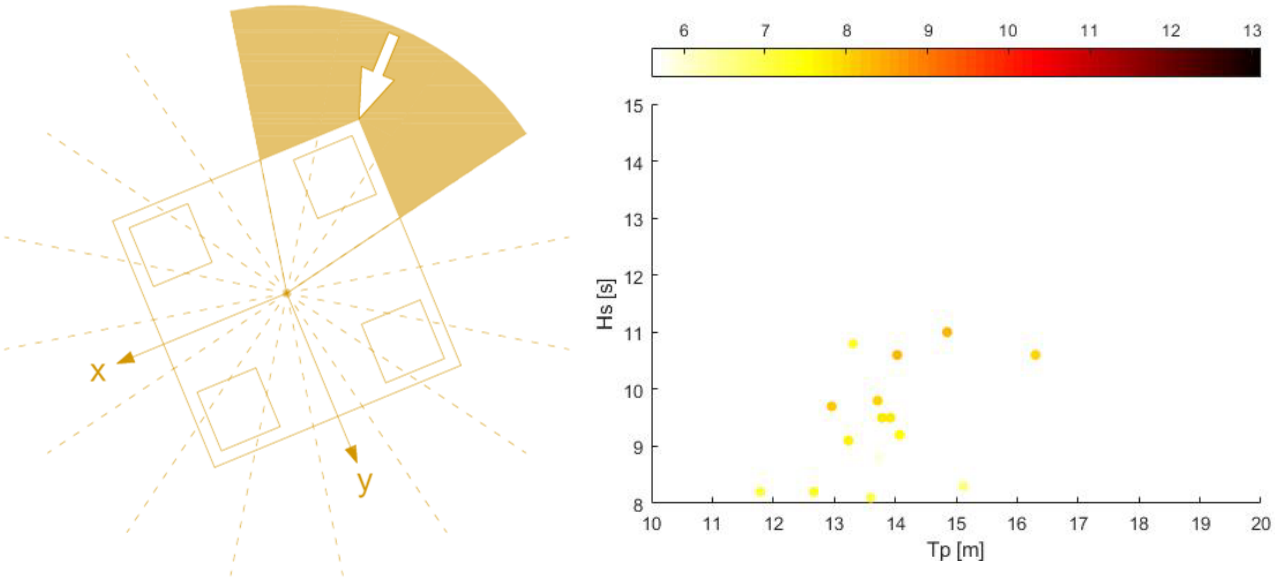

Figure 34: *MPSM at point 431 for all storm peaks with a threshold of* ***8 m****. 22.5° – 67.5° WAMIT.*

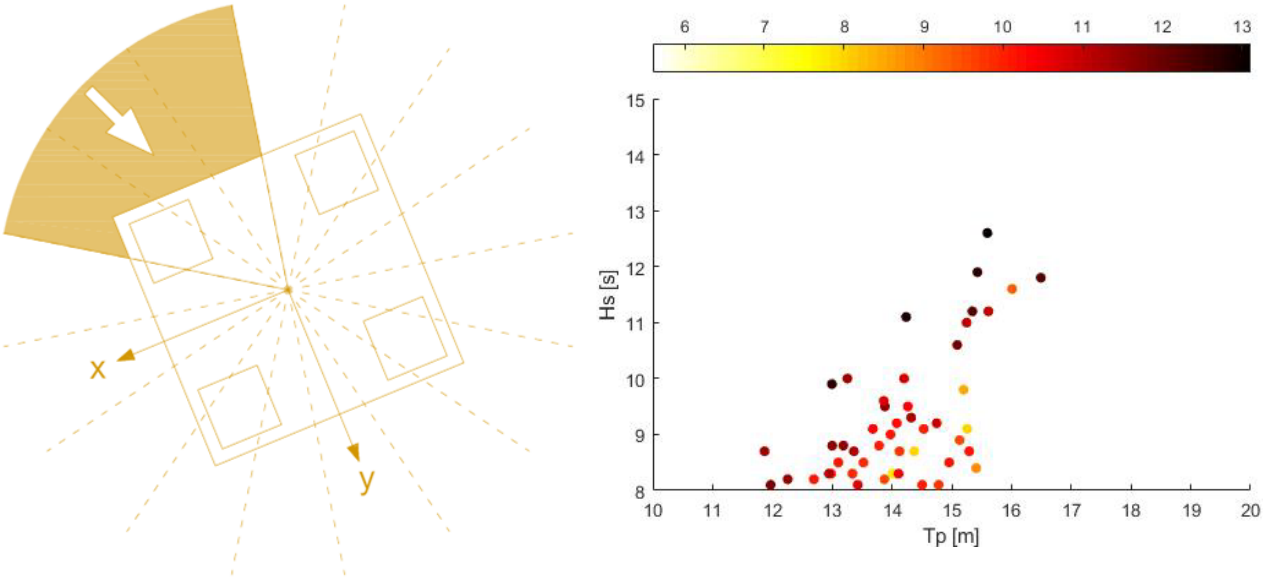

Figure 35: *MPSM at point 431 for all storm peaks with a threshold of* ***8 m****. 90° – 135° WAMIT.*

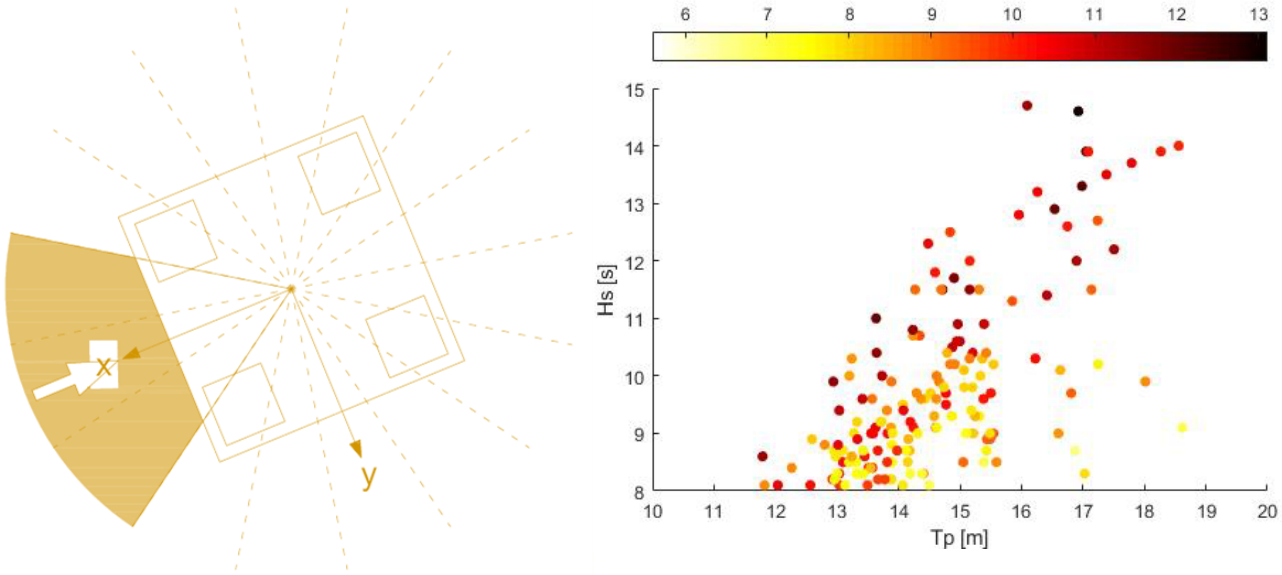

***Figure 36**: MPSM at point 431 for all storm peaks with a threshold of **8 m**. 157.5° – 202.5° WAMIT.*

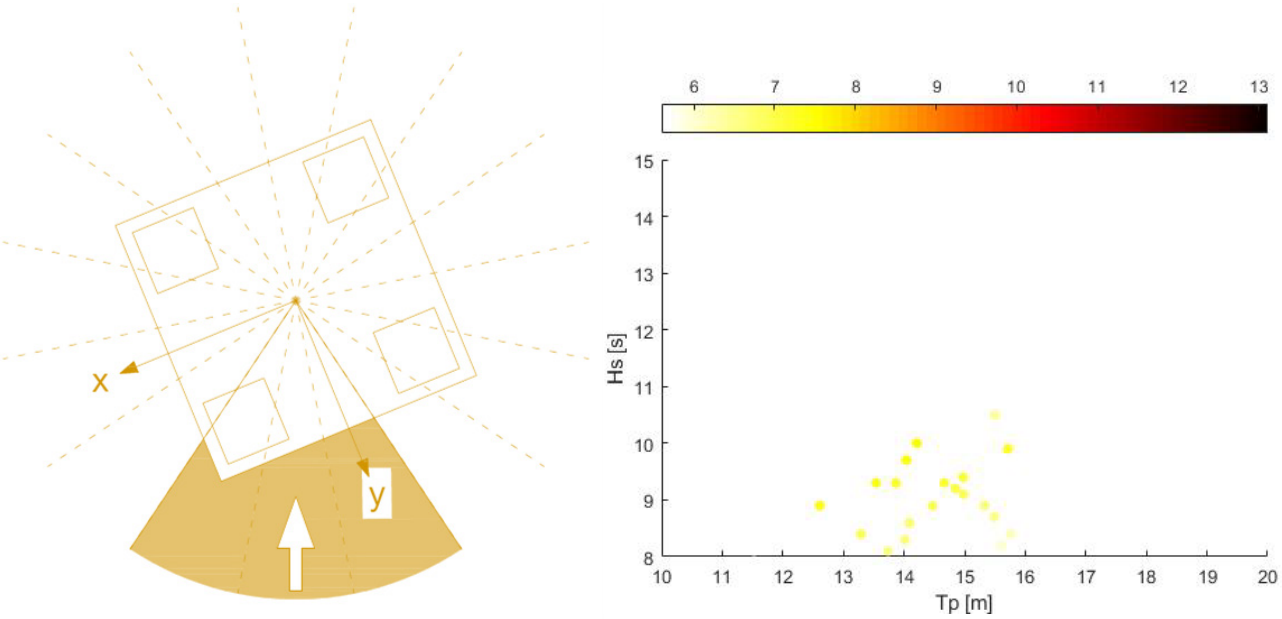

***Figure 37:** MPSM at point 431 for all storm peaks with a threshold of **8 m**. 225° - 270° WAMIT.*

H_s Extremes:

$$T_p \approx exp\left\{\mu(H_s) - \frac{\sigma(H_s)\, erf^{-1}(1-2*0.5)}{\sqrt{0.5}}\right\},\ \mu \text{ and } \sigma \text{ for all sea states} \qquad from\ (3.9)$$

***Table 2**: 1 in 100 years significant wave height and corresponding expected peak period*

100 years Hs [m]	Type of weibull distribution		
Expected Tp [s] (F=0.5)	**3 parameters**	2 parameters for Hs - threshold	3 parameters with λ = threshold
All steps with Hs > 6 m	**16.4**	17.3	16.6
	18.7	19.2	18.8
All steps with Hs > 7 m	**16.2**	16.9	16.4
	18.6	19.0	18.7
All steps with Hs > 8 m	**16.1**	16.6	16.2
	18.5	18.9	18.6
Storm peaks with threshold = 6 m	**16.2**	17.0	16.4
	18.6	19.1	18.7
Storm peaks with threshold = 7 m	**16.0**	16.6	16.2
	18.5	18.8	18.6
Storm peaks with threshold = 8 m	**15.8**	16.4	16.1
	18.4	18.7	18.6
All sea states	**18.3**	15.9	18.4
	19.8	18.5	19.9

***Table 3**: 1 in 10,000 years significant wave height and corresponding expected peak period*

10,000 years Hs [m]	Type of weibull distribution		
Expected Tp [s] (F=0.5)	3 parameters	2 parameters for Hs - threshold	3 parameters with λ = threshold
All steps with Hs > 6 m	**21.1**	23.0	21.2
	21.2	22.2	21.3
All steps with Hs > 7 m	**20.7**	22.3	20.8
	21.0	21.8	21.1
All steps with Hs > 8 m	**20.3**	21.8	20.4
	20.8	21.6	20.9
Storm peaks with threshold = 6 m	**21.6**	23.7	21.8
	21.5	22.5	21.6
Storm peaks with threshold = 7 m	**21.0**	22.8	21.3
	21.2	22.1	21.3
Storm peaks with threshold = 8 m	**20.5**	22.5	20.7
	20.9	22.0	21.0
All sea states	**24.5**	20.6	26.6
	22.9	21.0	23.0

Design sea states from contour plots:

***Table 4**: Design sea states (most severe) from contour plots*

ULS	H_s T_p	18.1 m 19.4 s
ALS	H_s T_p	23 m 21.3 s

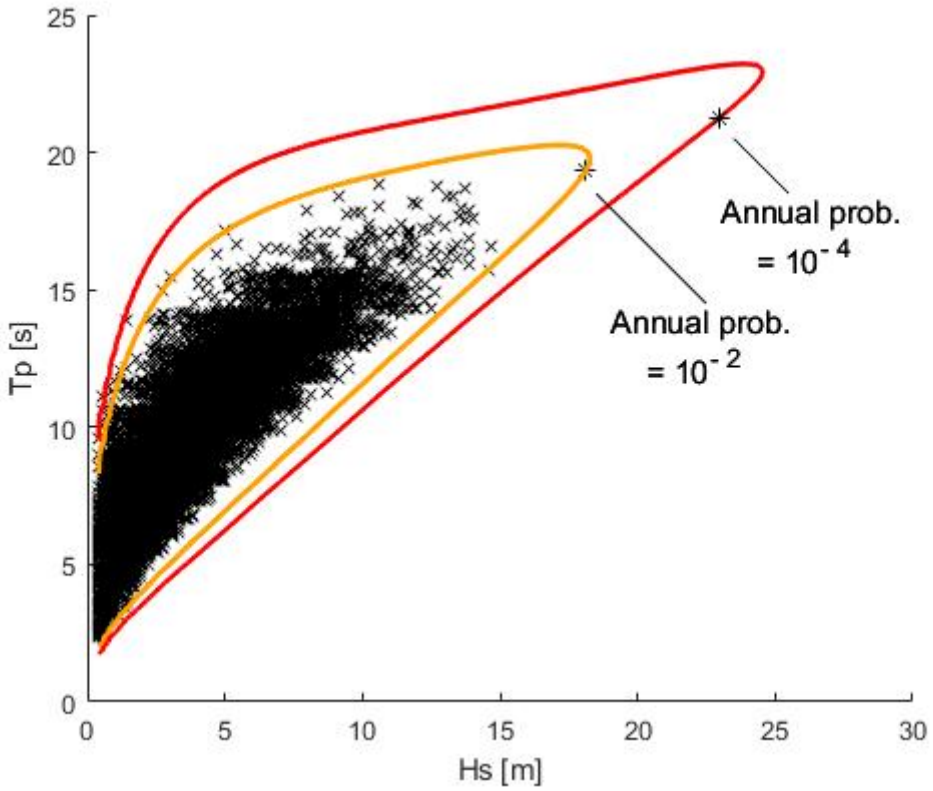

***Figure 38**: most severe sea states from contour plots (obtained from all wind seas)*

DISCUSSION

The present work has been done for an existing model of a semisubmersible that was to be built in the Norwegian continental shelf. The response properties of the structure as a floater were given from a FEM analysis and the dimensions of the deck are known; this is enough to conduct an airgap analysis when the wave data is introduced. Everything related to mass distributions, inertial properties, and added mass is reflected in the transfer functions (response properties). However, it is worth to remember that some design processes are iterative, such as that of a semisubmersible: the transfer functions consider an airgap, because the FEM analysis does require the detailed geometry of the underside. Changing the geographical location, and thus changing the characteristics of the sea -which is the one of the arguments of this thesis-, changes the airgap requirement and this would in fact change the response properties for a different airgap than the one the transfer functions were computed for. In a real project, the transfer functions would be re-computed after changing the dimension of the airgap, and then the whole procedure to determine the minimum airgap would be done again, until similar results are obtained. The main take of this thesis is that the whole procedure to determine the minimum airgap was developed in a complete way and can be run for any case of a column stabilised unit.

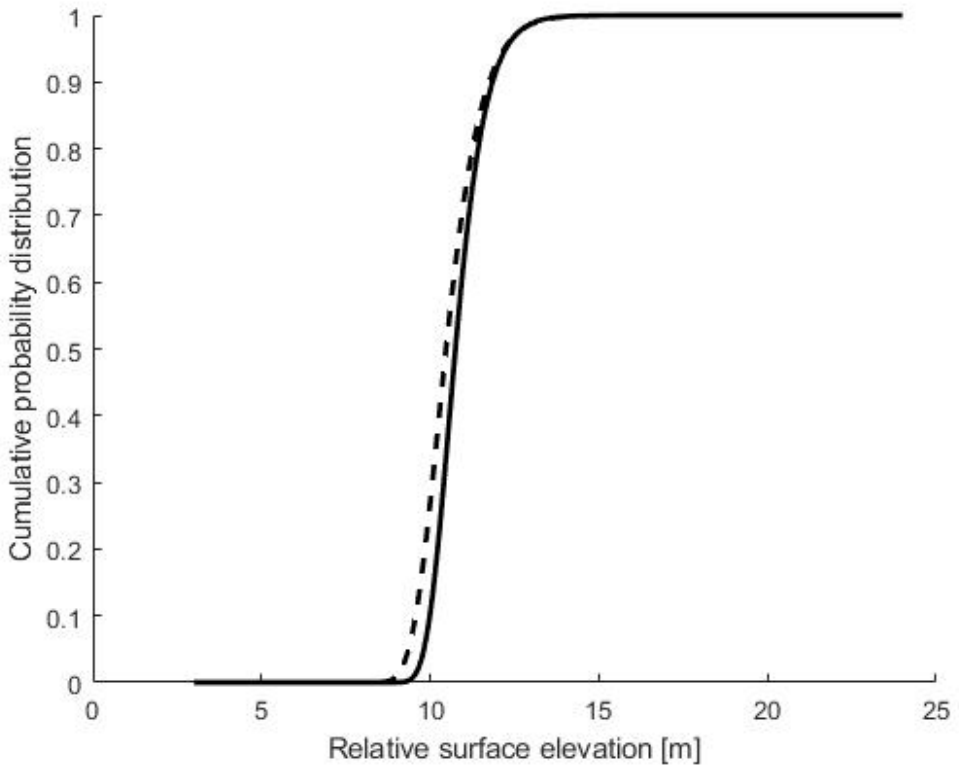

***Figure 39**: Comparison between the distribution of a storm maximum relative surface elevation for a storm peak (dashed) and for all of the steps. Cases computed for a threshold of 7 m.*

Some extra cases were computed for the ULS and ALS relative surface elevations when only the responses due to the storm peaks are analysed and also for the 100 and 10,000 year significant wave heights with different analysis approaches. For the relative surface elevations when looking at the storm peaks only (figure 39), it is obvious that they are smaller, but it might be worth considering for some response problems that it might only be the peaks that have an influence. For the extreme values of the significant wave height, it is the storm peaks that are important when fitting a probabilistic model. The extremes were also estimated from probability distribution fits that consider all the 3-hoour events above the threshold. While these results are not expected to be the best, tables 2 and 3 show that the differences between the two methods are very small. Other than the extra cases -which in this work might not be useful for more than comparing-, the probabilistic models included some variations; as it was mentioned a few times along the text, three versions of the Weibull distribution were used and the performance of the 3-parameter version with an artificial location was actually very close to the traditional 3-parameter distribution, just slightly more conservative.

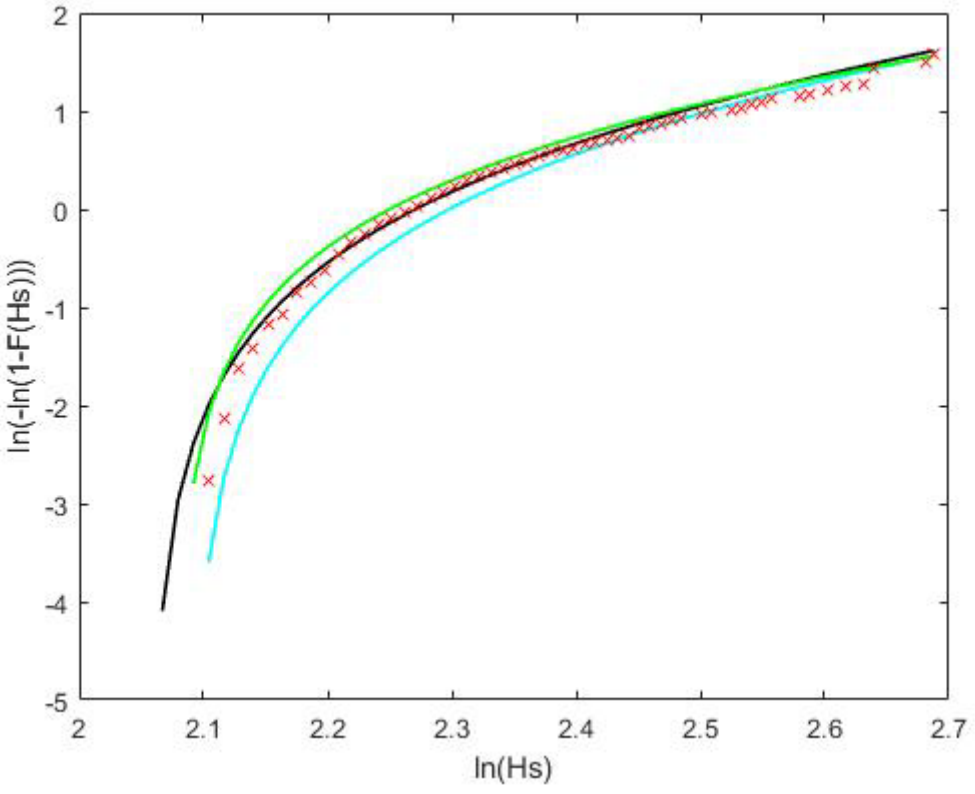

***Figure 40**: Fitted distributions of the 3-hour significant wave heights of the storm peaks with a threshold of 8 m. Black: normal 3-parameter Weibull, green: 2-parameter Weibull, cyan: 3-parameter Weibull with artificial location.*

One of the most important considerations in this thesis has been that the computation of the most probable storm maximum relative surface elevation -which are obtained for each storm and under each point- were done for the corresponding direction of each 3-hour event. The effect of this vs defining a direction of a storm an applying it for the whole storm is that the transfer functions are different for the different direction. This would certainly affect the results. For the lowest threshold (6 m) the longest storm resulted in 114 hours, I.e. 38 3-hour steps with an individual direction each. Even for some of the average-sized storms, the direction could change significantly over the course of their duration. The approach to determine the directions for the contour method was different though, the direction of an arbitrary sea state along a contour can't be estimated with certainty, which is why the extreme sea states were directed to a sector of several directions. From the storm severity scatter plots and the contours of the extreme relative surface elevations, it was clear that the worst sea states could, in fact, be assumed to come not from a specific direction from a sector. That is why WAMIT 135°, WAMIT 157.5° and WAMIT 180° were selected and then the 'sea-state maximum expected relative surface elevations were obtained for each case and the largest -for each point under the deck- were kept.

The wave asymmetry factor and another critical thing. It is clear that the waves are not sinusoidal and thus their height from the mean water level to the crests must be corrected. The factor was 1.2 for all points under the deck, but it is known that due to the disturbances of the waves under the platform their shape would change. A more precise approximation would consider a unique value for each location under the deck depending on the wave direction or even on the frequency. Defining the correct asymmetry factor is a task on its own and it was left out of this thesis. 1.2 is thought to be a safe value and there should not be any reason believe that there could be negative consequences from generalizing it when the value is on the high (conservative) side. It is important, however, to notice how much this affects in the assessment. A case was prepared with $\alpha = 1$ to see the extreme relative surface elevations for what would be sinusoidal waves (figures 41 and 42).

Finally, it should be pointed that the whole procedure is not restricted to semisubmersibles. It can be applied to any column stabilized floater, which include structures such as spars or semisubmersibles with different geometries. Ideally, the method will be part of different types of projects not necessarily related to the Oil and Gas industry, such as floaters for offshore wind turbines.

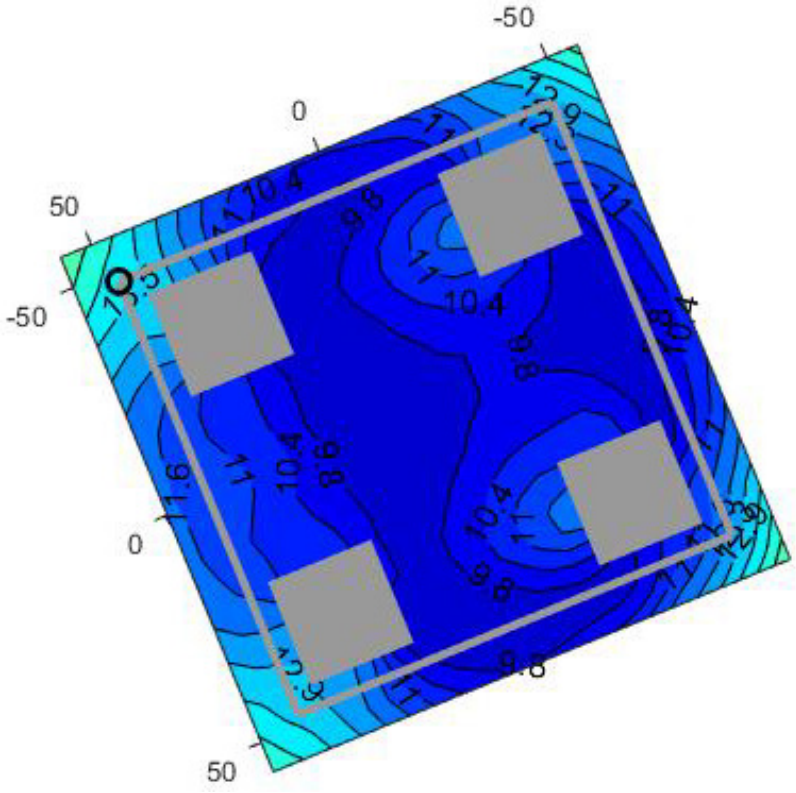

***Figure 41**: 100 year relative surface elevations from the analysis of the storm peaks with a threshold of 7 m. $\alpha = 1$.*

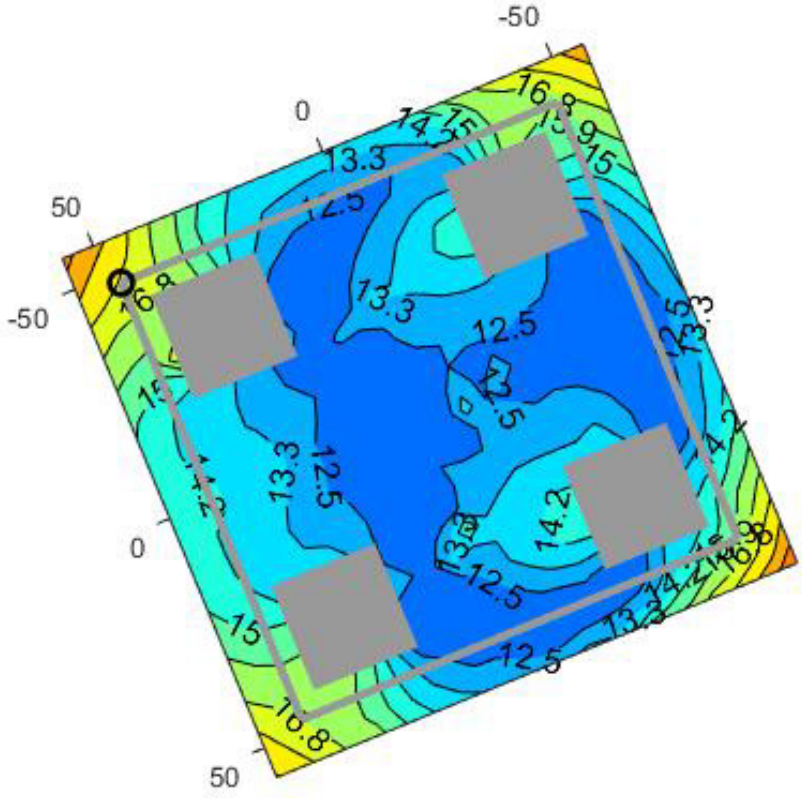

***Figure 42**: 10,000 year relative surface elevations from the analysis of the storm peaks with a threshold of 7 m. $\alpha = 1$.*

CONCLUSIONS

From figure 15 in the results it can be seen that threshold values of 6 and 7 meters yield similar results while a more significant deviation starts when higher thresholds are implemented. It is difficult to decide which value is the optimal, this depends on each particular problem. For the selected location, both 6 and 7 meters returned very similar results; and if the time of computation is considered important, a threshold 7 meters saves about half of the time. **The initial/design airgap requirement according to this study is 18 m for ULS design and 22 m for ALS design.**

The storm severity was defined as a measure of the relative surface elevation on a point for different storms when the directions of all their steps are considered. From the storm severity scatter plots, it was evident that the most severe storms come from the West-North-West if they are looked at carefully. The influence of a threshold on the storm severity by directional sector does not seem to have an effect, which is an expected outcome considering that the peaks and the steps close to them make for most of the effect on the relative surface elevation. A direction with severe storms could be related to a direction with steeper seas, although it was seen that the highest waves come from the East, but slightly from the South (from the wind rose in the problem setup). This means that waves from the North-West are the steepest, regardless of their height.

The contour plot method showed a good performance for the highest relative surface elevations. It was done for different percentiles of the distributions of the sea-state maximum relative surface elevation and the traditional 90% was more than satisfactory. According to the results presented here, it suggests to be a reliable method for estimating extremes, but relative surface elevations under the middle of the deck seem much higher compared to the POT method. This method is significantly less expensive in a computational aspect.

Regarding the extreme values of the significant wave height, results are very sensitive to the selection of a threshold and the type of fitted distribution. Despite sorting out significant wave height values lower than 0.4 m, the estimation of extremes for all sea states with a Weibull model gives unrealistically high values. It is subject to discuss on how this influences the results from the contour plots. **Extremes for ULS and ALS with the normal 3-parameter Weibull model are well around 16 and 21 m, correspondingly.**

RFERENCES

Veld, K. (2016, April 08). En hendelse hele bransjen vil bli berørt av. Retrieved April, 2019, from http://www.cosl.no/en-hendelse-hele-bransjen-vil-bli-berort-av

Haver, S. (2019). Airgap and safety: Metocean induced uncertainties affecting airgap assessments. Marine Structures,(63), 406-428. Retrieved January, 2019.

Skjeggedal, E. (2017). Wave-in-Deck Forces and Response of Semi-Submersibles(Master's thesis, NTNU, Trondheim, 2017). Trondheim: NTNU.

Ferreira, J.A. & Soares, C. G. (1998). An Application of the Peaks Over Threshold Method to Predict Extremes of Significant Wave Height. Journal of Offshore Mechanics and Arctic Engineering,3(120). Retrieved April, 2019, from https://www.researchgate.net/publication/245293243_An_Application_of_the_Peaks_Over_Threshold_Method_to_Predict_Extremes_of_Significant_Wave_Height.

Patiño, J. (2018). Assessing air-gap of semi-submersibles in the Northern North Sea(Master's thesis, University of Stavanger, 2018). Stavanger: UiS.

Appendix D of “Haver, S. (2018). METOCEAN MODELLING AND PREDICTION OF EXTREMES. University of Stavanger, NTNU”. Andersen, O. J. (2009). Correction of spectral peak period of NORA10 data base. Statoil.

Cheynet, E. (2016, November 08). ScatterWindRose.m. Matlab 9.1, R2016b. [Source code].

Kurian, V.J. Ng, C.Y., & M.S, Liew. (2012). Numerical investigation on dynamic responses of classic spar platforms: Long crested waves vs. short crested waves. Conference: Humanities, Science and Engineering (CHUSER). Retrieved May, 2019, from https://www.researchgate.net/publication/261054583_Numerical_investigation_on_dynamic_responses_of_classic_spar_platforms_Long_crested_waves_vs_short_crested_waves.

DNV GL. (2017). Prediction of air gap for column stabilised units (OTG-13).

Haver, Sverre. (2018). METOCEAN MODELLING AND PREDICTION OF EXTREMES (Unpublished doctoral dissertation). University of Stavanger, NTNU.

Tromans, P.S., & Vanderschuren, L. (1995). Response based design conditions in the North Sea: Application of a new method. 27th offshore technology conference, Houston, 1-4 May 1995.

Naes, A. & Moan, T. (2005). Probabilistic Design of Offshore Structures. Handbook of Offshore Engineering. Retrieved May, 2019, from https://www.sciencedirect.com/science/article/pii/B9780080443812500084.

Bai, Y., & Lin, W. (2016). Loads and Dynamic Response for Offshore Structures. Marine Structural Design,(7). Retrieved March, 2019, from https://www.sciencedirect.com/science/article/pii/B9780080999975000071.

History of offshore drilling units. (2015, June). Retrieved May, 2019, from https://petrowiki.org/History_of_offshore_drilling_units

Mathiensen, M., Goda, Y., Hawkes, P. J., Mansard, E., Martin, M. J., Peltier, E., . . . Van Vledder, G. (n.d.). Recommended practice for extreme wave analysis. Journal of Hydraulic Research. Retrieved February, 2019, from https://www.researchgate.net/publication/239395324_Recommended_practice_for_extreme_wave_analysis.

Gyory, J., Mariano, A. J., & Ryan, E. H. (n.d.). Surface Currents in the Atlantic Ocean: The Norwegian & North Cape Currents. Retrieved May, 2019, from https://oceancurrents.rsmas.miami.edu/atlantic/norwegian.html

Reistad, M., Breivik, Ø, Haakenstad, H., Aarnes, O., Furevik, B. R., & Bidlot, J. (2011). A high-resolution hindcast of wind and waves for the North Sea, the Norwegian Sea, and the Barents Sea. Retrieved May, 2019, from https://agupubs.onlinelibrary.wiley.com/doi/abs/10.1029/2010JC006402.

NORSOK STANDARD. (2007). Actions and action effects (N-003)

RECOMMENDED PRACTICE DET NORSKE VERITAS. (2010). ENVIRONMENTAL CONDITIONS AND ENVIRONMENTAL LOADS (DNV-RP-C205)

Haver, S., & Patiño, J. (2019). AIRGAP ASSESSMENT OF SEMI-SUBMERSIBLE ACCOUNTING FOR SIMULTANEOUS OCCURRENCE OF WIND SEA AND SWELL. Proceedings of the ASME 2019 38th International Conference on Ocean, Offshore, and Arctic Engineering.

APPENDIX

MSc theses 2019

Assessment of necessary airgap of semi-submersible using a peak-over threshold long term analysis

Student: JoséTorres

Background

Sufficient still water airgap is important both for fixed and floating platforms. What is a sufficient airgap according to the rules depends on the rule regime under which the platform is planned to be operating. All fixed platforms and floating platforms operating at one site for its design life time, platform design will follow the regulations provided by the Petroleum Safety Authority Norway, Framework Regulation and Facilities Regulations. For floating platforms operating as drilling rigs, there is an opening in the Framework Regulation for design platform in according to the Maritime Regulations. The latter approach means that platform has to fulfill class requirements from a recognized classification society, e.g. DNV-GL.

In the MSc focus shall be on a given semi-submersible platform. The rigid body transfer functions are made available. The aim of the MSc is to estimate q-probability airgap, $q = 10^{-2}$/year and $q = 10^{-4}$/year, for the worst location under platform deck accounting for joint occurrence of wind, wind-sea and swell sea. A consistent estimation of q-probability airgap requires that a long term analysis is performed. The platform shall in this thesis be operating in a position in the Norwegian Sea where weather conditions are similar to North Atlantic condition. NORA10 data for the years from September 1957 – September 2017 will be made available. In order to validate the airgap assessment procedure, the procedure should be applied to a case taken from the thesis of Julio Patino. Based on previous results the present study can be restricted to merely considering wind sea.

Long term response analysis shall in this thesis be performed using the "*all storms approach (POT)"*. An important part of this method is to choose a proper threshold defining the selection of storms. An important part of the air-gap assessment is to consider sensitivity of results to selected threshold.

A linear response analysis can be utilized for the short term analyses, but non-linearities in the surface elevation process shall be included in the analyses. A possibility is to utilize the approach proposed by DNV-GL – OTG13. The analysis can at first be done by neglecting wind speed. If time permits, one may consider to include effect of wind in the "all storm approach". As a minimum, effect of wind speed shall be discussed for a governing sea state both for $q= 10^{-2}$ per year and $q= 10^{-4}$ per year.

Below a possible division into sub-tasks is given.

1. The first thing to do is to modify the spectral peak period of the NORA10 hindcast data for the Norwegian Sea position. The recipe for that is found in the compendium used in Marin Technology and Marine Operations.

   Thereafter compressed database shall be stablished be identifying all wind sea storms exceeding 6m significant wave height. Sensitivity to chosen threshold shall be done by considering several threshold.

2. Use peak-over-threshold technique to estimate significant wave height of wind sea corresponding to annual exceedance probabilities of q= 0.01 and q = 0.0001. The method used should be clearly explained.

3. Perform and “all storm approach” for estimating the q - probability crest height using Rayleigh distribution for global crest heights of a stationary sea state. This is in agreement with a Gaussian assumption for the sea surface. Demonstrate the effect of accounting for non-linearities in the surface process.

4. Demonstrate how a short term analysis is utilized in order to establish the distribution function for the storm maximum relative crest heights (i.e. crest heights seen from the platform). This should include a demonstration of how the transfer function for the relative surface elevation is determined. Use a JONSWAP type of wave spectrum for wind sea.
   Discuss in detail how you model the effect of non-linearities in the incoming sea.
   Discuss the adequacy of the present approach.

5. Do the long term analyses for and estimate necessary still water airgap to avoid wave deck impacts for q = 0.01 and q = 0.0001.

6. Do an approximate long term analysis for the relative crest using the metocean contour analysis for the worst point under the platform.

7. Discuss the results of various analyses of the airgap variable for q = 10^{-2}/year and q = 10^{-4}/year.

8. Present the work in a scientific report and present conclusions regarding your main findings.

The candidate may of course select another scheme as the preferred approach for solving the requested problem. He may also involve other subjects than those mentioned above if found to be important for answering the overall problem; air-gap requirement for semi-submersibles.

The work may show to be more extensive than anticipated. Some topics may therefore be left out after discussion with the supervisor without any negative influence on the grading.

The candidate should in his report give a personal contribution to the solution of the problem formulated in this text. All assumptions and conclusions must be supported by mathematical models and/or references to physical effects in a logical manner. The candidate should apply all available sources to find relevant literature and information on the actual problem.

The report should be well organised and give a clear presentation of the work and all conclusions. It is important that the text is well written and that tables and figures are used to support the verbal presentation. The report should be complete, but still as short as possible.

The final report must contain this text, an acknowledgement, summary, main body, conclusions, suggestions for further work, symbol list, references and appendices. All figures, tables and equations must be identified by numbers. References should be given by author and year in the text, and presented alphabetically in the reference list. The report must be submitted in two copies unless otherwise has been agreed with the supervisor.

The candidate should give a written plan that describes the progress of the work mid-way through the MSc period. The plan can be limited to give a draft table of content for the MSc thesis, status regarding completion for the various chapters and what is consider the main remaining challenges. As an indication such a plan should be available by mid-April.

From the report it should be possible to identify the work carried out by the candidate and what has been found in the available literature. It is important to give references to the original source for theories and experimental results.

The report must be signed by the candidate, include this text, appear as a paperback, and - if needed - have a separate enclosure (binder, diskette or CD-ROM) with additional material.

Supervisor: Sverre Haver, UIS

The MATLAB codes are in a separate appendix in electronic form.